Title

The Dynamics and Resilience to Drought of Wetlands and Avian Metapopulations in a Coupled Human and Natural System

Author

Van Schmidt, Nathan Donald

Publication Date

2018

Peer reviewed|Thesis/dissertation

The Dynamics and Resilience to Drought of Wetlands and Avian Metapopulations in a Coupled Human and Natural System

By

Nathan D. Van Schmidt

A dissertation submitted in partial satisfaction of the

requirements for the degree of

Doctor of Philosophy

in

Environmental Science, Policy, and Management

in the

Graduate Division

of the

University of California, Berkeley

Committee in charge:

Professor Steven R. Beissinger, Chair
Professor Justin S. Brashares
Professor Norman L. Miller

Fall 2018

The Dynamics and Resilience to Drought of Wetlands and Avian Metapopulations in a Coupled Human and Natural System

by Nathan D. Van Schmidt

Abstract

The Dynamics and Resilience to Drought of Wetlands and
Avian Metapopulations in a Coupled Human and Natural System

by

Nathan D. Van Schmidt

Doctor of Philosophy in Environmental Science, Policy, and Management

University of California, Berkeley

Professor Steven R. Beissinger, Chair

In working landscapes where natural resource extraction co-occurs with habitat conservation, species are often structured as a metapopulation occupying fragmented patches of habitat. Because patches change due to human management decisions, understanding how metapopulations persist in working landscapes requires assessing both how the species' intrinsic factors drive turnover and how the behaviors of key actors drive patch changes. Coupled human and natural systems (CHANS) research uses a multidisciplinary approach to identify the key actors, processes, and feedbacks that drive the dynamics of a region. This dissertation integrates five diverse datasets—wildlife occupancy surveys, land-use change mapping, a survey of landowner decision-making, hydrological databases, and disease vector trapping—to assess how wetlands, irrigation, and two avian metapopulations function as a CHANS in the rangelands of the foothills of the California Sierra Nevada. The threatened, dispersal-limited black rail (*Laterallus jamaicensis*) and widespread, vagile Virginia rail (*Rallus limicola*) inhabit patchy wetlands throughout the foothills. The black rail has declined over the past decade, with drought and the arrival of West Nile virus potential causes. The first chapter assesses how the human-induced diversity of hydrological processes altered the CHANS' resilience to an exceptional disturbance, a historically severe drought from 2012–2015. The second chapter tests if the "rescue effect" (dispersing individuals preventing local extinctions) actually occurs as predicted by theory and occupancy models. The third chapter integrates these interdisciplinary datasets into a simulation model that combines agent-based models of land-use change with stochastic patch occupancy models of metapopulations, in order to (1) quantify the relative importance of different drivers of metapopulation dynamics, (2) test predictions of the behavior of metapopulations in dynamic landscapes, and (3) evaluate the potential impacts of mandated irrigation cutbacks during drought and wetland incentive policies on metapopulation persistence.

Complex metapopulation dynamics emerged from the CHANS, and irrigation water was critical for black rail persistence. Wetlands were primarily fed by "waste" from the irrigation system. Landowners and water sources showed response diversity to drought, increasing the resilience of the wetland landscape and maintaining the black rail metapopulation through the 2012–2015 drought. The rescue effect was operating for both rail metapopulations during this period, providing one of the first empirical validations of this process, and occurred at notably higher rates during the lowest precipitation year. However, inferences from occupancy models

were unreliable and underestimated the rescue effect (1) when using autoregressive measures that incorporated patch area, (2) when the species was not dispersal-limited, and (3) during a period of nonequilibrium metapopulation dynamics. Simulations showed rail metapopulations were strongly top-down regulated by precipitation, with synergistic negative impacts because droughts affected multiple system processes at the same time. The black rail decline was caused by the combination of West Nile virus and drought. Two key theoretical predictions were not borne out due to the CHANS' complexity. First, dispersal limitations of black rails did not result in greater sensitivity to patch change rates compared to Virginia rails, because patch heterogeneity affected patch change rates and the two species' colonization and extinction rates in different ways. Second, because incentive programs were coupled to CHANS dynamics they made the black rail metapopulation more sensitive to other parameters, not less. Drought irrigation cutbacks posed a substantial extinction risk that incentive policies were unable to reduce. Integrating "waste" water into regional wetland management may thus offer more cost-effective conservation than attempting to restore a lost "natural" state. These results highlight that conserving metapopulations in working landscapes requires assessing how human transformation of CHANS may create new diversity in system processes that benefits wildlife.

For Meagan,
the good earth on which this orchard grew.

Table of Contents

List of Figures

List of Tables

Acknowledgements

First and foremost I would like to thank my wonderful wife, Meagan Van Schmidt, to whom this dissertation is dedicated. She moved across the country so I could pursue this dream, accepted my working long hours and being away for months of fieldwork with understanding and encouragement, and provided me countless hours of material and emotional care. I'd further like to thank my family—Allen, Caryn, Katrina, and Peter Schmidt—and my other loved ones and friends—Holly Chandler, Abbey Hartland, Steve McClellan, and Craig Williams—who have supported me throughout the years and sharpened my mind by challenging my ideas.

My deepest gratitude towards my committee chair and guiding professor, Steve Beissinger, for teaching me how to think, plan, and write like a scientist. I'm also grateful for the mentorship of Laurie Hall and Jerry Tecklin, who taught me everything they knew about the wetlands of the Sierra Nevada foothills. This dissertation would not have been possible without the foundation laid by their research and guidance.

Numerous collaborators helped with this interdisciplinary research. I'd like to thank the team of coauthors on my first and third chapters: Lynn Huntsinger, Tracy Hruska, Marm Kilpatrick, Tony Kovach, Norm Miller, and José Oviedo. Many others also helped: my Cooperative Extension mentors, Van Butsic, Roger Ingram, Cass Mutters, and Sam Sandoval Solis; my many field and lab technicians, in particular Tricia Gardner, Caitlin Boise, and Eric Tymstra who were instrumental for several years; and Luke Macaulay, Sean Peterson, Orien Richmond, and Ben Risk who collected key pieces of field data.

Thank you to everyone else that provided feedback on this dissertation. First, the remaining members of my dissertation and qualifying committee: Justin Brashares, Rauri Bowie, and Maggi Kelly. There were many people who participated in the Beissinger Lab that reviewed numerous drafts of these papers, including Karl Berg, Katie LaBarbera, Aline Lee, Juan Li, Lu Liang, Sarah MacLean, Sean Maher, Toni Morelli, Oliver Muellerklein, Erica Newman, Patrick Kelley, Tierne Nickel, Eric Riddell, Soorim Song, Erica Spotswood, Henry Streby, and Corey Tarwater. I'd like to extend a special thank you to my officemate Kelly Iknayan for letting me pick her brain about statistical problems for years without complaint.

This research was funded by the National Science Foundation (DEB-1051342, CNH-1115069), the Sierra Foothills and Sacramento Audubon Societies, the Salvador de Madariaga program (PRX16/00452) of the Spanish Ministry of Culture and Education, and the USDA National Institute of Food and Agriculture.

Lastly, research on coupled human and natural systems is not possible without the "human" component. My heartfelt thanks to all of the people that generously participated in this study by granting access to their property, participating in interviews, or responding to the mail survey. The community of the Sierra foothills was a warm and welcoming place to call my temporary home. While this landscape has transformed over the past century, it remains—as Clarence King wrote in 1872—a place of "rich, dreamy quiet, with distance lost behind pearly hazes, with warm tranquil nights, dewless and silent… wear[ing] an aspect of patient waiting for a great change." I am profoundly grateful for the year of my life I spent living and learning there.

Chapter 1: Human-created diversity in hydrological processes increased resilience of a metapopulation of a threatened wetland bird to drought

1.1 Abstract

There is a wealth of research showing that human reductions in diversity of ecological processes can negatively affect ecosystems. However, the conceptualization of ecosystems as integrated with people within broader "coupled human and natural systems" suggests that the addition of novel types of human-induced diversity in system processes may likewise confer benefits. We explored this hypothesis by studying how socially created diversity mediated the impact of a historically severe drought on a network of wetlands in the foothills of the California Sierra Nevada containing a metapopulation of the threatened black rail (*Laterallus jamaicensis*). We examined (1) how differences in natural and irrigated water sources affected wetland's drying in response to drought, (2) how diversity in landowner's motivations for land ownership affected their irrigation use and response to drought, and (3) how this hydrological diversity affected the persistence of black rails. We found that wetlands were mostly fed by inefficiencies and leaks from the irrigation system. Wetlands with both natural and irrigated water sources were larger, wetter, and likelier to persist through drought because these sources showed response diversity by drying at different times. Wetlands with diverse water sources provided the best habitat for the black rail, and irrigation appeared responsible for its persistence through the drought. While profit-motivated landowners provided wetlands more irrigation during non-drought conditions, other landowner types were more likely to continue providing irrigation during drought. Our results highlight that conservation in socio-ecological systems requires assessing not only the value of historic ecological diversity, but also how novel types of socially-induced diversity may benefit ecosystems.

1.2 Introduction

Recognition of the complex links between people and ecosystems has fostered growing interest in coupled human and natural systems (CHANS, also called social-ecological or human-environment systems; Liu et al. 2007). CHANS are characterized by heterogeneity, cross-scale interactions, feedback loops, and multiple quasi-equilibrium states, resulting in complex nonlinear dynamics that hamper prediction of system behavior (Costanza et al. 1993, Schlüter et al. 2012). In lieu of controlling system behavior, resilience theory has come to dominate the CHANS literature as a way to promote sustainability by managing for resilience (Brown 2014, Allen et al. 2018). Resilience has been defined in multiple ways (Quinlan et al. 2015, Angeler and Allen 2016) with ongoing debate (c.f., Hodgson et al. 2015 and responses). "Ecological resilience" is the magnitude of disturbance a system can withstand and maintain critical relationships and functions (Quinlan et al. 2015). "Engineering resilience" focuses on stability, measured by resistance (how much the system changes in response to disturbance) and recovery (the speed with which a system returns to prior condition afterwards; Holling 1996). In the CHANS literature, resilience is generally equated with the concept of ecological resilience, but can be expanded to include social adaptability (e.g., learning; Angeler and Allen 2016, Quinlan et al. 2015). A consensus definition is emerging based on commonalities that broadly equates resilience as a system's capacity to persist or maintain function following disturbance, with

stability an aspect of resilience that can be quantified as resistance and recovery (Angeler and Allen 2016, Quinlan et al. 2015, Hodgson et al. 2015, Ingrisch and Bahn 2018).

Theory posits that resilience increases when stability is created by the diversity of agents and the linkages between them (Holling 1996). Diversity of agents (e.g., species or stakeholders) enhances system function if each plays a different role in the provisioning of services (functional diversity). Even when agents play the same role (functional redundancy), they can enhance resilience by responding differently to disturbance (response diversity; Elmqvist et al. 2003, Leslie and McCabe 2013) because diverse responses reduce the risk of losing functions if one agent type in the system fails (the portfolio effect; Hooper et al. 2005). Resilience theory arose from studies of how diversity in biological communities creates overall system resilience, even though individual system components (e.g., species populations) may be highly variable (Holling 1973, Folke 2006). However, research on functional and response diversity in other ecological and social systems is lacking (Leslie and McCabe 2013, Hruska et al. 2017). The application of resilience theory to CHANS has consequently been criticized as a vague naturalistic metaphor being inappropriately applied to fundamentally different social systems without empirical validation (Olsson et al. 2006, Brown 2014, Angeler and Allen 2016). Quantitatively evaluating if other kinds of ecological and social diversity promote function and resilience is necessary to establish the validity of resilience as a scientific theory of CHANS (Angeler and Allen 2016).

We examined the influence of functional and response diversity of natural and social agents on the function and resilience of the freshwater wetlands of California, a CHANS of conservation concern, to a historic drought (Fig. 1.1). Over 90% of California wetlands have

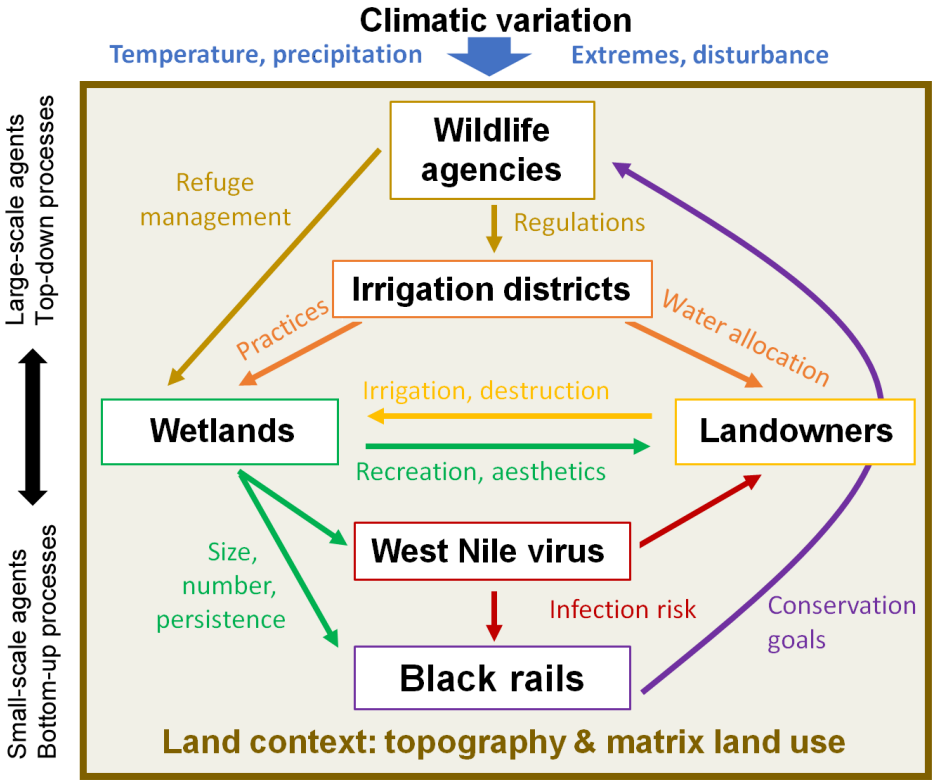

Figure 1.1. System flow diagram of the wetland coupled human and natural system in the Sierra Nevada foothills. System components are connected by key linkages; climate is an external force affecting all components, while land context structures the system and constrains changes.

been destroyed since 1850 (Lemly et al. 2000). In the Sierra Nevada foothills, however, numerous small (typically <1 ha) wetlands have been created, mostly on private lands that are comprised of large and small ranches in open oak (*Quercus* spp.) savannah and seasonal grasslands, rice (*Oryza sativa*) farms, and exurban and suburban residences(Richmond et al. 2010a). Landowners create wetlands by irrigating, and dry them by draining or reducing irrigation. Water is provisioned to landowners chiefly by two irrigation districts, which are governed by locally elected officials and respond to regulations from state agencies. Small wetlands provide important ecosystem services disproportionate to their size (Blackwell and Pilgrim 2011, Palta et al. 2017), exemplified in this CHANS by providing habitat for the secretive black rail (*Laterallus jamaicensis*), a threatened bird whose density is greater in foothills wetlands than in the larger wetlands of the San Francisco Bay (Girard et al. 2010). However, foothills wetlands also provide ecosystem disservices as habitat for mosquitoes that carry West Nile virus (WNV), an emerging infectious disease that threatens people and rails. Rail metapopulation dynamics, and potentially WNV transmission risk, are affected by the number, size, and persistence of wetlands (Risk et al. 2011). Our study included four years of historically severe drought (2012–2015; Diffenbaugh et al. 2015), followed by a wetter year (2016).

We tested whether functional and response diversity affected the CHANS' function and resilience to this historic drought. Following the recommendations of Quinlan et al. (2015), we utilized a multi-scale approach to quantify resilience that combined metrics with a holistic assessment of system dynamics. We used remote sensing, field surveys of wetlands, and a mail survey sent to landowners to quantify two types of diversity, wetland hydrological diversity and landownership motivation diversity, and determine their influence on five aspects of this CHANS: wetland abundance, wetland saturation, landowner irrigation behavior, black rail dynamics, and WNV transmission risk. Because CHANS operate across multiple scales we defined resilience at three scales: (1) individual wetlands maintaining ecosystem functions; (2) landowners maintaining wetlands; and (3) system-wide maintenance of water and wetlands sufficient for persistence of black rails and landowner livelihoods. Quantifying overall resilience of an entire CHANS is likely impossible, necessitating the assessment of the specific resilience of focal system components to focal disturbances (Quinlan et al. 2015, Angeler and Allen 2016, Allen et al. 2018). We focused on resilience to drought of water and rails because irrigation water shortages are an important concern of landowners (Huntsinger et al. 2017), and wetland habitat goals in central California focus on waterbirds and perennially saturated wetlands (Duffy and Kahara 2011), which are critical for black rails in the foothills (Richmond et al. 2010a).

1.3 Methods

1.3.1 Wetland data collection

The study area was the California's Sierra Nevada foothills EPA zone III eco-region (US Environmental Protection Agency 2013) in Yuba, Nevada, and southern Butte counties. We mapped all emergent wetlands >5×5 m within this area by manually interpreting summer 2013 GeoEye-1 0.4 m imagery in Google Earth 7.1.5. This minimum mapping unit included virtually all wetland patches in the study area and was less than the size of the smallest breeding home range we measured for black rails (0.16 ha; S.R. Beissinger, unpublished data). Areas covered by hydrophytes (*Typha* spp., *Scirpus* spp., *Juncus effusus*, *Leersia oryzoides*, or various sedges) were considered wetland. We included hydrophytes that appeared seasonally dried and buffered

5 m into any green vegetation present along the wetland-upland transition zone. Open water and rice were excluded. If imagery was ambiguous, we used Google Earth imagery from adjacent years to help distinguish if a wetland was present. Wetlands were considered separate patches if they were >100 m from another patch, had different water sources, or were distinct management units (e.g., separate ponds). Each wetland's geomorphology was classified as slope (shallow hillside flow), pond fringe, fluvial, rice fringe, irrigation ditch, or waterfowl impoundment.

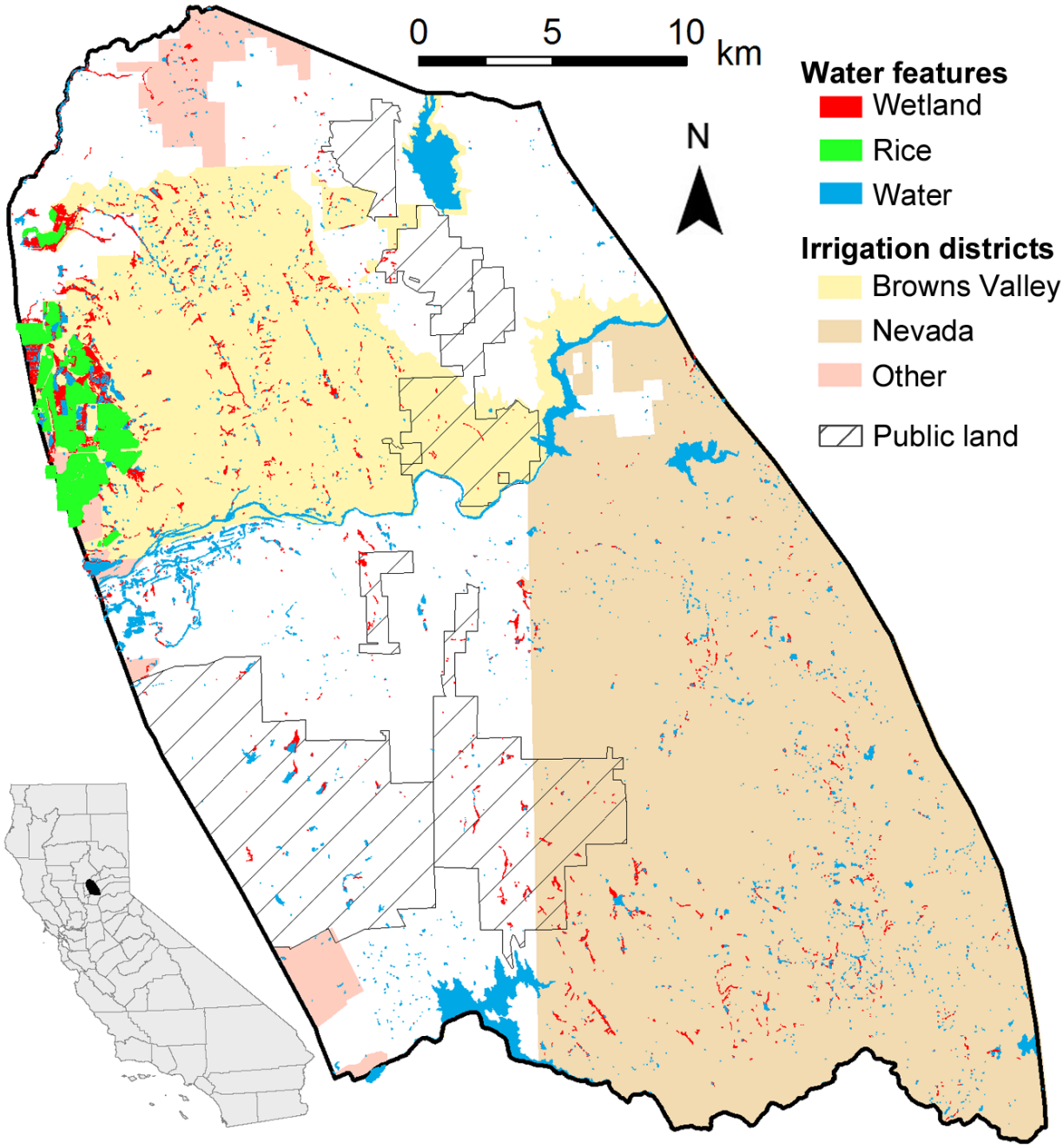

Figure 1.2. Water features >5×5 m in the foothills of the California Sierra Nevada study area, clustered within irrigation district service areas. Inset shows study area location in California.

We combined historic imagery and field data to determine the water sources of 934 wetlands (53% of 1,760 total wetlands). We classified the water sources of the 623 wetlands on the properties of landowner survey respondents (see *1.3.2 Social data collection*) using historical (1947–2015) aerial photographs of the landscape under different irrigation regimes to determine if natural springs or creeks existed before the addition of irrigation water. We also assessed all 222 wetlands on public lands and the remaining 16 rice fringe, 10 irrigation ditch, and 4 waterfowl impoundment wetlands on non-respondent properties to give us a comprehensive sample of these groups. We were able to gain property access to conduct field surveys of 271 wetlands (59 of which were newly assessed wetlands opportunistically added), supplementing our aerial interpretation with visual site inspections and interviews with landowners about water sources. All statistical analyses included only wetlands whose water sources were known.

To determine the total number and area of wetlands supported by each water source, we estimated the number and total area of the remaining 826 (47%) privately owned fringe, slope, and fluvial wetlands that were supported by each water source. We first calculated the percent and areal percent of each of the three types of wetlands supported by each water source in our n = 934 known-source wetlands. We then multiplied these percentages by the total number and area of unknown-source wetlands in each of these categories, and added them to the known-source wetlands in those categories. For example, for the number of spring-fed slope geomorphology wetlands (using only data from private lands):

$$\#\ \text{spring-slope} = \#\ \text{known spring-slope} + \#\ \text{unknown slope} \times \frac{\#\ \text{known spring-slope}}{\#\ \text{known slope}} \quad (1.1)$$

Confidence intervals were calculated based on the original proportions and then multiplied by the total number or area of unknown-source wetlands.

To assess the effects of water source on wetland hydrology, we resurveyed n = 117 wetlands for 14 periods: in the early wet season (January 8–27), late wet season (March 22–25), early dry season (May 17–June 20), and late dry season (July 15–August 15) from summer 2013–2016. At each visit we walked throughout the wetland with a map of aerial imagery and recorded the percent wetness (areal percent of wetland saturated with water). Not all wetlands could be sampled in all time periods due to access restrictions; we discarded any sites that were not visited ≥5 times and in both the dry and wet season, leaving n = 1343 observations. We compared the frequency of sites drying out (≤5% wetness) at least once during the drought between sites with only one, versus sites with both, water sources using a χ^2 test (R v3.4.3 base package *stats*; R Core Team 2013). To estimate to estimate the expected percent wetness of wetlands during each period we fit Tobit regressions (Tobin 1958) in R package *censReg* v0.5.26, with values censored at 0 and 1 and a random effect for site. Tobit regression is suitable for percent wetness data because wetlands could experience additional drying below 0% percent wetness (i.e., firm mud changing to cracked dry ground), while large inflows of water could cause flooding beyond 100% of the polygon saturated. We analyzed a model set that included water source (a factor: natural-only, irrigation-only, or both-source), wetland area (ln hectares), and interactions between these and each sampling period. For wetlands whose size varied annually (i.e., experienced changes in extent of hydrophyte cover) we used the maximum area (measured from aerial imagery) and corrected wetness estimates by multiplying the field-estimated percent wetness times the percent of the maximum area filled by the current area. We selected the best model via Akaike information criterion (AIC; Burnham and Anderson 2003). We excluded the impoundments (large, intensively managed waterfowl hunting wetlands found

only in the Central Valley) from this analysis because they had complex management cycles of water drawdowns and re-flooding. For reference, we included the prior 100 days' precipitation for the mean date of each sampling period, obtained from CIMIS weather station #84 near the center of our study area.

1.3.2 Social data collection

Data collection protocols for human subjects were approved by Committee for the Protection of Human Subjects (UCB-IRB protocol #2011-06-3324). From 2013–2016 we conducted 51 interviews with landowners and irrigation district employees about water management. In 2013–2014 we mailed a survey on land and water management, based on the Dillman Total Design method (Dillman et al. 2014), to a selection of regional landowners with properties ≥1.2 ha stratified by property size (see Huntsinger et al. 2017 for the survey). We sent surveys to $n = 862$ valid addresses, including 129 non-randomly selected landowners that were cooperators with our field research. There were $n = 470$ surveys returned (a 55% response rate), including 64 from non-random landowners. Because of the inclusion of these non-random responses, we report results on the respondents rather than the population; the proportion of landowners in each typology was similar between respondents and full population estimates (3.5% mean absolute difference).

We quantified social diversity by identifying six landowner typologies based on reported motivations for owning land, which has often been used to examine connections between motives and behavior (c.f., Ferranto et al. 2013, Sorice et al. 2014). Our survey asked respondents to score 20 reasons for owning land from 1 "not important at all" to 4 "very important" (Appendix S1.1: Table S2). We identified landowner typologies from $n = 354$ respondents who scored all the 20 reasons by performing a factor analysis, which finds linear relationships (factor loadings) between observed variables of interest (the reported reasons) and a smaller number of unobserved factors (the typologies). We identified six factors and labeled them as landowner types based on their shared characteristics of the subset of the 20 variables. For simplicity, we associated each variable to a single factor based its highest factor loading. Using the estimated factor loadings and the scores given by respondents, we obtained standardized values for each factor for each respondent that indicated which factor likely had the greatest influence on the landowner's reported motivations for land ownership. We then assigned each landowner to the typology for which that they had the highest standardized value.

We used these typologies in statistical tests for differences among respondents in their parcel characteristics and survey responses. We used our wetland mapping to count the number of natural-fed wetlands, irrigation-fed wetlands, ponds, and irrigated pastures on respondents' parcels in 2013. We used negative binomial generalized linear models (R v3.2.2, package *MASS*) to test for differences in number of water features. We used logistic regressions (NLOGIT v4.0) to analyze landowner responses to hypothetical water cutbacks (20%, 50%, or 100%) by modeling the probability of a landowner taking actions that would negatively impact wetlands or a landowner's livelihood (Appendix S1.1: Table S3). Wetland-impacting actions were "Repair leaks in ditches, pipes, dams and/or ponds", "Recycle and/or reuse tailwater, irrigation or pond runoff", "Stop or use less water to irrigate pasture(s)", and "Reduce area of irrigated pasture." Landowner-impacting actions were "Stop or reduce growing crops or gardening", "Sell livestock or reduce stocking rate", "Find other grazing land", "Sell some or all the land", "Purchase water from outside (non-district) sources", and "Change to a different land use."

1.3.3 Black rail data collection

We surveyed 237 wetlands for occupancy of black rails up to three times each summer from 2012–2016 using established broadcast survey methods (for details see Richmond et al. 2010a). We assessed the impact of water source diversity on the black rail metapopulation by fitting multi-season occupancy models (MacKenzie et al. 2003) using Program PRESENCE v11.7 (Hines 2013). Potential covariates for probabilities of initial occupancy (ψ), colonization (γ), and extinction (ε) we assessed were water source and three nuisance variables: area (natural log of hectares + 1), isolation (an autoregressive 7 km buffer radius measure obtained from Hall et al. (2018), and year (a set of dummy variables; not included on initial occupancy). Detection (p) only included year dummy variables as covariates. Continuous variables were standardized.

We implemented our occupancy modeling in two phases. First, to reduce the size of the model set we carried out a backwards model selection exercise for the three nuisance covariates. Water source was included in all models and AIC was used to assess model fit. The lowest AIC model included area as a covariate on ψ, γ, and ε, and year as a covariate on γ (Appendix S1.1: Table S4). Unlike previous studies in this system (Risk et al. 2011), there was only weak support (>3 ΔAIC) for connectivity influencing occupancy dynamics during this time period, possibly due to very low colonization rates during the drought. In the second phase we retained the nuisance variables from the best model and then ran a full model set of all possible water source combinations (Appendix S1.1: Table S5). For both phases, covariates were included for initial occupancy if they were included for either colonization or extinction.

Finally, we used AIC weights of the water source model set to calculate model-averaged estimates of occupancy in each year for an average wetland with each of the three water sources. Because area of wetlands significantly differed among water sources, we used the median area in our black rail sample for each category: 0.076 ha for natural-only, 0.168 ha for irrigation-only, and 0.284 for both-source. We used 95% confidence intervals calculated via the delta method to assess significant differences.

1.3.4 West Nile virus data collection

From June–October 2012–2014, we trapped mosquitoes at 63 wetlands (size range 0.03–6.7 ha) for 1,201 total site visits. We sampled 50 wetlands for one year and 13 wetlands in all three years. We visited each wetland weekly and set up four Center for Disease Control traps baited with dry ice, distributed along the wetland edge at ≥100 m intervals to capture spatial variation in mosquito densities; at some very small wetlands, shorter intervals needed to be used. The same trap locations were used at each visit. All mosquitoes caught were identified to species using morphological keys (Darsie and Ward 1981). For each wetland, we estimated the abundance of the main mosquito WNV vectors as the mean number of *Culex* mosquitoes caught per trap/night (from 4,710 trap/nights).

To estimate WNV prevalence at each wetland, we first extracted RNA using RNeasy kits (Qiagen) followed by RT-PCR (Qiagen) on 2,551 pools of 1–50 *Culex* mosquitoes (Kauffman et al. 2003). We included at least one positive and negative control alongside each set of 40 reactions and all WNV-positive pools were run twice to confirm presence of WNV. In the few cases where a pool tested positive and then negative, we conducted a third test to determine WNV status. We then used bias-reduced generalized linear models using package *brglm* in R (v3.13) with a binomial distribution and an offset for mosquito pool size to estimate WNV

prevalence using the presence/absence of WNV in 2,539 pools (mean 14.6 mosquitoes/pool). The full model included site, date, date^2, year, and interaction terms as predictors. The model with the lowest AIC (Appendix S1.1: Table S6) was used to estimate WNV prevalence, the mean probability of a *Culex* testing positive for WNV at each wetland across all dates. Finally, we estimated WNV transmission risk at each wetland as the mean abundance of WNV-infected *Culex* mosquitoes (mean *Culex* abundance × mean *Culex* WNV prevalence).

We used analysis of covariance to test for effects of water source on the abundance of all mosquitoes, abundance of *Culex*, WNV prevalence, and WNV transmission risk, while controlling for the effect of wetland size. We used a square root transformation on wetland size to equalize leverage and on all metrics involving mosquito abundance to maintain adequate homogeneity of variance.

1.4 Results

1.4.1 Water source diversity

We identified 1760 wetlands totaling 644.863 ha (Fig. 1.2) and quantified their hydrologic diversity based on water sources as natural-only (15% of sites), irrigation-only (62%), or both-source (24%). Most irrigated wetlands were created by inefficiencies and benign neglect, with 74% fed by leaks from ditches or ponds, oversaturated pasture or rice, or runoff (Fig. 1.3a). Wetlands were generally small (median = 0.090 ha, range: <0.001–11.459 ha), but both-source wetlands were significantly larger (median ± SE = 0.284 ± 0.053 ha) than irrigation-only (0.168 ± 0.015 ha) and natural-only wetlands (0.076 ± 0.007 ha; Kruskal-Wallis $n = 934$, $\chi^2 = 62.98$, with post-hoc Nemenyi pairwise tests $p = 0.0019$, 1.0×10^{-13}, and 2.0×10^{-8}). By increasing wetland size irrigation also increased wetness: wetlands were 7.6% wetter on average with each ten-fold increase in size (Appendix S1.1: Table S1), likely because the greater amount of overall water in larger wetlands resulted in inertia to drying.

Wetlands with diverse water sources were more resistant to drought. Sites with both water sources dried out (18.9 ± 0.7% SE) significantly less frequently ($\chi^2 = 6.25$, $p = 0.01$) compared to sites with only one water source (42.2 ± 0.8%). AIC model selection showed water source, but not wetland size, altered seasonal cycles of wetness during drought (Appendix S1.1: Table S1). Natural-only wetlands were more likely to dry in response to the drought during Mediterranean climate's dry summer, while irrigation-only wetlands were more likely to dry during the rainy winter (Fig. 1.3b; impoundments were excluded from this analysis). In a non-drought year (2016), wetness varied little among sites with different water sources across seasons, indicating that the pattern observed during drought was the result of response diversity.

1.4.2 Water management diversity

Factor analysis identified six landowner typologies based on motivations for owning land, similar to other studies in California (Ferranto et al. 2013): profit-oriented agricultural production ("profit," 16% of respondents); family, tradition, and a sense of belonging to the land ("tradition," 17%); the lifestyle associated with rural life ("lifestyle," 17%); environmental and wildlife protection ("environment," 15%); vacation and recreational use ("recreation," 20%); and financial investment ("investment," 15%; Appendix S1.1: Table S2). There were no significant differences among typologies in property size (range: 1.2–3237.5 ha, $F_{5,324} = 0.97$, $p = 0.43$), household income ($F_{5,293} = 1.44$, $p = 0.21$), or age ($F_{5,325} = 0.57$, $p = 0.72$).

Landowner typologies exhibited both functional redundancy and functional diversity in the types of water features on their landscape and their water management. All types had some irrigated features (Fig. 1.4a), and many types exhibited similar rates of water management actions (Fig. 1.4a–b). Profit-motivated landowners, and to a lesser extent tradition-motivated landowners, tended to have more irrigated water features and have more activate water management (Fig. 1.4a–b). Landowners in these groups were more likely to be ranchers or farmers ($F_{5,324} = 15.65$, $p = 8.3\times10^{-14}$). One ranch with numerous waterfowl impoundments strongly influenced the number of irrigation-fed wetlands of recreation-motivated landowners (Fig. 1.4a). While typical of hunting ranches in the Central Valley, recreation-motivated landowners elsewhere in the foothills had few irrigation-fed wetlands.

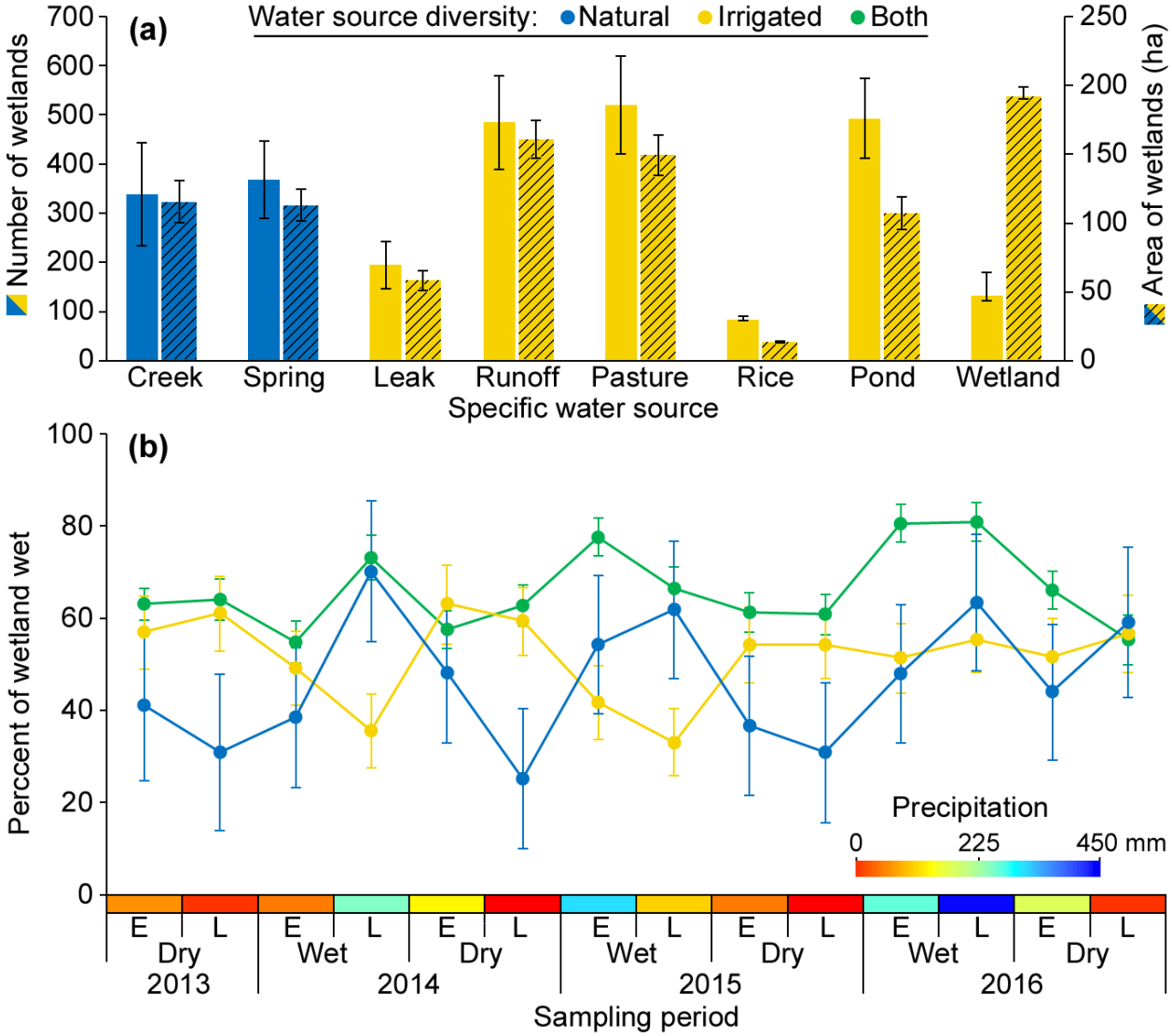

Figure 1.3. Sierra Nevada foothills wetland water source diversity. (a) Number and total area (± 95% CI) of wetlands supported by water sources; rice, pasture, pond, and wetland describe landowner's intended irrigation use. Wetlands with multiple sources (e.g., all both-source wetlands) are counted in multiple bars. (b) Mean (± SE) wetness (percent of surface saturated) of mean-sized wetlands over time (E = early and L = late in season) showed response diversity. The mean precipitation over the past 100 days for each period is shown for reference.

We quantified social response diversity by examining how landowners indicated they would respond to water cutbacks, which can be mandated by irrigation districts. Landowners said they would respond to water cutbacks by reducing water to pastures (31% of respondents), reusing runoff (8%), and repairing leaks (6%), which would affect up to 69% of the region's wetlands that were fed by these sources. Landowner adaptation to hypothetical water cutbacks

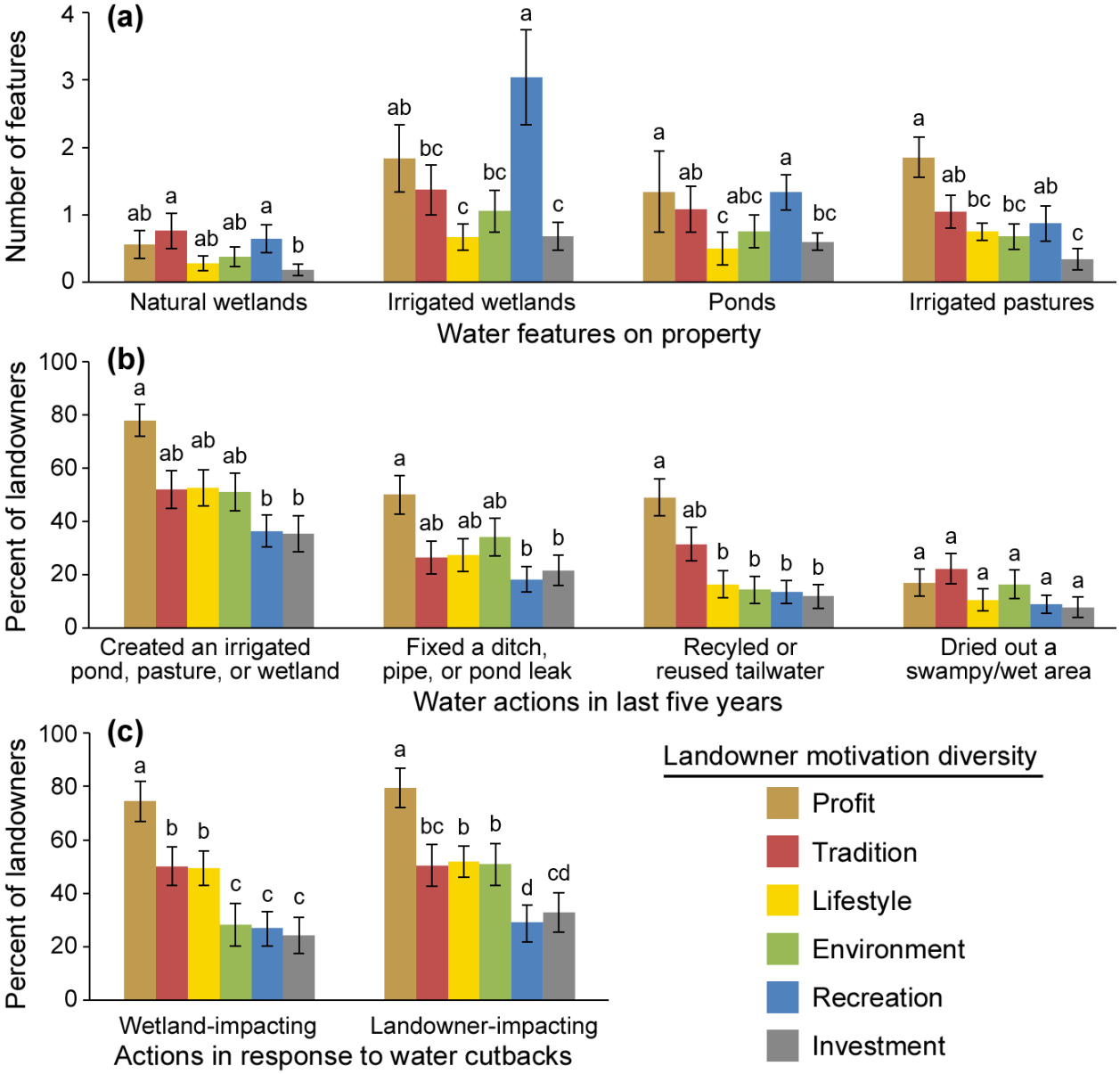

Figure 1.4. Functional (a & b) and response (c) diversity of Sierra Nevada foothills landowners based on landownership motivation typologies. Bars represent SE, and shared superscripts (*a*–*d*) represent groups without significant differences. (a) Expected number of different water-dependent features on a landowners' property (n = 351). (b) Proportion of landowners that took different water-management actions in the past five years (n = 323, 322, 327, and 333). (c) Proportion that responded to a hypothetical water cutback of 56.6% (mean value in survey) by taking adverse wetland-impacting (e.g., reducing irrigation) or landowner-impacting (e.g., reducing livestock stocking) actions (n = 274).

showed response diversity (Fig. 1.4c). Profit-motivated landowners were the most likely, and investment-motivated the least likely, to take actions that would dry wetlands (i.e., reduce irrigation; Appendix S1.1: Table S3). Profit-motivated landowners were also significantly more likely to suffer economic hardship, sell their land, or change livelihoods in response to water cutbacks (Fig. 1.4c; Appendix S1.1: Table S3). This may be because these landowners earned a higher percentage of their income from their land than other types ($F_{5,317} = 6.736, p = 5.6\times10^{-6}$).

1.4.3 Impact of hydrological diversity on rails and West Nile virus

Irrigation increased both the quantity and quality of wetland habitat for black rails. Natural-only wetlands had significantly lower rail occupancy than both-source wetlands in all years and irrigation-only wetlands during the drought (Fig. 1.5a). This effect was driven by two mechanisms. First, irrigation increased wetland size and larger wetlands were more likely to be occupied (Appendix S1.1: Table S4). Second, water source was an important predictor of occupancy even after accounting for wetland size, indicating that water source diversity increased habitat quality (Appendix S1.1: Table S5). Several very large natural-only wetlands had dramatic seasonal drying and were unoccupied by black rails during this study. By the drought's end, no black rails were detected in natural-only wetlands.

Irrigation increased WNV transmission risk by increasing the quantity, but not the quality, of wetland habitats for mosquitoes. Transmission risk increased with wetland size ($p = 0.045$, Fig. 1.5b) because mosquito abundance increased, while WNV prevalence was invariant (Appendix S1.1: Fig. S1). After controlling for wetland size, water source had no effect on transmission risk ($F_{2,59} = 0.30$, $p = 0.76$), indicating that the increased persistence of both-source wetlands did not affect WNV dynamics.

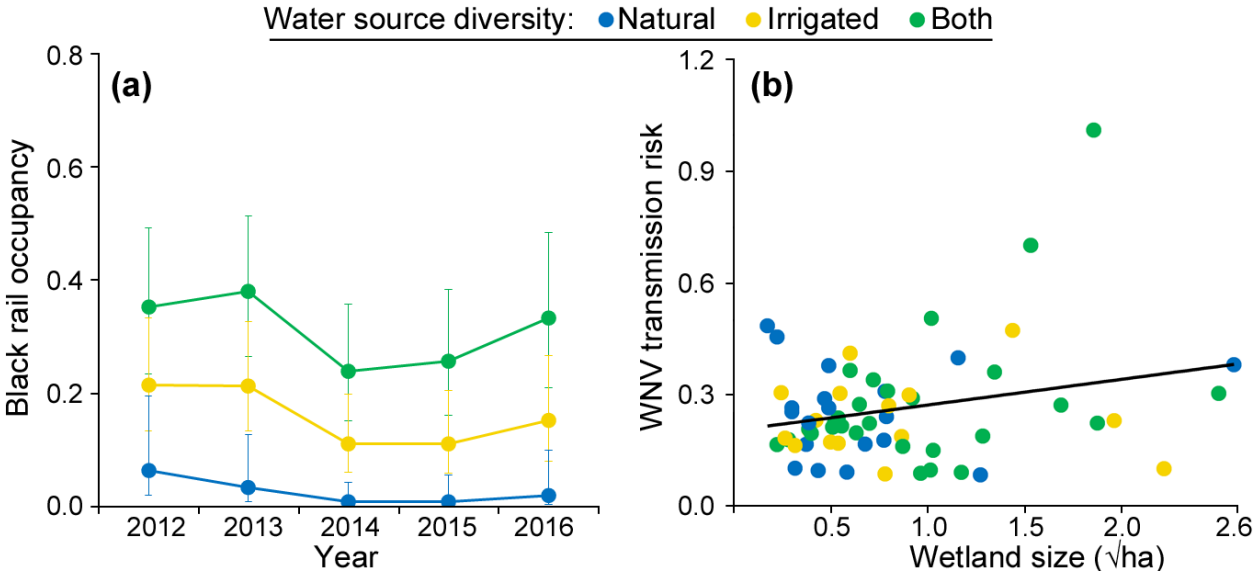

Figure 1.5. Impacts of Sierra Nevada foothills wetlands' hydrological diversity on maintenance of ecosystem function during drought. (a) Mean (± 95% CI) probability of occupancy by black rails for a median-sized wetland of each water source. (b) West Nile virus-infected *Culex* mosquito abundance increased with wetland size ($r^2 = 0.064$, $p = 0.045$).

1.5 Discussion

1.5.1 Hydrological diversity and metapopulation resilience

We found that the transformation of the Sierra Nevada foothills from a natural landscape to a CHANS has led to an apparent great increase in the abundance of wetlands (Fig. 1.2a). This increase was largely the result of accidental "waste" water, with 74% of irrigated wetlands fed by leaks, runoff, or oversaturated agriculture (Fig. 1.3a). Other studies of semi-arid irrigated agricultural areas have also found an abundance of wetlands fed by irrigation runoff (Moreno-Mateos et al. 2009, Sueltenfuss et al. 2013).

During the drought wetlands showed a diversity of drying cycles depending on their hydrological sources, illustrating response diversity (Fig. 1.3b). This pattern was not present in the non-drought year (2016), illustrating that these were different responses to this exceptional drought disturbance and not normal seasonal cycles. Natural wetlands had seasonal drying with winter-wet water cycles: they stayed wet during California's rainy Mediterranean winter but dried in the summer dry season (and other periods of low rainfall) during the drought (Fig. 1.3b). Irrigation-only wetlands had less dramatic fluctuations, but exhibited reverse-cycle seasonality: they were driest during the normally wet winter, when irrigation delivery generally ceased and ditches filled only from rain (Fig. 1.3b). Some irrigation-only wetlands also dried in the summer when irrigation ceased, possibly due to water conservation by landowners.

A diversity of water sources increased wetland resilience because sources responded differently to disturbance, exemplifying the portfolio effect. When irrigation water entered natural wetlands, it increased their resistance to drought by keeping them saturated due to differences in the timing of drying between the two water sources. Irrigation systems in California were engineered to alter the timing of water availability by storing precipitation in reservoirs to complement natural Mediterranean water cycles. The resulting reverse-cycle seasonality of irrigated wetlands mimics some historic Central Valley wetlands, which were fed by summer Sierra Nevada snowmelt. These have been disproportionately lost, creating a landscape with a higher proportion of winter-wet seasonal wetlands today than it had historically (Duffy and Kahara 2011). Thus, the transformation from a natural system to a CHANS has added human-created diversity that functionally replaced natural diversity, which had been lost or reduced. As in biological communities, adding variability to the system at one scale (individual water sources) increased system stability at a broader scale (individual wetlands; Holling 1996). While individual wetlands may re-saturate after drying (analogous to studies of resilience in community ecology showing populations of individual species fluctuating), severe drought may disturb water availability sufficiently to permanently disrupt the CHANS' ability to maintain functions at the landscape scale (e.g., by extirpating species).

We found that the black rail metapopulation would have likely been extirpated by the drought in the absence of this hydrologic diversity. No black rails were detected in natural wetlands by the end of the drought, though by two years later, in 2017, they had recolonized several spring-fed wetlands (S.R. Beissinger, unpublished data). Wetlands with diverse water sources provided the best habitat for the threatened black rail during normal and drought conditions, demonstrating increased function and resilience. Foothills irrigation development may also create disservices by expanding the amount of wetland habitat. However, the metrics we studied show irrigated wetlands offered more services (rail habitat provisioning) with fewer disservices (WNV risk) per hectare than natural wetlands.

These benefits likely extended to some other species and functions. Small agricultural wetlands support wetland-dependent and even some upland species (Moreno-Mateos et al. 2009, Palta et al. 2017). Perennial and reverse-cycle wetlands in California have increased invertebrate diversity and abundance, providing important food sources for wildlife (de Szalay et al. 2003). Reverse-cycle wetlands are now among the rarest in the Central Valley, resulting in overcrowding of breeding waterbirds that is exacerbated by water shortages and drought (Duffy and Kahara 2011). Perennial wetlands also create important habitat for migratory birds because spring drying renders wetlands unsuitable for migrating birds (Duffy and Kahara 2011). Reverse-cycle irrigated wetlands provide water quality-related ecosystem services, like their natural counterparts (O'Geen et al. 2007).

While our results highlight the value of water source diversity within wetlands, maintaining a diversity of water source combinations at the landscape scale is also advisable. At the landscape scale, summer-wet wetlands add to system resilience by increasing the diversity of wetland response and habitat types. Winter-wet, reverse-cycle, and non-seasonal wetlands each support overlapping but complementary sets of species and functions, and wetland networks should be managed to include hydrological diversity among wetlands (Duffy and Kahara 2011, Lunde and Resh 2012).

1.5.2 Maintaining a resilient landscape

Landowners steward wetlands in this region, as 93% of wetlands occurred on private land (Fig. 1.1). Landowners exhibited functional diversity, with different typologies stewarding different types of wetlands. Compared to the other typologies, tradition-motivated landowners had more natural-fed wetlands, profit-motivated landowners had more irrigation-fed wetlands, and recreation-motivated landowners had more of both types of wetlands (Fig. 1.4a). Overall, profit-motivated landowners had more irrigated water features (Fig. 1.4a) and were likelier to have created one recently (Fig. 1.4b). However, profit- and tradition-motivated landowners were likelier to fix leaks or reuse tailwater, actions that eliminate wetlands (Fig. 1.4b), possibly because they more often were ranchers or farmers. While these differences suggest functional diversity occurs in this CHANS, functional redundancy was also prevalent among landowner types. All types provided some irrigation, and many types exhibited similar water management (Fig. 1.4a, b). However, functional redundancy can maintain system function if responses to disturbance differ (Hooper et al. 2005).

Landowners showed response diversity in their responses to irrigation cutbacks during drought (Fig. 1.4c). In response to the drought, irrigation districts either ceased winter water sales during the drought's peak, or permanently stopped them, and summer water cutbacks were nearly implemented. Irrigation districts also banned runoff beyond property boundaries and dried wetlands by fixing irrigation ditch leaks. Although profit-motivated landowners had more water features (Fig. 1.4a), they were also more likely to state they would reduce irrigation should water be cut back (Fig. 1.4c). Other landowner types were likelier to maintain their water use under cutbacks, possibly because they purchased more water than they needed in order to maintain their water allocation (Huntsinger et al. 2017). Similarities among other typologies suggest that future studies could improve quantification of social diversity by grouping typologies that appeared functionally equivalent.

Under normal conditions with adequate rainfall, profit-motivated landowners irrigated more wetlands than other landowner types. Under disturbance conditions (i.e., drought and water cutbacks), however, profit-motivated landowners would reduce water to wetlands, while other landowner types would continue providing irrigation. This illustrates the value of response diversity even when one agent type performs best outside of disturbance conditions (Elmqvist et al. 2003). Thus, landowner diversity increases system function and resilience over time given oscillating environmental conditions, with some types performing better during drought and some during non-drought conditions.

The landowner diversity that maintains this diverse hydrological landscape could itself be undermined by severe water shortages. Profit-motivated landowners, whose income was more dependent on their land, were likelier to need to sell their land or change livelihoods in response to water cutbacks (Fig. 1.4c). This could potentially result in property turnover, reallocation of water, and shifting land use. The social costs of cutbacks, thus, fall disproportionately on those providing more wetland ecosystem services. This jeopardizes long-term CHANS sustainability by increasing the risk of transformation to a system with less irrigation-intensive land uses (e.g., exurban development). Disturbance that overwhelmed resilience in one part of the CHANS (social land use) may produce cascading effects in other parts (e.g., wetland function and resilience).

1.5.3 Diversity and resilience as a theory of CHANS

Some have argued that resilience in CHANS has become a metaphor without empirical validation (Olsson et al. 2006, Brown 2014). Our findings add evidence that social-ecological diversity can contribute to resilience via the same mechanisms as in community ecology (Leslie and McCabe 2013). Social and hydrological diversity in the foothills CHANS reflected functional diversity, redundancy, and response diversity, the cornerstones upon which resilience theory developed (Holling 1973). Profit-motivated landowners provided more wetland ecosystem services during normal conditions by adding more irrigation to the landscape. However, they were not as resistant to disturbance as other landowner types, which otherwise offered fewer ecosystem services and appeared redundant. Thus, social diversity increased function during both normal and disturbance conditions, creating a system of water provisioning to ecosystems that was more resilient to fluxes in water availability. Wetlands fed by diverse water sources had increased function and were more resistant to total drying during the drought, which was crucial in maintaining the regional persistence of a threatened bird that otherwise may have faced extirpation. Thus, transformation of the Sierra foothills into a hydrologically coupled human and natural system increased the resilience of the wetland network by adding social-ecological variability. Similar dynamics may occur in other regions where seepage and runoff from irrigation are key water sources for wetlands (Sueltenfuss et al. 2013, Palta et al. 2017). Studies determining whether similar mechanisms operate in other CHANS or impact other aspects of resilience (e.g., alternative stable states or cross-scale effects; Peterson et al. 1998, Liu et al. 2007) would be a promising direction for future research.

1.5.4 Sustainability implications

California is a globally important region for both agricultural production and wetland bird habitat (Duffy and Kahara 2011), and the state is under intense pressure to conserve water from the looming threat of droughts of greater frequency and intensity due to climate change

(Diffenbaugh et al. 2015, Christian-Smith et al. 2015). Irrigation districts and the state have responded to drought by encouraging water conservation and optimizing irrigation use, which may foster social system resilience if the conserved water is not subsequently allocated to other users. However, such attempts to engineer CHANS stability can lead to unintended consequences (Holling 1996, Folke 2006). Our research suggests this CHANS is vulnerable to this kind of top-down regulation, with few feedbacks to foster adaptation (e.g., incentives for landowners to preserve accidental wetlands). Most landowners valued wetland ecosystem services: 70.0% agreed that "I like wetlands because they attract wildlife." However, there is little institutional recognition of the importance of these wetlands. The California Dept. of Fish and Wildlife provides financial support to landowners for maintaining perennial water to intentional wetlands in the Central Valley (Duffy and Kahara 2011), but these programs do not extend to the "waste" water wetlands in the foothills. A complex set of physical and policy constraints leave irrigation districts few options to conserve water except by reducing the "waste" water that facilitates ecosystem resilience. Irrigation districts are incentivized to fix leaks, pipe earthen ditches, and discourage runoff because the conserved water can be sold off-district for higher prices (Huntsinger et al. 2017). Permanent irrigation infrastructure changes to conserve water will preclude recovery of some wetlands. For example, two landowner interviewees had leak-dependent wetlands with rails that were threatened or eliminated by an irrigation district fixing the leaks, despite opposition of the landowners. There is no requirement to monitor for black rails or other species before eliminating an anthropogenic wetland.

Resilience theory argues for shifting from policies intended to control and optimize exploitation of a system assumed to be stable to managing for the capacity of a system to cope with, adapt to, and shape change (Folke 2006). Allowing for "waste" water may provide this CHANS capacity to cope in the face of climate change, but will require recognizing tradeoffs between water conservation and ecosystem services within a policy framework. The definition of resilience in CHANS depends on goals and values (Brown 2014), and some policies could make either the social or natural components of a CHANS less resilient, producing distinct winners and losers (Allen et al. 2018). Water conservation policies could be balanced by including language that protects valued ecosystem services and recognizes the importance of irrigation for wetlands. Wetlands could be integrated into the water conveyance system; one4 interviewee with a leak-dependent wetland had worked with their irrigation district to do so. Finally, water cutbacks could be applied in multiple tiers, targeting low-value uses first (e.g., lawns). Deferring cutbacks for irrigators engaged in commercial agriculture, like profit-oriented landowners, would increase the resilience of social diversity in this CHANS, the ecosystem functions fostered by it, and regional food production.

Chapter 2: Direct observations of the rescue effect in two avian metapopulations show inferences from occupancy models are unreliable

2.1 Abstract

The "rescue effect" hypothesizes that less isolated patches are less likely to go extinct in metapopulations. This may be due to extinction and immediate recolonization between sampling periods (e.g., breeding seasons), or immigrants bolstering population sizes enough to prevent extinction altogether. However, these mechanisms have rarely been directly demonstrated and almost all supporting evidence is based on relationships between isolation and extinction. We directly measured the frequency of the "immediate recolonization" rescue effect for two avian metapopulations occurring in patchy wetlands by conducting patch occupancy surveys during the non-breeding season (winter) in addition to surveys during the primary breeding (summer) sampling period. We then assessed the reliability of inferences about the rescue effect derived from isolation-extinction relationships based on three different measures of isolation: the mean distance to the three nearest sites the species was detected at, and two connectivity indices (buffer radius and incidence function) that used autoregression to correct for unsurveyed sites. We compared results between two ecologically similar species with different dispersal capabilities, the dispersal-limited black rail (*Laterallus jamaicensis*) and the more vagile Virginia rail (*Rallus limicola*), which occur in the foothills of the California Sierra Nevada. The "immediate recolonization" rescue effect was operating in both metapopulations, and was more important during periods of more intense drought-induced disturbance. Inferences about the rescue effect from relationships between isolation and extinction were unreliable. Autoregressive measures performed worse than the simple distance measure of isolation and led to inaccurate conclusions. The rescue effect was underestimated more for Virginia rails; estimating the rescue effect based on inter-patch distances measures requires that patch isolation is the driving factor of colonization, but this may not be true for species whose dispersal is not distance-limited. Our results suggest lower power to detect the rescue effect during nonequilibrium periods compared to equilibrium periods, even though disturbance increased the strength of the rescue effect. We advise researchers seeking to understand if the rescue effect is operating in a metapopulation to supplement isolation-extinction relationships with sub-surveys between breeding seasons, in order to increase reliability of conclusions and better distinguish the mechanisms behind the rescue effect.

2.2 Introduction

Metapopulation theory is a dominant framework for assessing spatially structured populations, with hundreds of papers published annually on the topic (Fronhofer et al. 2012). Classical metapopulations are networks of local populations in discrete patches that are connected by dispersal, resulting in stochastic local extinctions and recolonizations that may eventually reach a dynamic equilibrium (Levins 1969, Hanski 1999). The Levins model is central to metapopulation theory, stating that large, well-connected patches are more likely to be occupied than small, isolated patches (Hanski et al. 1995, 1996). Larger patches should support larger populations and thus have lower probability of extinction (ε), while less isolated patches should receive more dispersing individuals and thus have higher probability of colonization (γ). The rescue effect hypothesizes that the additional immigrants less isolated patches receive should also lower their

extinction rates. The rescue effect is theorized to be a key mechanism by which multiple alternative stable equilibria in occupancy arise in metapopulations (Gotelli 1991, Hanski 1998, Vergara et al. 2016), and is particularly important for species with small local populations (Sutherland et al. 2012).

The rescue effect is widely assumed to operate in metapopulations (Vergara et al. 2016) but empirical observations of its occurrence are lacking (Sutherland et al. 2012, Eaton et al. 2014). The few studies that have directly tested the rescue effect have focused on colonization after experimental removal of individuals from a few patches or demographic rates within source-sink metapopulations with ≤5 patches (Henderson et al. 1985, Sinsch 1992, Carson et al. 2011, Lee and Bolger 2017). The preponderance of evidence for the rescue effect is inference from occupancy patterns that report a relationship between patch isolation and extinction probability (Bellamy et al. 1996, Hames et al. 2001, Franken and Hik 2004, Piessens et al. 2005, Ozgul et al. 2006, Ferraz et al. 2007, Schooley and Branch 2007, Foppen et al. 2008, Thornton et al. 2009, Heard et al. 2013, Eaton et al. 2014, Acevedo et al. 2015, and others). However, it is unclear whether the relationship between isolation and extinction represents rescue. Clinchy et al. (2002) called early attention to the possibility that occupancy patterns in support of metapopulation theory can be misleading because they reflect multiple ecological processes, such as spatially-correlated extinctions. Yet, studies continue to use occupancy data to infer dispersal rates and distances based on relationships between colonization and isolation metrics (Driscoll et al. 2014). While some studies have validated this approach (Dornier and Cheptou 2013, Hall et al. 2018), others found inferences were inaccurate (Poos and Jackson 2012).

While isolation-extinction relationships are well-documented (Vergara et al. 2016), the mechanism behind the rescue effect has received less attention. Metapopulation models frequently describe the rescue effect as the probability of extinction and immediate recolonization between breeding seasons or sampling periods ($\varepsilon\gamma$), following Hanski's (1994) incidence function model. Brown and Kodric-Brown (1977) originally proposed a demographic rescue mechanism based on island biogeography, where dispersers bolster population sizes sufficiently to prevent extinction altogether. Demographic rescue can be considered part of the source-sink concept (Pulliam 1988, Runge et al. 2006), since it describes the "sink" condition where a patch avoids extinction by receiving immigrants from other patches in the landscape. Brown and Kodric-Brown's definition is thus most associated with source-sink metapopulations that have larger populations and consistent occupancy (c.f., Sinsch 1992, Carson et al. 2011, Lee and Bolger 2017). Hanski's definition, because of its applicability to metapopulation occupancy models, remains primarily associated with metapopulations characterized by numerous patches that experience frequent colonization and extinction (c.f., Henderson et al. 1985, Hames et al. 2001, Sutherland et al. 2012). Studies often refer to these mechanisms interchangeably (c.f., Bellamy et al. 1996, Hanski 1999, Hames et al. 2001, MacPherson and Bright 2011, Sutherland et al. 2012) or do not describe a mechanism at all (c.f., Matthysen 1999, Ferraz et al. 2007, Eaton et al. 2014, Acevedo et al. 2015), only discussing isolation-extinction relationships. Understanding the actual mechanism by which these relationships arise is important because demographic rescue can maintain local genetic diversity, while immediate recolonization rescue does not (Stacey et al. 1997). We focus here on testing Hanski's immediate recolonization rescue effect (hereafter "the rescue effect") because our study was on the occupancy dynamics of metapopulations with small local population sizes and frequent occupancy turnover.

We directly tested for the rescue effect in metapopulations of two ecologically similar birds with different dispersal capabilities and used these results to assess the reliability of inferences from the isolation-extinction relationships. The threatened, dispersal-limited black rail (*Laterallus jamaicensis*) and the widespread, more vagile Virginia rail (*Rallus limicola*) are both permanent residents of a network of hundreds of small wetlands (mean 0.34 ha) in the foothills of the California Sierra Nevada (Richmond et al. 2010a, Risk et al. 2011). Occupancy surveys have been conducted annually during the breeding season for these metapopulations for over a decade, providing long-term data. Preliminary analyses of isolation-extinction relationships from 2002–2006 (Appendix S2.1), a time period with both metapopulations in dynamic equilibrium (Chapter 3), suggested the rescue effect was strong in black rails but was not supported for Virginia rails (Fig. 2.1, Appendix S2.1: Table S1). Thus, we predicted we would find evidence of the rescue effect for black rails but not for Virginia rails.

We tested for the rescue effect (extinction followed by recolonization between breeding seasons) by conducting additional occupancy surveys for both rails during the winter non-breeding seasons from 2013–2016. The arrival of West Nile virus and severe drought caused a decline in occupancy and non-equilibrium dynamics during this time period (Chapter 3). We

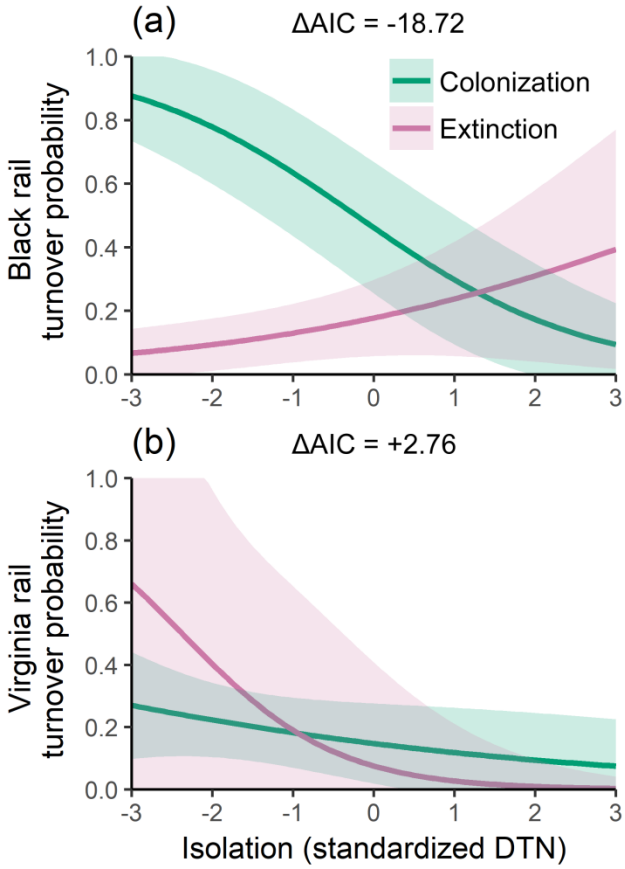

Figure 2.1. Preliminary analysis showing significant isolation effects on dispersal and rescue effects for metapopulations of black rails (a), but not Virginia rails (b), in the foothills of California's Sierra Nevada during a period of equilibrium (2002–2006; n = 205 & 204). Graphs show predicted values for an average wetland with different values of standardized isolation (the geometric mean distance to nearest 3 occupied sites ($\log_{10}$ (km + 1))). The shown relationships were only supported in AIC model selection for black rails.

compared the frequency of rescue expected from occupancy models against the actual occurrence. Lastly, we assessed the reliability of inferences about the rescue effect from isolation-extinction relationships in occupancy models using data from 2013–2016, comparing three different measures of isolation. Eaton et al. (2014) suggested the use of autoregressive models to correct for biases due to imperfect detection and unsurveyed sites, so we compared one simple measure (the distance to the three nearest sites with detections) to two more complex autoregressive measures (buffer radius and incidence function). Genetic analysis had validated the accuracy of the dispersal kernels represented by the autoregressive measures for black rails (Hall et al. 2018), but suggested the vagile Virginia rail was not dispersal-limited (Hall 2015).

2.3 Methods

2.3.1 Data collection

The study area was the zone III Sierra Nevada Foothills ecoregion (US Environmental Protection Agency 2013) in Nevada, Yuba, and southern Butte counties, plus a 1 km buffer to better quantify isolation of sites near the study area boundary (Fig. 2.2). Open oak savannah and seasonal grasslands dominated below 500 m elevation, and oak woodland and mixed deciduous-conifer forest at higher elevations. Land uses were chiefly a mix of ranches, exurban development, protected areas, and rice farms at the lowest elevations. Patchy natural and irrigation-created wetlands are found throughout this landscape from pooling irrigation runoff or leaks, along the fringes of ponds and creeks, and in large waterfowl hunting impoundments near rice farms. There was a historically severe drought from 2012–2015, overlapping with the main period of this study.

We surveyed 273 wetlands annually for black and Virginia rail occupancy from 2002–2016 during the breeding season (late May to early August). Wetlands were surveyed with call broadcast methods as described in (Richmond et al. 2008, 2010b), with up to 3 visits each summer (5 in 2002) to use in occupancy models that correct for detection probability (MacKenzie et al. 2003). Previous studies found no evidence of competition between black and Virginia rails (Richmond et al. 2010b), so we analyzed each species separately following Risk et al. (2011). To determine the actual frequency of the rescue effect that occurred, we resurveyed a subset of 125 wetlands during the non-breeding season (January 8th–29th) of 2014–2016 using the same methodology.

2.3.2 Occupancy modeling

We analyzed survey data using multi-season occupancy models in Program PRESENCE v12.19 (Hines 2013), which use detection histories from visits within years to estimate joint probabilities of detection (p), occupancy in the first year (Ψ), and colonization (γ) and extinction (ε) in subsequent years (MacKenzie et al. 2003). These probabilities can be specific to site i and year t by incorporating covariates with logit functions. The probability of occupancy after the first year can be estimated for each year as a derived parameter:

$$\psi_{i,t} = \psi_{i,t-1}(1 - \varepsilon_{i,t}) + (1 - \psi_{i,t-1})\gamma_{i,t} \quad (2.1)$$

Following other studies (c.f., Ferraz et al. 2007, Thornton et al. 2009, Heard et al. 2013, Eaton et al. 2014), we tested for evidence of the rescue effect from metapopulation dynamics by testing if isolation increased ε and decreased γ (i.e., a dispersal kernel) via Akaike information

criterion (AIC) model selection (Burnham and Anderson 2003).We tested three different measures of isolation with varying complexity. The simplest measure was the geometric mean distance to the nearest three occupied sites in the previous year (hereafter "DTN"), which we calculated using observations of occupancy uncorrected for detection probability.

We also used two autoregressive connectivity measures that took into account the area of source patches (a proxy for number of dispersers, following Moilanen and Nieminen 2002) and accounted for two sources of uncertainty, (1) the probability that surveyed sites where the

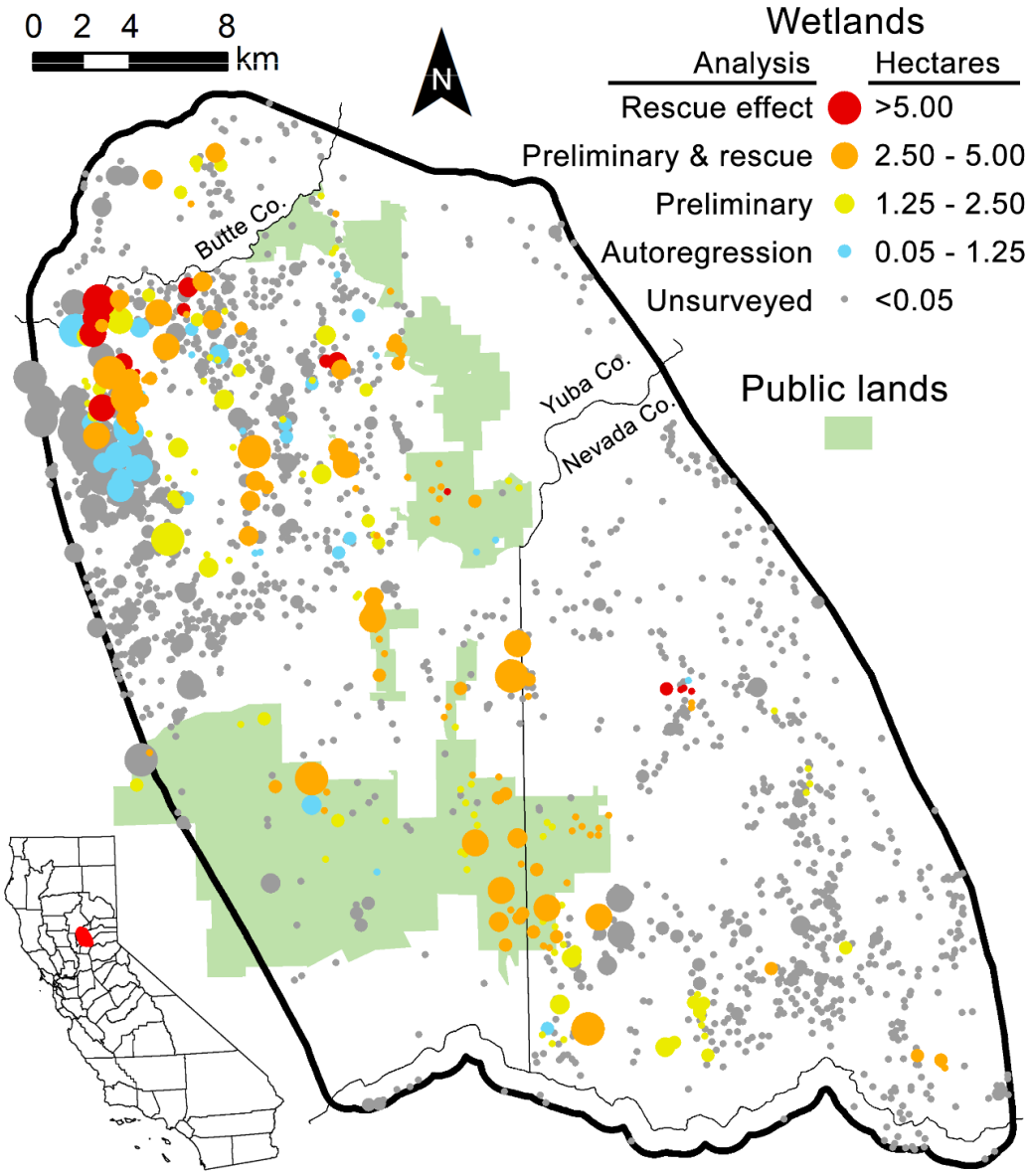

Figure 2.2. Sampling of wetlands within the Sierra Nevada foothills study area (inset: study area location relative to California). Color indicates the analysis their surveys were included in. Preliminary surveys were from 2002–2006, a period of equilibrium metapopulation dynamics; rescue effect surveys were from 2013–2016, a nonequilibrium period. Autoregressive isolation measures were calculated based on all wetlands ever surveyed (blue plus other colors) and incorporated estimated occupancy at unsurveyed wetlands.

species was not detected were actually occupied, and (2) the probability that unsurveyed sites were occupied. Both measures were estimated using the autoregressive model of Hall et al. (2018). This model utilized the full detection history of a site to estimate $\psi^c_{i,t}$, the probability that a site was occupied conditional on its detection history. It assumed no false positive detections, so for sites where a species was detected $\psi^c_{i,t} = 1$. For unsurveyed sites (all wetlands in this region were mapped in 2013; Chapter 1), $\psi^c_{i,t}$ was equal to occupancy as defined in Equation 1. The first autoregressive measure was a buffer radius measure ("BRM"). It summed the area of each potential colonist source patch *s* within a radius multiplied by its conditional occupancy probability:

$$BRM_{i,t} = \sum_{s \neq i} \psi^c_{s,t-1} A_s B_s \textbf{ where } B = 1 \textbf{ if } d_{i,s} \leq r \textbf{ and } B = 0 \textbf{ elsewise} \quad (2.2)$$

where A_s is the area of the colonist source patch, $d_{i,s}$ is the distance between the focal patch centroid and colonist source patch centroid, and r is a user-specified constant buffer radius. The second autoregressive measure was the incidence function measure ("IFM"). It summed the area of all patches on the landscape, multiplied by their conditional occupancy probability and a function representing the likelihood of successful dispersal decaying continuously over distance:

$$IFM_{i,t} = \sum_{s \neq i} \psi^c_{s,t-1} A_s e^{-\propto d_{i,s}} \quad (2.3)$$

where $1/\propto$ is the mean dispersal distance assuming a negative exponential kernel (Moilanen and Nieminen 2002).

All distances were in km and measures were transformed $\log_{10}$(measure + 1). While DTN was a single continuous measure, the BRM and IFM measures were calculated and fit for radius (r) and mean dispersal distance ($1/\propto$) values of 1–10, 15, 20, 25, and 30 km, with the largest distances approximating unlimited dispersal across the study area. For black rails, the BRM-7 km and IFM-4 km fit best and were validated with genetic data (Hall et al. 2018). For Virginia rails we carried out an equivalent analysis, which found that BRM-20 km and IFM-10 km best fit the data (Appendix S2.2). Differences in scale between isolation metrics is expected, because the IFM models the mean dispersal distance while the BRM models the domain over which the majority of dispersal occurs (Hall et al. 2018).

For each species, we used AIC model selection to assess whether there was evidence for rescue effects for each isolation measure competing in a single model set. We fit models with data from 2013–2016 for the 125 wetlands that were also surveyed during the same period in the winter non-breeding season to ensure both methods of measuring the rescue effect used the same set of sites. In all occupancy models assessed, we included covariates that were found to be important predictors of rail metapopulation dynamics in this region (see Appendix S3.1): patch area ($\log_{10}$ (ha +1)), elevation (m), slope (a categorical variable indicating whether the wetland lacked a central water body), categorical variables indicating whether the wetland's water source was irrigation-only (the reference category), natural-only, or both-source, and precipitation (mean monthly over the November–May rainy season). All continuous variables were standardized. Because models in Appendix S3.1 were fit to survey data from all years, some variables were omitted to ensure convergence over the smaller time window of this study. For black rails, the base (i.e., no isolation measures) model was:

$$\Psi_i \sim \text{Area} + \text{Slope} + \text{Both-source} + \text{Natural-only} \quad (2.4)$$

$$\gamma_{i,t} \sim \text{Area} + \text{Slope} + \text{Both-source} + \text{Precipitation} \quad (2.5)$$

$$\varepsilon_{i,t} \sim \text{Area} + \text{Slope} + \text{Both-source} + \text{Precipitation} \quad (2.6)$$

For Virginia rails the base model was:

$$\Psi_i \sim \text{Area} \quad (2.7)$$

$$\gamma_{i,t} \sim \text{Area} + \text{Precipitation} \quad (2.8)$$

$$\varepsilon_{i,t} \sim \text{Area} + \text{Both-source} + \text{Natural-only} + \text{Elevation} + \text{Precipitation} \quad (2.9)$$

Year-specific detection probabilities were included for both species to account for differences in surveyors, and "no playback" was included as a categorical variable in Virginia rail models for visits in 2004–2005 when only black rail calls were played. We then ran a model set for each species that included the DTN, IFM, and BRM on γ only, ε only, or both. To allow for direct comparison of these results with the preliminary analysis that drove our study (Fig. 2.1), we also ran model sets for DTN, BRM, and IFM models for 2002–2006 data (Appendix S2.1). The "DTN γ, ε" models for each period for black and Virginia rails are in Appendix S2.1: Tables S2–S3. We graphed the estimated rescue effect for an average site within our full sample (median area = 0.47 ha, median elevation = 123 m, slope geomorphology, both water sources). For comparison with DTN's measure of isolation, the BRM and IFM measures of connectivity were multiplied by -1 when graphed.

2.3.3 Determining the frequency of the rescue effect

We determined the frequency of the rescue effect using summer-winter-summer occupancy trends from 2013–2016. For example, a "1-0-1" history of detecting rails across summer-winter-summer surveys at a site would indicate the rescue effect (extinction and recolonization between breeding seasons), while a "0-0-1" history would indicate a spring colonization. This method of estimating the frequency of the rescue effect makes several assumptions. First, it assumes that no additional rescues occur between the two breeding and non-breeding sampling periods (e.g., a 1-1-1 history assumes no extinctions and recolonizations in the time between each 1-1 pair). This assumption will be violated to some degree in all real metapopulations, and if severe violations are suspected additional sub-sampling could obtain more precise estimates. Second, it requires that the species is generally resident in patches and does not move seasonally between separate breeding and non-breeding habitats.

We used naïve estimates of occupancy based on naïve estimates of occupancy that were not corrected for detection probability with occupancy models, in order to avoid comparing one set of modeled results to another modeled result. To determine if ignoring imperfect detection would be problematic, we used occupancy models to estimate site-level detection rates (p*) in each sampling period. We fit the base model for each species to the full winter-summer dataset, substituting season-specific intercepts for annual rainy season precipitation. Site-level detection probabilities ranged 0.90–0.97 in summer and 0.96–1.00 in winter (Appendix S2.1: Table S4), indicating that ignoring imperfect detection would not seriously bias results.

We calculated the expected frequency of the rescue effect as predicted by theory (Hanski 1999) for each year as the mean value of $\varepsilon_{i,t}\gamma_{i,t}$ across sites (from a model without isolation effects to minimize "double-counting" the rescue effect), for the same set of sites visited in the direct measurement for each year. This method may slightly underestimate the expected frequency of the rescue effect because estimates of $\varepsilon_{i,t}$ naturally incorporate any rescue effect,

Table 2.1. Full-season dynamics of black rail and Virginia rail metapopulations occupying wetlands in the foothills of the California Sierra Nevada. Estimated probabilities (standard errors in italics) represent the likelihood of a wetland that started that year occupied or unoccupied undergoing that transition history (equivalent to γ/ε). "SWS" indicates the naïve occupancy estimates for summer-winter-summer for that pair of years. Expected probabilities are from a summer-only occupancy model without isolation effects.

Initial occupancy	**Transition history (SWS)**	**Black rail**			**Virginia rail**		
		2014	**2015**	**2016**	**2014**	**2015**	**2016**
Expected ($\varepsilon_{i,t}\gamma_{i,t}$)	Rescue effect (101)	0.023	0.015	0.007	0.098	0.089	0.081
Occupied	Rescue effect (101)	0.212 *(0.071)*	0.057 *(0.039)*	0.105 *(0.050)*	0.219 *(0.073)*	0.045 *(0.031)*	0.043 *(0.030)*
	Remains occupied (111)	0.485 *(0.087)*	0.743 *(0.074)*	0.789 *(0.066)*	0.406 *(0.087)*	0.659 *(0.071)*	0.739 *(0.065)*
	Fall extinction (100)	0.182 *(0.067)*	0.143 *(0.059)*	0.053 *(0.036)*	0.188 *(0.069)*	0.091 *(0.043)*	0.065 *(0.036)*
	Spring extinct-ion (110)	0.121 *(0.057)*	0.057 *(0.039)*	0.053 *(0.036)*	0.188 *(0.069)*	0.205 *(0.061)*	0.152 *(0.053)*
Unoccupied	Winter-only habitat (010)	0.038 *(0.026)*	0.054 *(0.026)*	0.053 *(0.026)*	0.167 *(0.051)*	0.138 *(0.043)*	0.136 *(0.042)*
	Remains un-occupied (000)	0.906 *(0.040)*	0.851 *(0.041)*	0.803 *(0.046)*	0.667 *(0.064)*	0.662 *(0.059)*	0.636 *(0.059)*
	Fall colon-ization (011)	0.000 *(0.000)*	0.000 *0.000)*	0.066 *(0.028)*	0.056 *(0.031)*	0.169 *(0.047)*	0.121 *(0.040)*
	Spring colon-ization (001)	0.057 *(0.032)*	0.095 *(0.034)*	0.079 *(0.031)*	0.111 *(0.043)*	0.031 *(0.021)*	0.106 *(0.038)*

which decreases $\varepsilon_{i,t}$ and therefore $\varepsilon_{i,t}\gamma_{i,t}$; however, it is a useful approximation with that constraint in mind. We compared these expected values to the observed frequencies to determine whether the rescue effect was occurring at rates expected by theory.

2.4 Results

2.4.1 Frequency of the rescue effect

The rescue effect occurred for both black rails and Virginia rails (Table 2.1). Contrary to predictions, rescue effects were of comparable magnitudes for both species: the mean probability of rescue effect for an occupied site over all three years was 0.123 ± 0.032 for black rails and 0.090 ± 0.027 for Virginia rails (mean ± SE). Of patches that appeared to be continuously occupied from one breeding season to the next, 6–35% actually represented the rescue effect. In 2015 and 2016, occurrence of the rescue effect for black rails and Virginia rails was slightly above and slightly below expected values, respectively. In 2014, occurrence of the rescue effect was notably higher than expected for both species (Table 2.1).

Table 2.2. AIC model selection table for isolation effects on colonization and extinction rates of two rail species occupying wetlands in the foothills of California's Sierra Nevada, 2013–2016 (n = 125). Base model included area, slope, water source, rainy season precipitation, and elevation (Virginia rail only) as covariates. DTN = distance to nearest 3 sites with detections; BRM = autoregressive buffer radius measure; IFM = autoregressive incidence function measure.

Black rail					**Virginia rail**				
Model	**ΔAIC**	**AIC**	***w***	***K***	**Model**	**ΔAIC**	**AIC**	***w***	***K***
DTN γ	0.00	769.59	0.453	20	IFM γ*, ε*	0.00	963.19	0.523	17
DTN γ, ε	0.21	769.8	0.408	21	IFM ε*	2.19	965.38	0.175	16
DTN ε	5.06	774.65	0.036	20	BRM γ*, ε*	2.98	966.17	0.118	17
Base	5.55	775.14	0.028	19	BRM ε*	4.13	967.32	0.066	16
BRM ε	6.27	775.86	0.020	20	IFM γ*	4.73	967.92	0.049	16
IFM ε	6.76	776.35	0.015	20	BRM γ*	5.75	968.94	0.030	16
IFM γ	6.97	776.56	0.014	20	Base	7.29	970.48	0.014	15
BRM γ	7.33	776.92	0.012	20	DTN ε	7.52	970.71	0.012	16
BRM γ, ε	8.16	777.75	0.008	21	DTN γ*	8.73	971.92	0.007	16
IFM γ, ε	8.34	777.93	0.007	21	DTN γ*, ε	8.88	972.07	0.006	17
Null	79.87	849.46	0.000	4	Null	123.29	1086.48	0.000	4

* Anti-rescue or anti-colonization effect (opposite direction predicted by theory)

Our non-breeding surveys also provided information on the wintering habitat use of each species and the annual timing of extinction and colonization (Table 2.1). The proportion of sites occupied only in the winter was consistent across years for both species, and generally slightly lower than the proportion of sites experiencing the rescue effect for black rails (mean ± SE rate across years of 0.049 ± 0.015 winter-only versus 0.123 ± 0.032 rescue effect), but higher for Virginia rails (0.146 ± 0.028 versus 0.090 ± 0.027) except for in 2014. For black rails, extinction was slightly more common in the fall (0.123 ± in fall versus 0.076 ± 0.026 in spring) and colonization notably less common (0.025 ± 0.011 versus 0.079 ± 0.019) and not observed at all in two of the three falls. For Virginia rails, extinction was less common in the fall (0.107 ± 0.029 versus 0.180 ± 0.038) while colonization occurred at roughly equal rates during both seasons (0.119 ± 0.025 versus 0.081 ± 0.021).

2.4.2 Inferences from occupancy modeling

In contrast to preliminary analysis (Appendix S2.1), AIC model selection for the 2013–2016 model set showed only weak support for the rescue effect for both species (Table 2.2). For black rails, DTN was modestly supported in model selection (-0.49 ΔAIC compared to model without isolation). BRM and IFM effects on colonization were not supported despite these measures being validated as accurate by genetic dispersal estimates (Hall et al. 2018). Black rails showed extinction probability increasing with isolation (i.e., the rescue effect) for all three measures, but with high uncertainty (Fig. 2.3a–c). In 2014 and 2015, higher extinction rates due to low

precipitation (Appendix S2.1: Table S2) during the 2012–2015 drought meant that an average wetland was predicted to be almost entirely dependent on the rescue effect to avoid extinction (Appendix S2.1: Fig. S2a–f). For Virginia rails the rescue effect was mostly unsupported, with anti-rescue effects (isolation decreasing the extinction rate; Clinchy et al. 2002) having much greater cumulative AIC weight than rescue effects (0.882 versus 0.018; Table 2.2). DTN was the only measure that predicted rescue effects (Fig. 2.3d). There was approximately equal support for inclusion and exclusion of the DTN rescue effect, with its inclusion resulting in slightly worse AIC (0.23 ΔAIC; Table 2.2). In contrast to our empirical measurement of the rescue effect for Virginia rails, IFM and BRM showed well-supported anti-rescue and anti-colonization effects: isolated sites were less likely to go extinct and more likely to be colonized (Fig. 2.3e–f). Effects were similar during 2014 and 2015 (Appendix S2.2: Fig. S2g–l) for Virginia rails due to weaker precipitation effects on extinction and colonization rates (Appendix S2.1: Table S3).

2.5 Discussion

2.5.1 The rescue effect and environmental stochasticity

Our results demonstrate that the "immediate recolonization" rescue effect occurred in a rail metapopulation at rates similar to those predicted by theory (Hanski 1994) in most years. The rescue effect occurred for 5.7% of occupied sites in 2015 and 10.5% in 2016 for black rails, and 4.5% and 4.3% for Virginia rails (Table 2.1), reasonably close to expected values across years of

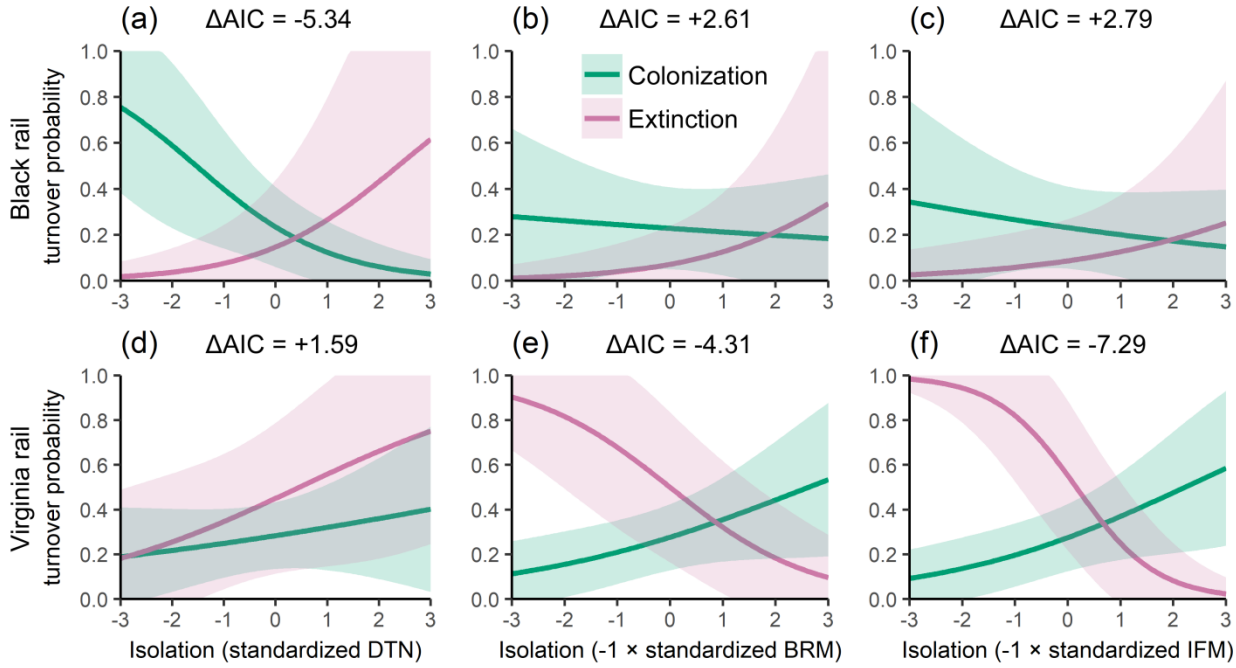

Figure 2.3. An average wetland's predicted isolation effects on metapopulation dynamics of (a–c) black rails and (d–f) Virginia rails in the foothills of California's Sierra Nevada during a period of nonequilibrium metapopulation dynamics from 2013–2016 (n = 125; 2016 values shown). DTN = distance to nearest 3 sites with detections; BRM = autoregressive buffer radius measure; IFM = autoregressive incidence function measure. ΔAIC values show the amount of support for including both graphed relationships compared to a model without isolation effects (negative values indicate improvement).

1.5% and 8.8% for each species respectively. However, 2014 was a notable exception, when the rescue effect occurred at a much higher proportion of sites, 21.2% and 21.9% for black and Virginia rails respectively. Precipitation is a strong driver of metapopulation dynamics in this system (Appendix S2.1: Tables S2–S3), and 2014 featured an exceptionally dry autumn, with only 90 mm of rainfall prior to our January surveys, compared to 318 mm in 2015, and 203 mm in 2016 (California Dept. of Water Resources 2018). Years of lower autumn rainfall were strongly correlated with frequency of the rescue effect for both black rails (R^2 = 0.95) and Virginia rails (R^2 = 0.75), which may explain the moderately higher than expected frequency of rescue for black rails in 2016 as well. The highest rates of fall extinction during the study occurred in 2014 (Table 2.1) and created a pulse of recolonizations the following spring compared to other winters. An alternative explanation is that individuals abandoned drying patches in autumn and then returned to them later in the spring when rains had begun. However, this seems less likely given that there was not a corresponding increase in winter-only habitat use observed in 2014 (Table 2.1). Thus, the importance of the rescue effect to metapopulation dynamics may vary greatly across years due to environmental stochasticity, potentially increasing its frequency well above what would be expected by theory.

2.5.2 Unreliability of isolation-extinction relationships

We found that inferences about the rescue effect based on the relationship between isolation and extinction were unreliable. Positive isolation-extinction relationships were only modestly supported for black rails, while they were generally unsupported for Virginia rails (Table 2.2). However, direct measurement showed that the rescue effect was occurring at comparable rates for both species (Table 2.1). Because connectivity acts as a positive feedback on metapopulation occupancy, inaccurate inferences about isolation can have serious consequences. Poos and Jackson (2011) found metapopulation viability models using dispersal estimates fit from occupancy patterns underestimated metapopulation extinction risk by several orders of magnitude compared to those that used direct measurements of dispersal. We found inferences were more unreliable and less powerful (1) when measures incorporated patch area and autoregressive estimates of occupancy probability, (2) for species that were not dispersal-limited, and (3) when fit to periods of decline and nonequilibrium metapopulation dynamics.

Relying on isolation-extinction relationships to demonstrate the rescue effect requires isolation to be the driving factor behind patch colonization. Our isolation metrics did not predict colonization for Virginia rails well (Table 2.2). Because Virginia rails are not dispersal-limited (Risk et al. 2011, Hall 2015), distance-based isolation metrics were unable to reliably model the presence of the rescue effect. While metapopulation theory was formulated for classical metapopulations with distinct local breeding populations, its utility for modeling threatened species living in fragmented habitats has resulted in broad application to a continuum of situations including spatially structured "patchy populations" with inter-patch movement and without distinct local breeding populations (Hanski 1998, Olivier et al. 2009). Classical metapopulations may be rare in nature (Fronhofer et al. 2012), and many apparent metapopulations may more closely approximate the dispersal-unlimited Virginia rail. Occupancy models applied to entire communities frequently draw conclusions about the rescue effect across multiple species (c.f., Ferraz et al. 2007). Our results suggest that the continuum of dispersal abilities and the resulting degree of metapopulation structuring complicates cross-species comparisons of occupancy inferences, which should be interpreted with caution.

Contrary to predictions (Moilanen and Nieminen 2002, Eaton et al. 2014), complex measures incorporating patch area and autoregressive predictions of occupancy at patches where the species was not detected performed worse than a simple measure, the geometric mean distance to the nearest three patches where the species was detected. For black rails, IFM and BRM predicted isolation effects in line with theory (Fig. 2.3b–c) but had low support (Table 2.2), despite genetic validation of these measures (Hall et al. 2018). For Virginia rails, the BRM and IFM failed completely, predicting that isolated sites were less likely to go extinct (Fig. 2.3e–f). However our direct measurement of the rescue effect (Table 2.1)—and the fact that DTN models estimated rescue effects in line with theory (Fig. 2.3d)—suggests that these were not actual anti-rescue effects but a problem with the autoregressive measures. The autoregressive BRM and IFM modeled the area of nearby habitats multiplied by their predicted occupancy, so these measures represent not only actual dispersers received by a patch but also the amount of highly suitable habitat nearby. Because the Virginia rail was not dispersal-limited, autoregressive measures of isolation may, instead of modeling a lack of dispersers, have modeled a lack of other nearby suitable patches for individuals to disperse into, leading to decreased ε and increased γ within isolated patches (Hale et al. 2015). Our results suggest that autoregressive measures of isolation should be used with caution, and their effectiveness is in need of further study.

The rescue effects we estimated for black rails from occupancy models fit to 2013–2016, a nonequilibrium period of declining occupancy, were markedly less well-supported than those in preliminary models fit to data from 2002–2006, an equilibrium period with higher occupancy (Appendix S2.1). For Virginia rails, no models with isolation had good support (all <2 ΔAIC compared to the base model without isolation; Appendix S2.1: Table S1) but estimated parameters were uncertain in preliminary models due to low detectability in the first years of the study (Appendix S2.1: Table S3). However, AIC model selection consistently supported the rescue effect for black rails for all three measures during equilibrium, with DTN still the best-supported metric (Appendix S2.1: Table S1, Fig. S1a–c). Recurrent droughts from 2007–2009 and 2012–2015, and the arrival of West Nile virus, caused declines in the black rail metapopulation and a shift to nonequilibrium dynamics characterized by periodic spikes in extinction and drops in colonization (Appendix S3.3: Fig. S5). This transition appeared to reduce the strength of the rescue effect in model selection (Table 2.2 compared to Appendix S2.1: Table S1), though this study confirmed that the rescue effect was still operating. This loss of statistical power may be because the increased annual stochasticity in colonization and extinction due to drought and generally lower rates of colonization (Appendix S2.1: Table S2) left occupancy models unable to determine the influence of the rescue effect. In contrast to the estimated reduction in the rescue effect during this period of drought, direct measurement of the rescue effect found that it was strongest during the year of greatest drought disturbance, 2014. This worryingly suggests that the power of occupancy models to detect the rescue effect may be lower when the rescue effect's importance for maintaining occupancy is actually higher.

2.5.3 Applications and future directions

We were able to confirm that the "immediate recolonization" rescue effect of Hanski (1994) occurred by using supplementary occupancy surveys during the non-breeding season. This method allowed empirical estimation of this rescue effect from easy to gather detection-nondetection data, without relying on inferences from isolation-extinction relationships. However, it does not produce unbiased estimates of the true frequency of the rescue effect. It

assumes additional rescue effects do not occur in-between breeding and non-breeding sampling periods (e.g., within each fall or spring), which is likely violated to some degree in real metapopulations. Unbiased estimates would require near-constant monitoring. Despite these biases, additional surveys conducted between breeding seasons can still provide information on the immediate recolonization rescue effect that is more reliable than inferences from breeding season occupancy data alone. It can act as a relative index for the frequency of the rescue effects between comparable species, as illustrated here (Table 2.2). Furthermore, it can help distinguish the mechanisms behind observed isolation-extinction relationships, which is important for conservation because between demographic rescue maintains local genetic diversity while immediate recolonization rescue does not (Stacey et al. 1997). Isolation-extinction relationships are frequently assumed to be the result of demographic rescue (c.f., Hames et al. 2001, Piessens et al. 2005, Foppen et al. 2008), but we found that immediate recolonization rescue occurred at (or in excess of) theoretically expected overall rates and could explain the isolation-extinction relationships observed in black rails without assuming dispersers prevented declining populations from local extinction. While a rigorous determination of the importance of each mechanism for the rescue effect requires tracking individual dispersal events and local population dynamics, this is impractical at the scale of metapopulations (Driscoll et al. 2014). Given the paucity of attempts to directly measure the rescue effect, we suggest that future studies use these methods and continue to develop new ones, to more rigorously interrogate this important but understudied aspect of metapopulation dynamics.

Chapter 3: Integrating social and ecological data to model metapopulation dynamics in coupled human and natural systems

3.1 Abstract

Understanding how metapopulations persist in dynamic working landscapes requires assessing the behaviors of key actors that change patches as well as intrinsic factors driving turnover. Coupled human and natural systems (CHANS) research uses a multidisciplinary approach to identify the key actors, processes, and feedbacks that drive metapopulation and landscape dynamics. We describe a framework for modeling metapopulations in CHANS that integrates ecological and social data by coupling stochastic patch occupancy models of metapopulation dynamics with agent-based models of land-use change. We then apply this framework to metapopulations of the threatened black rail (*Laterallus jamaicensis*) and widespread Virginia rail (*Rallus limicola*) that inhabit patchy, irrigation-fed wetlands in the rangelands of the California Sierra Nevada foothills. We collected data from five diverse sources (rail occupancy surveys, land-use change mapping, a survey of landowner decision-making, climate and reservoir databases, and mosquito trapping and West Nile virus testing) and integrated them into an agent-based stochastic patch occupancy model. We used the model to: (1) quantify the drivers of metapopulation dynamics, and the potential interactions and feedbacks among them; (2) test predictions of the behavior of metapopulations in dynamic working landscapes, and (3) evaluate the impact of three policy options on metapopulation persistence (irrigation district water cutbacks during drought, incentives for landowners to create wetlands, and incentives for landowners to protect wetlands). Complex metapopulation dynamics emerged when landscapes functioned as CHANS, highlighting the importance of integrating human activities and other ecological processes into metapopulation models. Rail metapopulations were strongly top-down regulated by precipitation, and the black rail's decade-long decline was caused by the combination of West Nile virus and drought. Theoretical predictions of the two metapopulations' responses to dynamic landscapes and incentive programs were complicated by heterogeneity in patch quality and CHANS couplings, respectively. Irrigation cutbacks during drought posed a serious extinction risk that neither incentive policy effectively ameliorated.

3.2 Introduction

Ecologists have increasingly focused on conserving species in "working landscapes" where agriculture, forestry, and other forms of resource extraction co-occur with habitat conservation (Franklin and Lindenmayer 2009, Kareiva and Marvier 2012). Working landscapes are frequently characterized by fragmented remnant habitat patches within a matrix of land uses providing less suitable habitat (Gimona and Polhill 2011). Species occupying these patchy landscapes are often structured as a metapopulation (Levins 1969, Hanski 1999). Habitat patches in working landscapes are dynamic due to human-caused changes in land use. Theory suggests that if the rate of patch change exceeds colonization, occupancy will decline, possibly resulting in metapopulation extinction (Anderson et al. 2009). Land-use change can also interact with other aspects of global change, such as climate change and emerging diseases (Wolfe et al. 2005, Brook et al. 2008, Hof et al. 2011, Altizer et al. 2013). Thus, understanding the dynamics of metapopulations in working landscapes requires integrating metapopulation ecology with both

biophysical and social sciences to assess the behaviors of key actors that drive change in landscape structure in these coupled human and natural systems (CHANS).

CHANS research uses an interdisciplinary approach to identify and analyze the key system components and the processes linking them across scales (e.g., landowners and regulating agencies), which presents a number of modeling challenges. By its nature, this research generally requires the integration of longitudinal data collected with a diversity of methodological tools from different disciplines (Liu et al. 2015). These data may differ greatly in spatiotemporal scales, resolution, structure, and processes, impeding their combination into a joint likelihood. CHANS tend to be idiosyncratic and context-specific, requiring data integration methods that are flexible enough to be readily adapted to novel data formats and systems. Integrating these data is a serious challenge that has been identified as one of the most pressing questions in CHANS research (Kramer et al. 2017). CHANS frequently have feedback loops, spatiotemporal heterogeneity, and thresholds in system state, which can result in emergent nonlinear dynamics that traditional statistical models fail to predict (Alberti et al. 2011, Liu et al. 2015). This complexity, coupled with the fact that metapopulations occur at a landscape scale that typically impedes experimentation, makes simulation modeling an especially useful tool for understanding land-use change and metapopulation dynamics as a coupled system (Ims 2005).

Here we present a general framework for integrating social and ecological data to model metapopulations in CHANS by combining agent-based models (ABMs; also called multi-agent or individual-based models) with stochastic patch occupancy models (SPOMs), an easily parameterized and commonly used metapopulation simulation tool. We then apply this approach to determine the main drivers of the metapopulation dynamics of two closely related, secretive marsh birds in the wetlands of a working landscape—irrigated rangelands in the foothills of the California Sierra Nevada—and evaluate how various policy options affect the metapopulations.

3.3 A framework for integrating data to model metapopulations as CHANS

ABMs are a particularly promising tool for analyzing CHANS because they can simulate the behavior of one or more classes of individual agents (e.g., landowners, institutions, wildlife, and habitat patches) to examine the collective patterns and complex dynamics that result (Liu et al. 2015). ABMs emerged from computer science and employed abstract simulations to develop theory, but have become commonly used in CHANS research to link individual or household behaviors to landscape-scale effects (e.g., land-use change; An 2012). ABM software (such as NetLogo; Wilensky 2018) stores sets of dynamic variables for each agent and structures them spatially in a simulated environment, which for CHANS is generally a map constructed from GIS layers. Submodels—individual processes performed by an ABM agent that are usually algorithms (e.g., regression equations)—are programmed to govern the behavior of agents and their effects on other agents. For example, a logistic regression estimating the probability of a "landowner" agent clearing their land of forests could be coded to remove all "forest patch" agents on their property if enacted during the simulation. By mechanistically linking empirical submodels, ABMs can integrate disparate data collected via different disciplinary methodologies to intuitively represent system components as different agents embedded in a common environment (Janssen and Ostrom 2006). Differences in scale and structure among processes are resolved by specifying relationships among agents represented across space and time (An 2012).

An empirical ABM framework that models change in the size and distribution of habitat patches on a landscape can be readily combined with a SPOM that simulates changes in species' occupancy state (present or absent) in each dynamic patch (Sjögren-Gulve and Hanski 2000) to jointly model the emergent dynamics of land-use and metapopulations in CHANS (Fig. 3.1). The landscape, represented by cell-based rasters of environmental layers (e.g., elevation), structures the system spatially. At the largest spatial and hierarchical scale, exogenous drivers (e.g., climate) affect one or more of the three classes of agents: governance institutions, resource users, and patches. Government institutions impose policies that incentivize or discourage different decisions of resource users (e.g., landowners) under their jurisdiction. Land-use change decisions of resource users are then modeled as functions of these policies, interactions with neighbors, and their own heterogeneous characteristics as well as those of their patches (equivalent to individual variation). For example, in this paper we use regression on social survey data to estimate the probability of landowners responding to policies in different ways (a "heuristic rule-based" decision-making model), but there are many other types of land-use change submodels (see Parker et al. 2003 and An 2012 for reviews). These decisions result in the creation, elimination, or modification of the resource user's patches. Finally, a SPOM is run over the resulting dynamic patches. Each patch's occupancy state is stochastically initialized in the first year with probability Ψ, and stochastically changes in subsequent years as a first-order Markov process. Occupied patches can go extinct with probability ε, and unoccupied patches can be

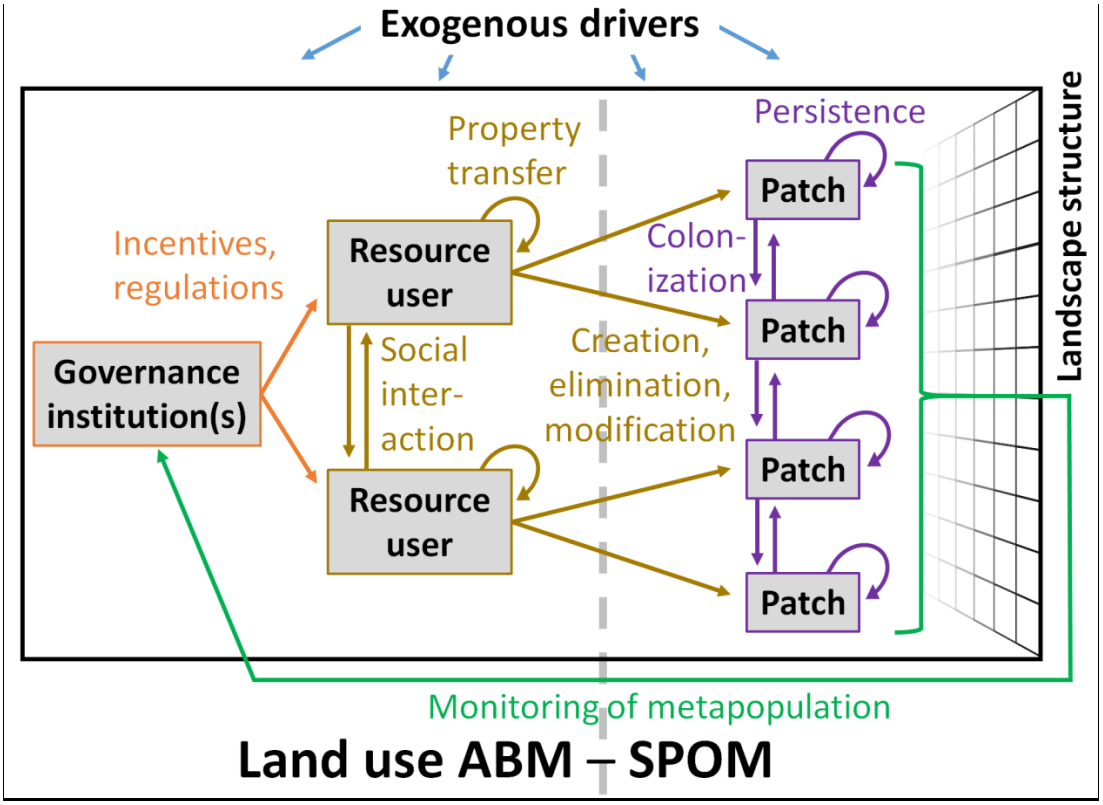

Figure 3.1 Conceptual diagram showing how a stochastic patch occupancy model (SPOM; right of dashed line) can be readily combined with an agent-based model (ABM; left of dashed line) to simulate metapopulations over habitat patches in dynamic landscapes. Agents (gray boxes), which may been heterogeneous, exist in a spatially explicit representation of the landscape and execute empirically-fit processes (arrows) that affect other agents under their spatial domain.

colonized with probability γ. These probabilities are patch-specific: theory posits ε is primarily a function of patch's area and γ of its connectivity to other occupied patches (i.e., sources of colonists), but other habitat covariates can also be included via logistic regression equations in occupancy models (Hanski 1999, MacKenzie et al. 2003). The metapopulation status and provisioning of ecosystem services can then feedback to institutions' decision-making.

Utilizing this ABM-SPOM framework to model metapopulations has a number of advantages. It allows for assessment of conservation strategies that require participation of social actors, such as "payment for ecosystem services" incentive policies (Gimona and Polhill 2011). ABMs can flexibly accommodate a wide range of situations with modular submodels (e.g., this paper includes disease dynamics but excludes interactions between landowners). Previous ABMs integrating land-use change and wildlife have either represented wildlife dynamics simply by using patch characteristics as a proxy for biodiversity (Guzy et al. 2008, Brady et al. 2012, Schouten et al. 2013), or utilized models simulating intra-patch population dynamics or decision-making of individual animals (Guillem et al. 2009, Anselme et al. 2010, Parry et al. 2013, Iwamura et al. 2014). While the former approach offers limited insights into metapopulation dynamics in working landscapes, the latter requires knowledge of species-specific population dynamics that, when unavailable, impedes generalization across systems. There is a need for mid-level models that realistically represent important dynamics while being tractable and generalizable (O'Sullivan et al. 2016). SPOMs use detection/non-detection data that are often easier to obtain than estimates of population sizes or vital rates, especially if these vary spatially or temporally (Sjögren-Gulve and Hanski 2000). SPOMs are most suitable for large networks of discrete patches with small local populations, where turnover in patch occupancy may occurred between years (Sjögren-Gulve and Hanski 2000). Incidence function models can estimate γ and ε with patch area and connectivity effects from just a single season of field surveys (Hanski et al. 1996). Surveys over multiple seasons allows for fitting of logistic regression models that incorporate habitat- and year-based covariates of turnover, and multiple resurveys within each season can correct for imperfect detection using hierarchical occupancy models (MacKenzie et al. 2003).

3.4 Applying the framework to rail metapopulations in the Sierra foothills

In the foothills of the California Sierra Nevada, irrigation by landowners has greatly increased the size and number of small wetlands (mean area = 0.37 ha; Richmond et al. 2010a). These wetlands support metapopulations of two closely-related, secretive marsh birds, the smaller, dispersal-limited black rail (*Laterallus jamaicensis*) and the larger, more vagile Virginia rail *(Rallus limicola)* (Richmond et al. 2010b, Hall et al. 2018). The California subspecies of black rail (*L. j. corturniculus*) is listed as a California State Threatened Species due to habitat loss (Eddleman et al. 1988), while the other US subspecies (*L. j. jamaicensis*) is proposed to be listed as Threatened under the Endangered Species Act. In the foothills, occupancy of black rails has declined since 2007, coinciding with the arrival of West Nile virus (WNV) which was a probable cause (Risk et al. 2011). Because wetlands also provide habitat for WNV mosquito vectors, irrigated wetlands may increase regional WNV infection risk. However, 2007–2009 and 2012–2015 were historically severe drought years, offering another possible cause of decline. Drought and climate change not only threaten to dry natural wetlands, they also threaten the stability of regional water supplies that maintain irrigated wetlands, which provide key black rail habitat (Richmond et al. 2010a). Water cutbacks by irrigation districts to conserve water during drought

may force landowners to reduce irrigation and encourage the conversion of ranchland to exurban development (Huntsinger et al. 2017). Thus, the persistence of wetlands and rails in the Sierra Nevada foothills strongly depends on the land-use decisions of landowners.

We developed an ABM-SPOM, the Wetlands-Irrigation CHANS Model (WICM), for this region. Modeling CHANS begins by defining a system's key actors and processes: we focus on climate as an exogenous forcing, irrigation districts and the California Department of Fish and Wildlife (hereafter "the wildlife agency") as governance institutions, landowners as resource users, and wetlands as patches providing habitat to both rails and WNV (Fig. 3.2a). We parameterized WICM by collecting data from five diverse sources: rail occupancy surveys, land-use change mapping, a survey of landowner decision-making, climate and irrigation district databases, and mosquito trapping and WNV testing.

The objective of our analysis was to evaluate (1) the dominant drivers of metapopulation dynamics and decline, and potential interactions and feedbacks among them, and (2) the impact of policy options on metapopulation persistence. We selected three policy scenarios for assessment based on pre-survey interviews with stakeholders: water cutbacks by irrigation districts during drought, incentives for landowners to create wetlands, and incentives for landowners to protect wetlands. The wildlife agency is actively developing conservation plans for the black rail; incentives were modeled after similar programs in the adjacent Central Valley (Duffy and Kahara 2011), which do not currently extend to the foothills. Local irrigation districts and the State Water Resource Control Board are under pressure to conserve water in the face of recent severe droughts, which prompted revisions of water cutback policies (Huntsinger et al. 2017). There is a need for the integrated assessment of the potential effects of these policies on the black rail, which can account for the linkages between social, climatic, and disease dynamics, in order to inform state conservation plans and water policy.

We test theoretical predictions of metapopulation dynamics in CHANS by comparing results for the dispersal-limited black rail to the more vagile Virginia rail (Richmond et al. 2010b). Following the conclusions of Gimona and Polhill (2011), we predicted that incentive programs would reduce the importance of other drivers of metapopulation extinction risk because they bolster the species overall. We predicted that wetland creation incentives should lead to landowners increasing the number of small wetlands, which in turn should increase the occupancy of black rails more than Virginia rails because the former can occupy smaller patches (Richmond et al. 2010b) and the resulting connectivity would reduce dispersal limitations (Sjögren-Gulve and Hanski 2000). Conversely, occupancy of black rails should be more sensitive than Virginia rails to higher rates of wetland patch change because they are less able to (re-)colonize patches (Amarasekare and Possingham 2001).

3.5 Methods

3.5.1 Data collection

Study area boundaries were the Sierra Nevada Foothills eco-region (US Environmental Protection Agency 2013) for Nevada, Yuba, and southern Butte counties (see Fig. 3.2b for a map and Appendix S3.1 for a description). Our climate model was based on projected regional precipitation values from the CCSM RCP 8.5 climate scenario (Flint and Flint 2012), because present greenhouse gas emission trends are closest to this scenario (Sanford et al. 2014). Information on irrigation districts and the state wildlife agency was obtained from interviews,

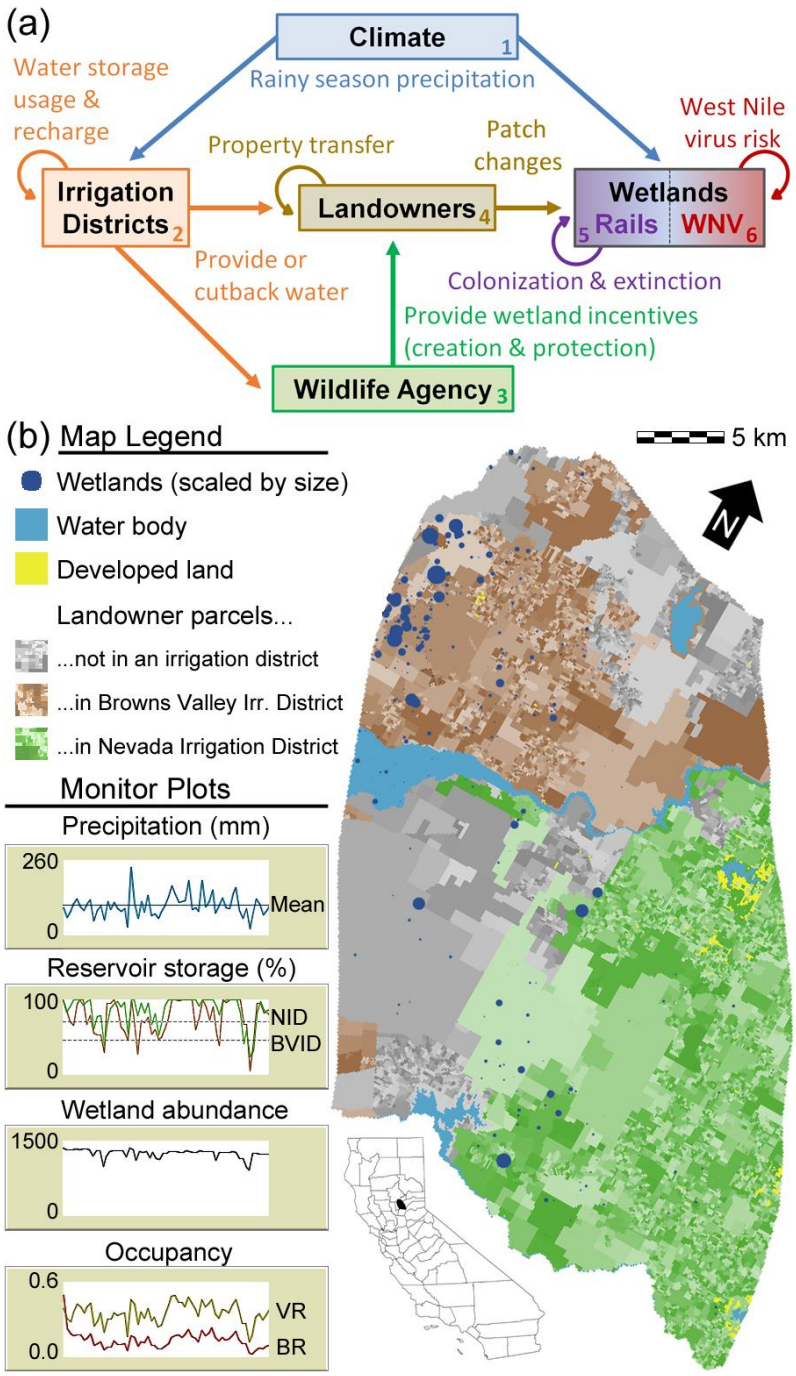

Figure 3.2. Design of the agent-based Wetlands-Irrigation CHANS Model (WICM). (a) Simplified flow diagram of main model processes: agents (boxes) execute processes (arrows) that affect other agents under their spatial domain (numbers indicate order of execution). (b) WICM's graphical user interface. A simulated map displays wetlands, landowners, and irrigation districts, and defines their hierarchical spatial relationships; bottom inset shows study area location in California. Monitor plots let users track how variables change after each simulated year (x-axis); the end of a single characteristic run is shown. Reservoir storage (solid lines) and thresholds for drought 20% water cutbacks (dotted lines) are shown for for Nevada (NID) and Browns Valley (BVID) Irrigation Districts. BR = black rail and VR = Virginia rail.

reservoir databases, and published documents. We acquired a map of 2010 parcel layers from county assessors, and designed and mailed a survey on land and water management to 862 range and oak woodland landowners with properties ≥1.2 ha from the study area (see Huntsinger et al. 2017 for details and the survey). Parcels <1.2 ha (a regional cutoff for Residential Agricultural zoning) were excluded from the study and model, as they were suburban and generally lacked wetlands. We obtained 466 valid questionnaires (54% return rate).

We mapped all 1759 emergent wetlands (minimum mapping unit 5×5 m), as well as all open water bodies and rice fields, by manually interpreting summer 2013 0.4 m imagery in Google Earth 7.1.5 (Google Inc.). We classified wetlands into four geomorphology types: slope (hillside with no open water body), fluvial (edge of creek), fringe (of a pond or rice field), or impoundment (for waterfowl hunting). We classified the water sources of 934 wetlands (53%) as natural-only, irrigation-only, or both-source. Natural water type was further classified as creek or spring. Irrigation type was classified as pasture, leak, rice, runoff (from multiple properties), or water feature (intentional wetland or pond). We used historical imagery to track wetlands over time (1947–2016; Appendix S3.2: Table S1) to measure how changes in irrigation created, eliminated, or changed the area of wetlands in this landscape. We recorded the annual area and irrigation state (presence/absence) of all field-surveyed wetlands (see below). We also tracked the parcels of landowner-survey respondents, mapping all wetlands found on parcels in any of the 6 years preceding our survey (2009–2014). We conducted annual presence-absence broadcast surveys for black rail and Virginia rail occupancy at 273 wetlands (43% of the 2013 acreage) during the breeding season 2002–2016 (methodology described in Richmond et al. 2008, 2010b). We trapped mosquitoes at 80 wetlands from June–October 2012–2014 (6,385 trap/nights), with weekly visits where we placed up to 3 CDC traps baited with dry ice. We used RNA testing to estimate mosquitoes' WNV prevalence. See Appendix S3.1 for more details on data collection.

3.5.2 Model design and overview

Studying CHANS and constructing an ABM is an exercise of iterative, incremental progress and redesign (Alberti et al. 2011). We developed the conceptual model in Fig. 3.2a from observations during early field studies of black rails. WICM was based on disciplinary theories that drove the design of underlying submodels, which were linked regression equations empirically fit from field data. We next refined it via interviews with landowners and water district employees, who helped focus our data collection and modeling on the key processes presented below. After collecting data we re-assessed our model, gathering additional data where needed (e.g., reservoir data) and excluding some processes that turned out unimportant (e.g., baseline rates of new wetland creation). We next provide an overview of the resulting design.

We constructed WICM in NetLogo v6.0.3 (Wilensky 2018). The model represents the CHANS as three types of spatially explicit agents—wetlands, landowners, and irrigation districts—overlaid on a 100 m resolution raster map of the study area (Fig. 3.2b). We chose this resolution because it was just below the minimum size of landowner parcels surveyed (1.2 ha), resulting in little information loss while increasing computational efficiency. Raster cells (what NetLogo calls "patches") have variables representing spatial covariates (elevation and distance to rice) and the spatial domains of landowner parcels and irrigation district service areas. Climate and the state wildlife agency are single entities affecting the whole model. Irrigation districts are agents that provide irrigation to landowners within their service areas. Landowners are agents with their own variables, and make decisions that affect wetlands originating on their property.

Wetlands are represented as points with associated variables (e.g., area). Rails and WNV are represented as variables stored by wetlands (i.e., wetlands have *black rail occupancy* = 0 or 1). The model starts with a 2013 landscape and runs on an annual time step for 50 to 100 years.

Annual processes in WICM are governed chiefly by regression equations parameterized from field data (Table 3.1) and executed in an order approximating the seasonal cycle or sampling period used when gathering data (Fig. 3.2a). First, during the winter rainy season, precipitation is generated based on the RCP 8.5 climate scenario (Flint and Flint 2012). Irrigation districts then update their reservoir water storage by subtracting water used over the previous summer and by adding recharge based on winter rainfall, and may implement 20–50% water allocation cutbacks if minimum storage thresholds are not met. The wildlife agency offers wetland protection and creation incentives. The protection incentive program permanently prevents landowners from turning irrigation off for their largest wetland (excluding impoundments, rice fringes, fluvial creeks, and wetlands fed by runoff from other properties). The wetland creation incentive program provides landowners with ~0.12 acre-feet/day of water to create a new wetland on their property. Total water allocation for creation incentives was capped at 2% of each district's storage; because created wetlands use additional (i.e., surplus) irrigation water, during water cutbacks they were all turned off and new enrollments suspended. These policies represent different strategies for promoting wetland habitats—one aims to maintain wetlands during drought and one to increase wetlands outside of drought. Landowners may transfer their property to a new landowner due to sale or death, and then make a series of irrigation decisions. Wetland patches first stochastically change their irrigation state (on or off) based on empirical baseline rates. Next, landowners can respond to irrigation cutbacks (if implemented) by permanently fixing leaks, temporarily cutting off water from pasture or rice fields until cutbacks are lifted, or deciding to sell their land in the next year (or some combination of these). When irrigation is turned off, wetlands shrink in size if fed by both irrigated and natural water sources, or are eliminated altogether if fed by irrigation only. Landowners then decide whether to participate in incentive programs, and may enroll in each only once. Next, rail colonization and extinction occurs during late spring (matching the onset of our field surveys) by running a SPOM over the new landscape. Wetlands eliminated by turning off irrigation go extinct. Finally, WNV vector strength is determined by wetland distribution as mosquito densities peak in late summer, which affects the probability of rail colonization and extinction in the following year (i.e., due to disease mortality over the winter). In the fall, measurements are taken and time steps forward.

In the following sections we present a brief summary of each empirical submodel, discuss its implementation in WICM, and describe the coded processes that link submodels. These sections are organized by agent type according to the general framework in Fig. 3.1, and approximate the schedule of execution of processes described above and in Fig. 3.2a. Appendix S3.1 contains a comprehensive description in the standard format for ABMs.

3.5.3 Parameterization of exogenous processes

Rainy season precipitation—We used the mean monthly precipitation over the rainy season (Nov–May); this metric accounted for the majority of rainfall and coincided with the timing of districts' recharge and decision-making. We stochastically generated annual precipitation based on the 2017–2099 RCP 8.5 data, to which we fit both a lag-1 autoregressive model (Salas 1993) and a non-autoregressive model using R package *stats* (v3.4.3; R Core Team 2013). We used the

Table 3.1 Summary of data integration in the WICM agent-based stochastic patch occupancy model. Most submodels are stochastic regressions; "summary" indicates summary statistics (no regression) and ^{D} indicates deterministic submodel. "Tables" lists the Appendix S3.1 table number of the final model / Appendix S3.2 table number of the model selection table; "T" indicates see text of Appendix S3.1 (no table). ψ represents initial occupancy probability, γ colonization probability, and ε extinction probability.

Agent (data source)	Process	Regression	Final submodel	Tables
Climate (RCP 8.5 model)	Rainy season precipitation	Summary	Precipitation (Nov–May) ~ Normal(μ, σ)^2	T / T
Irrigation districts (interviews and reservoir databases)	Water storage usage & recharge	Tobit or summary	Water storage used ~ Normal(μ, σ)	5 / T
			Water storage recharge ~ Normal(Precipitation, σ)	5 / T
	Provide or cutback water	N/A^{D}	If reservoir levels drop below thresholds, implement water cutbacks	5 / T
Wildlife agency (scenario design)	Provide wetland incentives	N/A^{D}	If no cutbacks, provide incentives	T / T
Landowners (mail survey)	Initialization & property transfer	Multinomial	Landowner typology ~ Property area	6 / 8
		Hurdle-Poisson	Going to sell land ~ Intercept-only	T / T
			Year until sell land ~ Poisson(μ)	
		Summary	Age ~ Normal(μ, σ)	T / T
		Summary	Pr(Death) ~ Exponential(Age)	T / T
	Patches changes (cutback actions)	Logistic	Pr(Land-seller) ~ Typology	9 / 11
			Pr(Pasture-cutter) ~ Typology + Elevation + Property area + Property area^2	9 / 12
			Pr(Rice-cutter) ~ Intercept-only	9 / T
			Pr(Leak-fixer) ~ Typology + Property area	9 / 13
	Patches changes (incentive actions)		Pr(Protection incentive participant) ~ Typology + Elevation	10 / 14
		Logistic	Pr(Creation incentive participant) ~ Typology + Elevation + NID	10 / 15
Wetlands (aerial mapping)	Initialization	Multinomial	Water source type ~ Geomorphology + Property area + No irrigation district + Landowner	1 / 2
			Irrigation type ~ Both-source + Geomorphology + Elevation + Property area + Wetland area + # wetlands + Landowner	2 / 3
			Natural type ~ Geomorphology + Landowner	3 / 4
		Logistic	Pr(Irrigation initially active) ~ Impoundment	4 / 5
		Tobit	Both-source wetlands' percent natural area ~ Intercept-only	T / 6
	Patch changes (baseline rates)	Logistic	Pr(Irr. activation) ~ Natural-only + Precipitation + Impoundment + Site	7 / 9
			Pr(Irr. deactivation) ~ Precipitation + Impoundment + Leak + Pasture + Runoff + Site	8 / 10
		Summary	New irrigated size ~ Gamma(α, β)	T / T
Wetlands: Rails (presence-absence surveys)	Colonization & extinction (black rail)	Occupancy model (logistic)	ψ ~ Wetland area + Water source + Slope + Fluvial	11 / 16
			γ ~ Wetland area + Precipitation + Water source + Geomorphology + WNV risk + Connectivity	
			ε ~ Wetland area + Precipitation + Water source + Geomorphology + WNV risk	
	Colonization & extinction (Virginia rail)	Occupancy model (logistic)	ψ ~ Wetland area	11 / 17
			γ ~ Wetland area + Precipitation	
			ε ~ Wetland area + Precipitation + Water source + Elevation	
Wetlands: WNV (mosquito trapping)	West Nile virus risk	Log-normal^{D}	Mosquito abundance ~ % wetland (2.5 km buffer) + Rice distance	12 / 18
			Mosquito WNV prevalence ~ Mosquito abundance + Rice distance	13 / 19

model without an autoregressive term ($\mu = 1.023$, $\sigma = 0.189$) because it had a lower AIC (ΔAIC=1.98).

3.5.4 Parameterization of governance institutions

Initialization—We modeled Browns Valley Irrigation District (BVID) and Nevada Irrigation District (NID) based on polygon maps of water district service areas (U.S. Bureau of Reclamation and California Department of Water Resources 2009). Extents of irrigation district service areas (and landowner properties; see below) were represented in the model by converting polygons to 100 m raster maps and loading them into NetLogo's raster cells.

Water storage usage & recharge—For each district we combined information from online databases using summary statistics and normal Tobit regressions to estimate storage usage and recharge per mm of precipitation (Appendix S3.1: Table S5). Annual storage was then updated by subtracting used water (which was proportionately increased by incentive programs or decreased by cutbacks) and adding water recharge, up to the max storage.

Provide or cutback water—If the new storage fell below thresholds (set based on irrigation district reports; Appendix S3.1: Table S5), 20% or 50% cutbacks were implemented for that year.

Provide wetland incentives—Based on the scenarios we designed, the wildlife agency activates protection policies, and creation policies for all irrigation districts without active water cutbacks.

3.5.5 Parameterization of resource users

Initialization—Landowners were implemented into the model as spatial agents based on 2010 parcel layers, converted to a 100 m raster and loaded into NetLogo. We modeled landowner diversity by conducting factor analysis on survey respondents' ratings of 24 possible motivations for owning their property (Appendix S3.2: Table S7), as has been done in other studies (Ferranto et al. 2013). This classified landowners as one of six typologies: investment-, environment-, lifestyle-, profit-, recreation-, or tradition-motivated. These landowner characteristics were then used as covariates for the probabilities of landowners taking actions within the patch change submodels. Private landowners' characteristics were initialized stochastically via multinomial regression (Appendix S3.1: Tables S6; Appendix S3.2: Table S8). Public landowners were deterministically assigned, and did not change or respond to cutbacks and incentive programs.

Property transfer—New landowner characteristics were assigned (via multinomial regression as above) when property was transferred because landowners either died or reached the year they planned to sell in. Rates were fit from survey data (Appendix S3.1). If a property was not transferred, the landowner's age increased and their "years to sell" decreased by one

Patch changes (cutback actions)—Our patch change model simulated a Markov process where an existing wetland transitioned between two irrigation states, on (1) or off (0), based on rates estimated from survey and field data (i.e., a heuristic rule-based model; An 2012). We used this framework, rather than an economic or vegetation successional model, because landowners reported in interviews that water use decision-making was driven by diverse, often non-economic factors (e.g., tradition or amenities; Huntsinger et al. 2017), and because field observations showed that wetlands were able to quickly form wherever there was sufficient water. We parameterized landowner's responses to irrigation water cutbacks during drought via

four logistic regressions (NLOGIT v5.0) that assigned landowners to groups based on a survey question asking if they would respond to hypothetical water cuts of ≥20% by (1) selling their land, (2) repairing leaks, (3) reducing pasture irrigation, or (4) reducing rice irrigation (Appendix S3.1: Table S9, Appendix S3.2: Tables S11–S13). These response options were based on landowner interviews; ponds and impoundments were excluded because landowners reported they were unlikely to be affected (see Appendix S3.1). Landowners in each group took their relevant actions (i.e., turning irrigation off) on their wetlands when cutbacks occurred (see *3.4.2 Model design and overview*).

Patch changes (incentive actions)—We used logistic regression (NLOGIT v5.0) on responses to a survey question asking whether landowners would be interested in protecting a wetland for a one-time payment or creating a wetland if given free water (Appendix S3.1: S10, Appendix S3.2: Tables S14–S15). Landowners that were interested were assigned to protection-landowner and creation-landowner groups when initialized. They then had an annual enrollment probability of 0.0526 (based on observed rates for a similar policy; see Appendix S3.1). Protection participants received a one-time payment of $10,000 from the wildlife agency to protect their wetland. Creation participants received enough water to create a ~0.57 ha slope wetland; created wetland size was estimated from State Wildlife Area data (see Appendix S3.1). The annual water cost, paid by the wildlife agency, was $550.00 (BVID) or $893.10 (NID; prices from district documents).

3.5.6 Parameterization of patches

Initialization—Wetlands were loaded into the WICM as points and had their characteristics assigned based on actual data (if available), or stochastically generated during initialization via regressions (Appendix S3.1: Tables S1–S4; Appendix S3.2: Table S2–S5) following Berger and Schreinemachers (2006). Both-source wetlands' areas were divided into natural and irrigated areas based on historic tracking data (text of Appendix S3.1; Appendix S3.2: Table S5).

Patch changes (baseline rates)—We estimated baseline rates of change in wetlands using our patch change data from 2001–2016, assuming contemporary rates represented future dynamics. We used mixed logistic regression (R package *lme4* v1.1) to estimate probabilities of irrigation activation or deactivation (Appendix S3.2: Tables S9–S10; Appendix S3.1: S7–S8). We included a random effect for site to account for repeat sampling of the same wetlands, as is common for time series data (Bell and Jones 2015). Newly irrigated natural wetlands had their irrigated area predicted with a Gamma distribution ($\alpha = 0.878$, $\beta = 2.228$) fit from mapping data. We did not model the creation of new wetlands because contemporary rates were negligible (Appendix S3.1).

Colonization & extinction (black and Virginia rails)—We modeled the metapopulation as a SPOM, parameterized by fitting multi-season occupancy models (MacKenzie et al. 2003) in R package *unmarked* (v0.12) to our rail presence-absence data. These models jointly estimate probabilities of initial occupancy (Ψ), colonization (γ), and extinction (ε) with covariates on each parameter. Previous studies found no evidence of competition between black and Virginia rails, so we simulated their dynamics separately (Risk et al. 2011). Connectivity was modeled with an autoregressive buffer radius metric (Appendix S3.1) that had previously been found to fit best for black rails and was validated with genetic data (Hall et al. 2018). This connectivity metric incorporated occupancy probability at sites within the buffer radius that were unsurveyed or had

non-detections. The remaining covariates for γ and ε were assessed via model selection: precipitation, WNV risk, elevation, geomorphology type, and water source type (Appendix S3.2: Table S16–S17, Appendix S3.1: Table S11). In WICM, any wetlands smaller than the minimum breeding home range size of radio-tracked black and Virginia rails (0.16 and 0.28 ha, respectively; S.R. Beissinger, unpublished data) were automatically set unoccupied.

West Nile virus risk—We used linear regressions to model mosquito abundance (mean # *Culex* spp. caught per trap-night) and WNV prevalence at each wetland as a function of wetland area in a 2.5 km buffer and other covariates (Appendix S3.2: Tables S18–S20; Appendix S3.1: Tables S12–S13). We estimated WNV risk as the product of these metrics (a well-established predictor of spatial variation in WNV cases with a strong theoretical basis; Kilpatrick and Pape 2013).

3.5.7 Simulation analyses

Simulations were run using R package *RNetLogo* (v1.0.4). To determine drivers of current CHANS dynamics, we conducted sensitivity analysis with drought cutbacks but no incentives for 50-year projections. We used ±25% and ±10% perturbations for all top-level parameters of the model (i.e., not beta parameters), as well as the beta parameters for rail colonization (γ) and extinction (ε). Initial results showed the system was highly sensitive to precipitation, so we also tested its mean and SD We replicated simulations 4000 times and calculated the mean percent change from a no perturbation scenario as:

$$\frac{\text{Output metric with perturbation} - \text{Output metric without perturbation}}{\text{Output metric without perturbation}} \quad (3.1)$$

for three metrics: (1) each species' mean metapopulation size (excluding the first 10 years as burn-in), (2) each species' minimum metapopulation size for each iteration (as a proxy for quasi-extinction risk; Beissinger and Westphal 1998), and (3) the mean wetland abundance (i.e., the number of wetlands that had natural water sources or were actively irrigated). We defined the metapopulation size as the number of occupied wetlands, and used this rather than the occupancy rate because wetland abundance varied across simulations.

We assessed the influence of incentive programs after 50 and 100 years by running scenarios with and without irrigation cutbacks: (1) no incentives, (2) wetland creation incentives, (3) wetland protection incentives, and (4) both incentives. To determine WNV's influence on the system, we also ran a scenario without WNV, incentives, or cutbacks. We replicated simulations 8000 times and recorded ending and minimum metapopulation sizes for each species. Our model lacked mechanisms to cause extinction vortices, so we choose a minimum metapopulation size threshold of 25 wetlands (<5% occupancy on the 2013 landscape) to represent a quasi-extinction risk, as wetlands in this region are small and often support only a few breeding pairs (Appendix S3.1). Finally, to test if incentives reduced the importance of other drivers of quasi-extinction risk, we ran sensitivity analyses for a drought cutback scenario with both incentives (4000 replicates) with ±25% perturbation. We then compared the absolute percent changes to the corresponding percent changes from the no incentives scenario, using Welch's *t*-tests (Benjamini-Hochberg correction for a 0.05 false discovery rate) to identify significant differences.

3.5.8 Model validation

We used 2017–2018 rail occupancy data that was not included in model fitting to validate WICM's ability to accurately predict metapopulation dynamics. To estimate 2017 and 2018 colonization and extinction rates corrected for detection probability, we fit multi-season occupancy models with different annual γ, ε, and p intercepts for each year to the field data. We then ran simulations, replicated 2000 times, that were initialized in 2002 and run through 2018 with the observed annual precipitation values and with WNV first entering the system in 2007. We only used wetlands with identical site boundaries between the field dataset and model (n = 260). To validate our land-use change model, we randomly selected 10% of regional wetlands (n = 176) and assessed their active water sources in 2017 via Google Earth imagery. We replicated simulations 2000 times, initialized to 2013 and run through 2017 with observed precipitation values. Following Schreinemachers and Berger (2011), we tested whether each metric's measured 95% CIs included the mean simulated rates for the same sets of wetlands.

3.6 Results

3.6.1 Model behavior

Validation tests indicated our model accurately predicted metapopulation and land-use change dynamics (Fig. 3.3). Modeled values were within the 95% CI of independent field data for all measures except Virginia rail colonization in 2017, which fell just below the confidence limit. The model correctly predicted an increase in occupancy for both species in 2017, which was the second rainiest year on record in California. However, it slightly underestimated the occupancy increase due to unusually high October 2017 rainfall, which was not captured in our precipitation metric (mean Nov–May, the typical rainy season); adding this extra precipitation to the model boosted model values close to expected values for both species (data not shown).

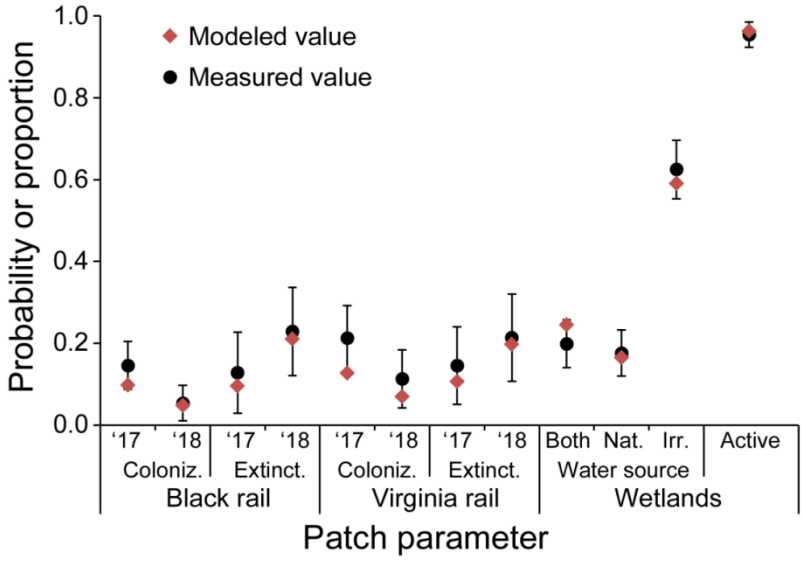

Figure 3.3. Validation analysis comparing sampled probabilities of colonization and extinction for black and Virginia rail metapopulations (n = 260 sites for 2017 and 2018), and proportions of wetlands fed by natural, irrigated, or both water sources, and with at least one active water source (n = 176 sites for 2017 only), to a WICM simulation of the California Sierra Nevada foothills that used actual precipitation values. Bars represent 95% CIs.

A characteristic run illustrating CHANS dynamics with drought cutbacks and no incentive policies is shown in Fig. 3.2b. Simulations exhibited relatively stable wetland numbers with balanced wetland irrigation activation and deactivation rates, but periodic drops in wetland numbers occurred when landowners reduced irrigation during drought cutbacks. Severe droughts typically caused cutbacks in only one irrigation district, while rarer, exceptional droughts caused cutbacks in both. Black rail occupancy declined in early years, because initial occupancy (ψ) was fit from pre-WNV levels; thereafter, occupancy reached a stochastic equilibrium. However, severe droughts caused occupancy declines that required up to a decade to recover. Virginia rail dynamics similarly stabilized at a stochastic equilibrium punctuated by drought-induced drops in occupancy, but exhibited greater annual stochasticity. The two species had fairly synchronous dynamics due to similar effects of precipitation. WNV risk was not retained in Virginia rail occupancy models during model selection (Appendix S3.1: Table S18), but was detrimental to both colonization and extinction rates of black rails (Appendix S3.2: Table S11). Wetlands near rice fields in the Central Valley had an order of magnitude higher WNV risk compared to wetlands upslope and away from rice agriculture (~1.5 vs. ~0.15 infected *Culex* per trap/night), similar to elsewhere in California (Kovach and Kilpatrick 2018). Wetlands with more wetland land cover within 2.5 km also had higher WNV risk (Appendix S3.3: Table S19). Thus, WNV introduced a negative feedback between wetland abundance and rail occupancy that most affected large, well-connected wetlands, which were otherwise the most likely to be occupied.

3.6.2 Drivers of rail metapopulation dynamics

This CHANS of wetlands in a working landscape was more sensitive to variation in precipitation by an order of magnitude compared to other modeled processes, with rail metapopulation dynamics (Fig. 3.4), quasi-extinction risk (Appendix S3.3: Fig. S1), and abundance of wetlands (Appendix S3.3: Fig. S2) all exhibiting similar patterns of sensitivity. A precipitation term was in 7 submodels; it was retained in every AIC model selection procedure in which it was tested (Appendix S3.2). Sensitivity to precipitation was driven primarily by its mean, but quasi-extinction risk also showed sensitivity to changes in precipitation variability. Irrigation district water storage capabilities and usage also exerted moderate effects for rails (Fig. 3.4) and strong effects for wetland abundance (Appendix S3.3: Fig. S2). After precipitation, the strongest drivers of metapopulation dynamics were those that directly affected occupancy, the colonization and extinction rates (γ & ε); mean metapopulation size was equally sensitive to γ and ε (Fig. 3.4), while quasi-extinction risk was more sensitive to ε (Appendix S3.3: Fig. S1). Virginia rails were generally less sensitive than black rails, but exhibited similar patterns. However, Virginia rails were relatively more sensitive to the minimum wetland size (Fig. 3.4b) because it was larger than for black rails, so a similar percent change caused more wetlands to be affected. There were other differences in sensitivity between rail species as well, with strong to moderate effects of connectivity, slope geomorphology, and WNV for black rails, and of patch change rates and elevation for Virginia rails. Most other parameters, including landscape and landowner initialization parameters (Appendix S3.3: Fig. S2–S3), had insignificant effects (Appendix S3.3).

3.6.3 Effects of irrigation cutback and wetland incentive policies

Prior to the arrival of WNV, black rails had higher occupancy than Virginia rails, but models suggested the virus more than halved black rail metapopulation size while Virginia rails were unaffected (Pre-WNV versus None in Fig. 3.5a–b; see Appendix S3.3: Fig. S5 foractual

occupancy trends). Likewise, in all other scenarios black rail ending and minimum metapopulation size (Fig. 3.5a–b) after 50 years was about half that of Virginia rails (Fig. 3.5c–d). Results were similar for 100 year projections (Appendix S3.3: Fig. S4a–b).

Minimum black rail occupancy reached precariously low levels when irrigation districts implemented water cutbacks during drought. Then, over a quarter of the simulations dropped below 25 occupied wetlands (~5% occupancy; Fig. 3.5c, red dashed line) within 50 years, and nearly half fell to that level within 100 years (Appendix S3.3: Fig. S4c–d).

Wetland creation incentives were effective at bolstering metapopulation size of both species outside of drought years, but also increased variation in occupancy (Fig. 3.5a–b). Creation incentives increased the total metapopulation size for Virginia rails more than for black rails, due to higher overall occupancy rates of Virginia rails. However, creation incentives were more effective at increasing the proportion of wetlands occupied for black rails, increasing their ending occupancy by 45.6% of its original value compared to 19.6% for Virginia rails. In the

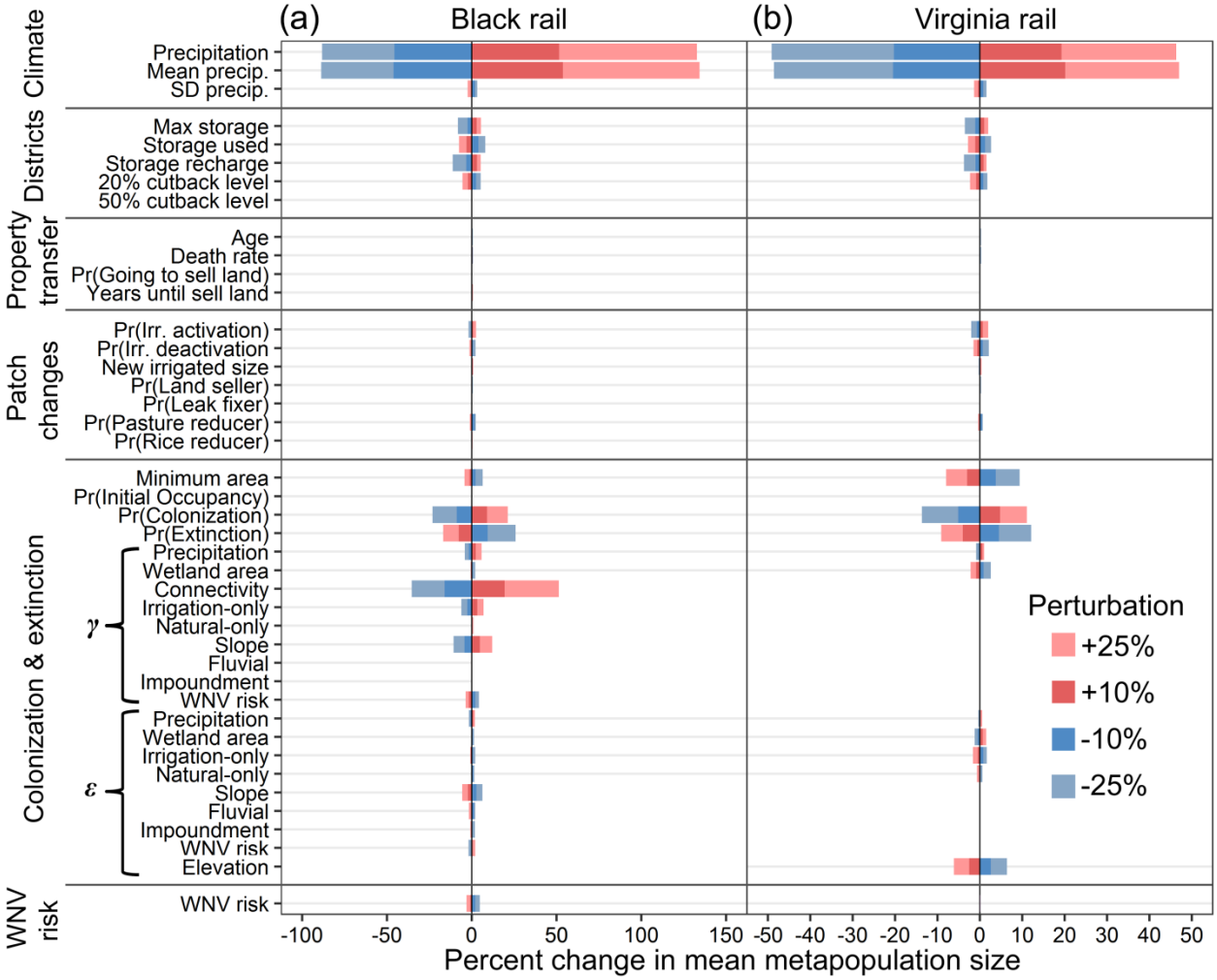

Figure 3.4. Sensitivity analysis of black and Virginia rail for WICM input parameters used in the simulation of the California Sierra Nevada foothills with drought cutbacks and no wetland incentives. Virginia rails were less sensitive to system dynamics overall. Parameters labeled γ and ε are regression parameters for colonization and extinction probabilities, respectively.

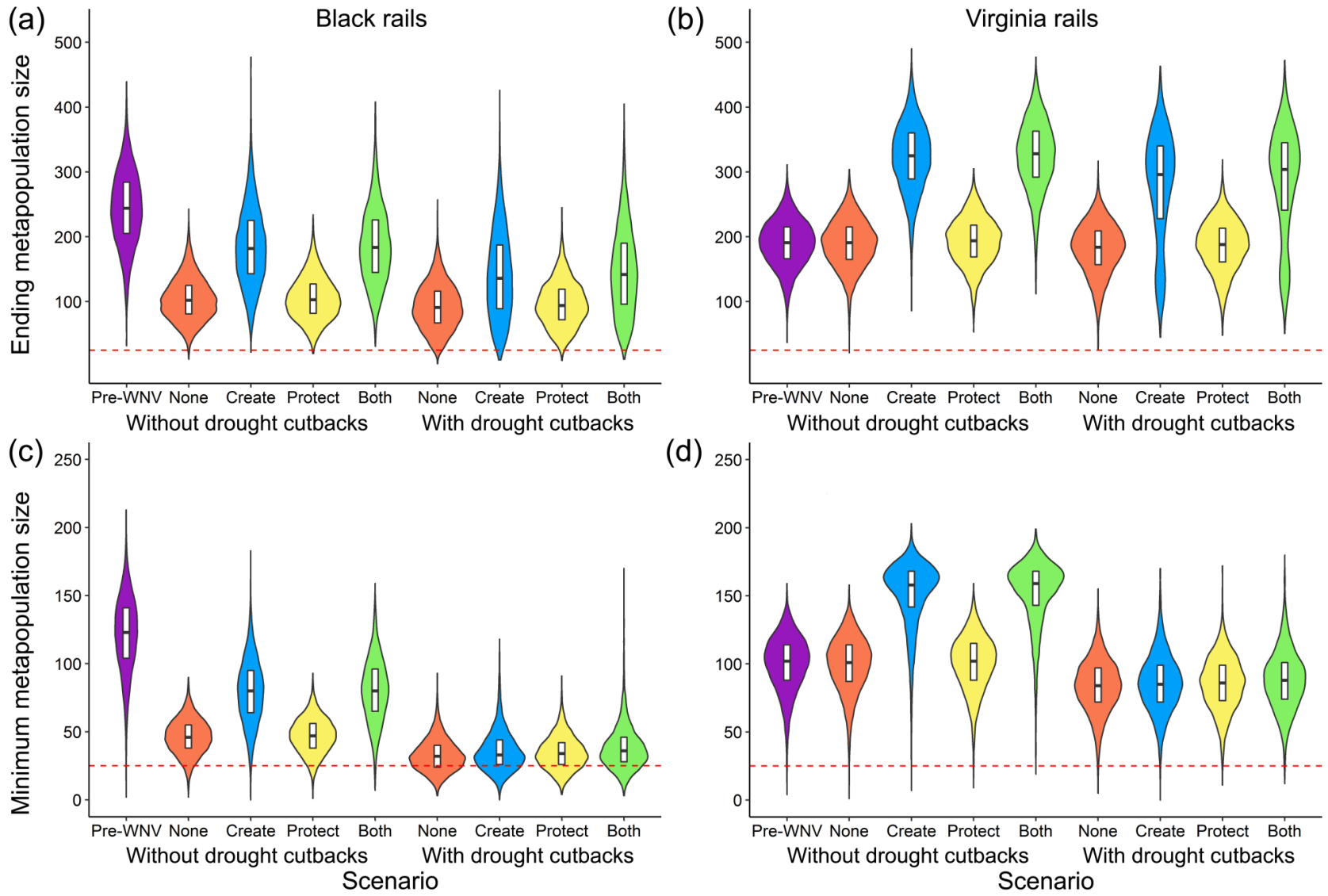

Figure 3.5. Ending metapopulation size and minimum metapopulation size (used as a measure of quasi-extinction risk) for black rails and Virginia rails in the California Sierra Nevada foothills, projected for 50 years in WICM for 8 different scenarios. Bar shows median and boxplots show 1st–3rd quantiles.

absence of drought cutbacks, creation incentives increased black rails' minimum metapopulation size over 50 years by 78.5% on average (Fig. 3.5c), greatly reducing their quasi-extinction risk. However, this benefit disappeared with water cutbacks during drought (reduced to only a 9.3% increase). Similar patterns were seen for Virginia rails but, because this species was widely distributed beyond the boundaries of our study area and had higher colonization rates, it faced little risk of metapopulation extinction (Fig. 3.5d). Creation incentives had high landowner participation rates, as this program reached the 2% reservoir storage cap on water allocation within a mean of 5 years. There were 277.0 ± 0.2 SD new wetlands created at an annual cost for water of $233,336.

Wetland protection incentives had little effect (<5% change) on ending or minimum metapopulation size of either rail species after 50 years in all scenarios (Fig. 3.5). This was partly because protection had lower landowner participation rates than creation incentives; participation was uncapped and grew linearly from 170.7 ± 11.6 wetlands by year 50 to 310.0 ± 14.1 protected wetlands by year 100. After 100 years, protection incentives had a small effect for black rails when coupled with drought cutbacks, increasing their ending and minimum metapopulation size by 7.3% and 12.2% (7 and 3 more occupied wetlands, respectively). Virginia rail ending and minimum metapopulation size was still unaffected after 100 years (≤5% change). The mean annual cost of protection incentives for the first 50 years was $33,509 (3.35 wetlands/year).

There was a moderate reduction in quasi-extinction risk when wetland protection incentives were combined with wetland creation incentives (Fig. 3.5c–d). The combination increased black rail minimum metapopulation size 15.8% after 50 years and 18.8% after 100 years (~5 new occupied wetlands in both cases) compared to the scenario without incentives. For Virginia rails, combining incentives showed weak effects only at 100 years (a 6.1% increase), due to their larger minimum metapopulation size.

Incentive policies made black rail quasi-extinction risk more sensitive to precipitation and irrigation storage, as well as slope geomorphology wetlands (the type created by incentives; Fig. 3.6). They reduced sensitivity to several parameters, all of which were not tied to the

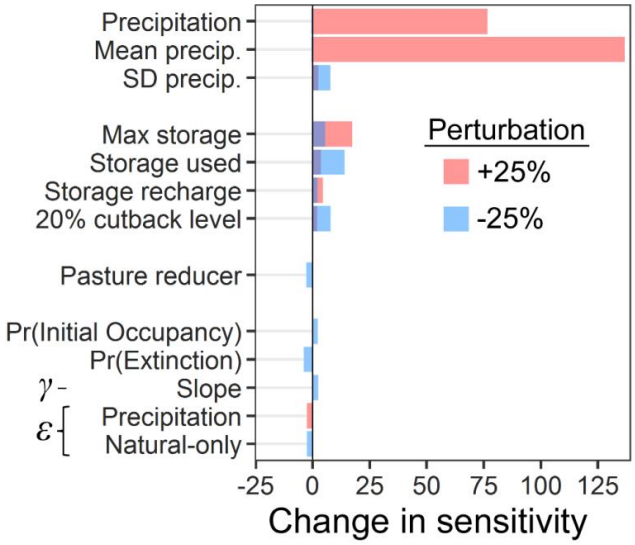

Figure 3.6. Significant differences (Welch's *t*-tests with Benjamini-Hoochberg 0.05 false discovery rate) in sensitivity (percent change) between scenarios with drought cutbacks and incentives, compared to scenarios without incentives (the baseline).

dynamics of creation-incentive wetlands, such as the proportion of landowners that turned off pasture wetlands during drought and precipitation's direct effects on rail extinction rates.

3.7 Discussion

3.7.1 Drivers of metapopulation dynamics in a CHANS

Our model showed that the precipitous decline of the black rail metapopulation was caused by a combination of WNV and drought. WNV halved the occupancy, while droughts created periodic spikes in extinction probability and reductions in colonization probability (Appendix S3.3: Fig. S5). The ability to deduce drivers of observed metapopulation dynamics by reproducing emergent, qualitative patterns is an important benefit of ABMs (Grimm et al. 2005). We found little evidence of WNV impacting Virginia rails (Appendix S3.1: S37); WNV infection and mortality rates vary substantially among avian species (Kilpatrick et al. 2013).

The CHANS was strongly driven by precipitation and the ability of irrigation districts to store it in reservoirs, further illustrating the importance of severe drought events (Fig. 3.4). The RCP 8.5 climate scenario projects a 6.6% drier climate with 19.5% greater variance compared to contemporary levels for the study region. Even these levels of change could cause large shifts in system state due to the extremely high sensitivity of rail metapopulation dynamics and wetland numbers in our model to precipitation. Precipitation affected rails directly as a covariate for colonization and extinction (Appendix S3.1: Table S11), by increasing the baseline probability of irrigation being turned or kept off in drier years (Appendix S3.1: Table S7–S8), and by landowner responses to drought cutbacks (Appendix S3.1: Table S9). Occupancy was less sensitive to direct effects of precipitation on colonization and extinction (Fig. 3.4a), indicating that sensitivity to precipitation was caused chiefly by irrigation decisions of landowners that changed wetland abundance. However, quasi-extinction risk was sensitive to effects of precipitation as a covariate for extinction probability (Appendix S3.3: Fig. S1a), suggesting that natural drying of wetlands during drought (observed in the field; S.R. Beissinger, unpublished data) is also a risk to the metapopulations. Irrigation cutbacks are thus a synergistic threat, causing wetlands to disappear when rails are already stressed from drying wetlands. Both species were surprisingly insensitive to parameters controlling the number of landowners that responded to drought cutbacks, indicating that the frequency of drought disturbance was more important than its magnitude.

The complexity of CHANS makes anticipating threats and controlling system behavior difficult, so fostering CHANS' resilience to different disturbances is an important management goal (Schlüter et al. 2012). Gimona and Polhill (2011) found that incentive programs reduced the sensitivity of metapopulation extinction risk to all other model parameters, creating resilience to perturbations of the other components of the CHANS. In contrast, we found that the addition of incentives greatly increased metapopulation sensitivity to precipitation (Fig. 3.6), although incentives did reduce sensitivity to some threats (e.g., landowners reducing pasture irrigation). This occurred in WICM because the provisioning of water for wetland creation incentives was conditional on staying above drought thresholds, while Gimona and Polhill's incentive programs were decoupled from system dynamics. Thus, an incentive scheme's ability to reduce extinction risk sensitivity may depend on whether the policy is exogenous to the CHANS dynamics.

Species differences in wetland habitat preferences complicated relationships between patch change (i.e., elimination and creation) rates and colonization abilities predicted by theory.

The limited dispersal abilities of black rails should make them more sensitive to patch change rates than Virginia rails because black rails are at greater risk of patch changes outpacing (re-) colonization abilities (Amarasekare and Possingham 2001). However, Virginia rails showed greater sensitivity to baseline patch change rates (Fig. 3.4). This likely occurred because Virginia rails used impoundment wetlands, which frequently dried and were re-irrigated (Appendix S3.1: Table S16–S18), but black rails rarely used these sites (Appendix S3.1: Table S11) which often are flooded too deeply (Richmond et al. 2010a). However, black rails were much more sensitive than Virginia rails to patch change due to drought, as shown by their greater sensitivity to precipitation and irrigation district parameters (Fig. 3.4). This difference may also be partly due to wetland heterogeneity; cutbacks affected pasture- and leak-fed wetlands, which were more often of the slope geomorphology type (Appendix S3.1: Table S2) preferred by black rails (Fig. 3.4a). Metapopulation theory has increasingly focused on the effects of patch quality differences and patch dynamics (Ranius et al. 2014). Our results show that in CHANS these processes can interact in complex ways, with heterogeneity in patch quality able to overshadow or exacerbate the influence of different drivers of patch change.

3.7.2 Utility and limitations of data integration via agent-based modeling

The ABM-SPOM framework allowed us to combine quantitative field data from wildlife occupancy surveys, social science surveys, land-use change mapping, climate models, and insect disease vector trapping. This integration resulted in important findings—such as direct effects of drought on wetland drying appearing much less important than its impacts on landowner irrigation behavior, and incentive schemes to foster resilience being less effective if coupled to CHANS dynamics. These findings would not have been evident from a standard SPOM or from the assessment of field data because they emerged from the coupling of multiple processes. A traditional SPOM would likely underestimate the true risk of metapopulation extinction by failing to account for the threat posed by irrigation cutbacks, which was identified from our ABM. Another key benefit of ABMs is their ability to model individual heterogeneity (Parker et al. 2003). This was crucial to our finding that the theoretical relationship between dispersal and patch change rates in metapopulations was not borne out in this system because patch heterogeneity affected colonization, extinction, and patch change rates in different ways.

Integrating different kinds of data to model CHANS is an evolving process (Alberti et al. 2011) that is enabled by the flexible ABM framework. Constructing an ABM-SPOM for a new system may seem daunting, but it begins by simply developing a conceptual model of the key social actors and ecological processes (i.e., Fig. 3.2), which can be coded into an initial draft of an ABM. Coding an ABM with "fake" parameters before beginning data collection has numerous benefits: it can clarify ambiguities in thinking, ensure that the correct data are gathered, provide an ongoing base for data integration, and be iteratively redesigned as necessary. NetLogo's simple programming language makes coding submodels remarkably easy, while the ABM-SPOM framework can be implemented in more advanced programming languages if needed.

Data types differ in their ease of incorporation into an ABM. Occupancy data for SPOM parameterization is relatively easy to collect and analyze. On the other hand, land-use change ABMs can be difficult to parameterize (Bousquet and Le Page 2004). However, if some parameters lack data, a range of plausible values can be estimated from expert opinion and the uncertainty this introduces into model behavior can be assessed via sensitivity analysis (c.f.,

Iwamura et al. 2014). In other situations, it may be pragmatic for ecologists to gather and integrate SPOM data into existing land-use change ABMs focused on farmland (Guillem et al. 2009, Brady et al. 2012, Schouten et al. 2013), urban growth (Guzy et al. 2008), vegetative succession (Anselme et al. 2010), or other systems (Parker et al. 2003), rather than reinvent the wheel. Such efforts could rapidly expand the number of studies of metapopulations in CHANS, and help to identify general principles for their conservation.

Uncertainty in model outcomes arises from uncertainty in model input parameter estimates, alternative model design choices, errors in data collection, and errors in model construction, all of which propagate through model results (Evans 2012). The use of sensitivity analyses to assess uncertainty is standard in ABMs due to their complexity (Evans 2012, Lee et al. 2015). Our sensitivity analyses showed extreme sensitivity to precipitation, suggesting that uncertainty in climate change models likely overwhelms other sources. However, model construction choices also added uncertainty to WICM, because data availability necessitated simplifications that reduced realism. Our reservoir model was a statistical approximation that did not model hydrologic flows or temperature increases, which threaten water supplies by reducing snowpack and increasing evaporation from reservoirs. Also, our model of water cutbacks during drought only focused on wetlands fed by pasture, rice, or irrigation leaks, and assumed that landowners responded by ceasing irrigation and drying these wetlands entirely rather than by reducing wetland size, which may happen in some situations. Thus, our results likely overestimated some effects of drought on wetland persistence, but this was offset by our assumption that water feature- and runoff-fed wetlands were unaffected by irrigation water cutbacks (Appendix S3.1). Lastly, we did not model parcel subdivision and land-use change outside of wetlands, which may have important effects in this CHANS over the coming decades. Thus, our results are best viewed as a useful approximation of CHANS behavior, rather than representing the system with total accuracy.

3.7.3 Conservation implications

Achieving sustainable CHANS requires an integrated systems approach to avoid "solutions" to natural resource problems that produce unforeseen negative consequences. ABMs are a particularly promising tool for quantitatively assessing such tradeoffs (Liu et al. 2015). Our model suggests that a negative externality may arise as a result of recently revised water conservation policies in California for increased water cutbacks during drought (Huntsinger et al. 2017). In the absence of water cutbacks during drought, only 5% of model runs had black rail metapopulation size falling below a threshold within 50 years where extinction could become a grave concern, and wetland creation incentives were effective at reducing this risk (Fig. 3.5b). However, a serious extinction risk to black rails occurs if irrigation districts mandate water cutbacks during drought, with one-quarter and one-half of the model iterations falling below this threshold within 50 and 100 years, respectively.

While our simulations should not be viewed as predictions of future conditions, they do provide information on how this CHANS is likely to respond, which can inform decisions (Bousquet and Le Page 2004, Liu et al. 2015). Neither of our assessed incentive policies—protecting wetlands and providing free water to landowners outside of drought cutback years—was effective at ameliorating risk to black rails from drought or reducing their sensitivity to precipitation. Creation-incentive wetland programs had high rates of landowner interest (Appendix S3.2: Table S15), but were more expensive and their gains in occupancy during

normal precipitation years disappeared when irrigation water was cutback during drought. Thus, adding wetlands outside of drought years did not bolster overall occupancy sufficiently to reduce the risk posed by drought cutbacks. Wetland protection schemes designed to encourage landowners to continue irrigating their wetlands were cheaper, but yielded only slight reductions in extinction risk over very long time periods. Sensitivity analysis (Fig. 3.4) suggested additional ways to reduce extinction risk, especially by increasing the water storage capacity of irrigation districts (Appendix S3.3). If combined with guaranteed water allocations for wetlands that were preserved during drought, this may be a politically feasible middle ground, providing landowners with additional and more secure water supplies and environmental benefits to trade-off against the impacts of reservoir construction.

We found that water conservation policies encouraging landowners to reduce irrigation "waste" that feeds wetlands, even if only during drought years, may reduce rail metapopulations to near extinction thresholds. Recent studies have documented similar systems where irrigation runoff and leaks have created numerous patchy wetlands that support bird communities in Europe (Moreno-Mateos et al. 2009) and semi-arid regions in the Western US (Sueltenfuss et al. 2013, Palta et al. 2017). Our study is the first to assess how water conservation policies impact such systems, and suggests caution is needed. Humans have caused profound loss of natural wetlands and existing environmental policies have focused on preventing their further degradation. However, some wetland species may have suffered an "extinction debt" (Tilman et al. 1994) from loss of natural wetlands, and are persisting primarily due to the presence of irrigated wetlands. Integrating accidental wetlands into regional water management goals may provide more cost-effective conservation benefits than attempting to restore a lost "natural" state.

References

Acevedo, M. A., R. J. Fletcher, R. L. Tremblay, and E. J. Meléndez-Ackerman. 2015. Spatial asymmetries in connectivity influence colonization−extinction dynamics. Oecologia 179:415–424.

Alberti, M., H. Asbjornsen, L. A. Baker, N. Brozovic, L. E. Drinkwater, S. A. Drzyzga, C. A. Jantz, J. Fragoso, D. S. Holland, T. A. Kohler, J. Liu, W. J. McConnell, H. D. G. Maschner, J. D. A. Millington, M. Monticino, G. Podestá, R. G. Pontius, C. L. Redman, N. J. Reo, D. Sailor, and G. Urquhart. 2011. Research on coupled human and natural systems (CHANS): approach, challenges, and strategies. Bulletin of the Ecological Society of America 92:218–228.

Allen, C., H. Birge, D. Angeler, C. Arnold, B. Chaffin, D. DeCaro, A. Garmestani, and L. Gunderson. 2018. Quantifying uncertainty and trade-offs in resilience assessments. Ecology and Society 23.

Altizer, S., R. Ostfeld, P. Johnson, S. Kutz, and C. Harvell. 2013. Climate change and infectious diseases: from evidence to a predictive framework. Science 341:514–519.

Amarasekare, P., and H. Possingham. 2001. Patch dynamics and metapopulation theory: the case of successional species. Journal of Theoretical Biology 209:333–344.

An, L. 2012. Modeling human decisions in coupled human and natural systems: Review of agent-based models. Ecological Modelling 229:25–36.

Anderson, B. J., H. R. Akçakaya, M. B. Araújo, D. A. Fordham, E. Martinez-Meyer, W. Thuiller, and B. W. Brook. 2009. Dynamics of range margins for metapopulations under climate change. Proceedings of the Royal Society B 276:1415–1420.

Angeler, D. G., and C. R. Allen. 2016. Quantifying resilience. Journal of Applied Ecology 53:617–624.

Anselme, B., F. Bousquet, A. Lyet, M. Etienne, B. Fady, and C. Le Page. 2010. Modelling of spatial dynamics and biodiversity conservation on Lure mountain (France). Environmental Modelling & Software 25:1385–1398.

Beissinger, S. R., and M. I. Westphal. 1998. On the use of demographic models of population viability in endangered species management. The Journal of Wildlife Management 62:821–841.

Bell, A., and K. Jones. 2015. Explaining fixed effects: random effects modeling of time-series cross-sectional and panel data. Political Science Research and Methods 3:133–153.

Bellamy, P. E., S. A. Hinsley, and I. Newton. 1996. Local extinctions and recolonisations of passerine bird populations in small woods. Oecologia 108:64–71.

Berger, T., and P. Schreinemachers. 2006. Creating agents and landscapes for multiagent systems from random samples. Ecology and Society 11.

Blackwell, M. S. A., and E. S. Pilgrim. 2011. Ecosystem services delivered by small-scale wetlands. Hydrological Sciences Journal 56:1467–1484.

Bousquet, F., and C. Le Page. 2004. Multi-agent simulations and ecosystem management: a review. Ecological Modelling 176:313–332.

Brady, M., C. Sahrbacher, K. Kellermann, and K. Happe. 2012. An agent-based approach to modeling impacts of agricultural policy on land use, biodiversity and ecosystem services. Landscape Ecology 27:1363–1381.

Brook, B. W., N. S. Sodhi, and C. J. A. Bradshaw. 2008. Synergies among extinction drivers under global change. Trends in Ecology & Evolution 23:453–460.

Brown, K. 2014. Global environmental change I: A social turn for resilience? Progress in Human Geography 38:107–117.

Burnham, K. P., and D. R. Anderson. 2003. Model selection and multimodel inference: a practical information-theoretic approach. Springer Science & Business Media.

California Dept. of Water Resources. 2018. CIMIS station reports. https://cimis.water.ca.gov/WSNReportCriteria.aspx.

Carson, H. S., G. S. Cook, P. C. López-Duarte, and L. A. Levin. 2011. Evaluating the importance of demographic connectivity in a marine metapopulation. Ecology 92:1972–1984.

Christian-Smith, J., M. C. Levy, and P. H. Gleick. 2015. Maladaptation to drought: a case report from California, USA. Sustainability Science 10:491–501.

Clinchy, M., D. T. Haydon, and A. T. Smith. 2002. Pattern does not equal process: what does patch occupancy really tell us about metapopulation dynamics? The American Naturalist 159:351–362.

Costanza, R., L. Wainger, C. Folke, and K.-G. Mäler. 1993. Modeling complex ecological economic systems. BioScience 43:545–555.

Darsie, R. F., and R. A. Ward. 1981. Identification and geographical distribution of the mosquitoes of North America, north of Mexico. Mosquito Systematics Supplement 1:1–313.

Diffenbaugh, N. S., D. L. Swain, and D. Touma. 2015. Anthropogenic warming has increased drought risk in California. Proceedings of the National Academy of Sciences 112:3931–3936.

Dillman, D. A., J. D. Smyth, and L. M. Christian. 2014. Internet, phone, mail, and mixed-mode surveys: the tailored design method. John Wiley & Sons.

Dobson, A. D. M., and S. K. J. R. Auld. 2016. Epidemiological implications of host biodiversity and vector biology: key insights from simple models. The American Naturalist 187:405–422.

Dornier, A., and P.-O. Cheptou. 2013. Inferring contemporary dispersal processes in plant metapopulations: comparison of direct and indirect estimates of dispersal for the annual species *Crepis sancta*. Heredity 111:1–7.

Driscoll, D. A., S. C. Banks, P. S. Barton, K. Ikin, P. Lentini, D. B. Lindenmayer, A. L. Smith, L. E. Berry, E. L. Burns, A. Edworthy, M. J. Evans, R. Gibson, R. Heinsohn, B. Howland, G. Kay, N. Munro, B. C. Scheele, I. Stirnemann, D. Stojanovic, N. Sweaney, N. R. Villaseñor, and M. J. Westgate. 2014. The trajectory of dispersal research in conservation biology. Systematic Review. PLOS ONE 9:e95053.

Duffy, W. G., and S. N. Kahara. 2011. Wetland ecosystem services in California's Central Valley and implications for the Wetland Reserve Program. Ecological Applications 21:S128–S134.

Eaton, M. J., P. T. Hughes, J. E. Hines, and J. D. Nichols. 2014. Testing metapopulation concepts: effects of patch characteristics and neighborhood occupancy on the dynamics of an endangered lagomorph. Oikos 123:662–676.

Eddleman, W. R., F. L. Knopf, B. Meanley, F. A. Reid, and R. Zembal. 1988. Conservation of North American rallids. The Wilson Bulletin 100:458–475.

Elmqvist, T., C. Folke, M. Nyström, G. Peterson, J. Bengtsson, B. Walker, and J. Norberg. 2003. Response diversity, ecosystem change, and resilience. Frontiers in Ecology and the Environment 1:488–494.

Evans, A. 2012. Uncertainty and error. Pages 309–346 *in* A. J. Heppenstall, A. T. Crooks, L. M. See, and M. Batty, editors. Agent-based Models of Geographical Systems. Springer Netherlands, Dordrecht.

Ferranto, S., L. Huntsinger, C. Getz, M. Lahiff, W. Stewart, G. Nakamura, and M. Kelly. 2013. Management without borders? A survey of landowner practices and attitudes toward cross-boundary cooperation. Society & Natural Resources 26:1082–1100.

Ferraz, G., J. D. Nichols, J. E. Hines, P. C. Stouffer, R. O. Bierregaard, and T. E. Lovejoy. 2007. A large-scale deforestation experiment: effects of patch area and isolation on Amazon birds. Science 315:238–241.

Flint, L. E., and A. L. Flint. 2012. Downscaling future climate scenarios to fine scales for hydrologic and ecological modeling and analysis. Ecological Processes 1:2.

Folke, C. 2006. Resilience: The emergence of a perspective for social–ecological systems analyses. Global Environmental Change 16:253–267.

Foppen, R. P. B., J. P. Chardon, and W. Liefveld. 2008. Understanding the role of sink patches in source-sink metapopulations: reed warbler in an agricultural landscape. Conservation Biology 14:1881–1892.

Franken, R. J., and D. S. Hik. 2004. Influence of habitat quality, patch size and connectivity on colonization and extinction dynamics of collared pikas *Ochotona collaris*. Journal of Animal Ecology 73:889–896.

Franklin, J. F., and D. B. Lindenmayer. 2009. Importance of matrix habitats in maintaining biological diversity. Proceedings of the National Academy of Sciences 106:349–350.

Fronhofer, E. A., A. Kubisch, F. M. Hilker, T. Hovestadt, and H. J. Poethke. 2012. Why are metapopulations so rare? Ecology 93:1967–1978.

Gimona, A., and J. G. Polhill. 2011. Exploring robustness of biodiversity policy with a coupled metacommunity and agent-based model. Journal of Land Use Science 6:175–193.

Girard, P., J. Y. Takekawa, and S. R. Beissinger. 2010. Uncloaking a cryptic, threatened rail with molecular markers: origins, connectivity and demography of a recently-discovered population. Conservation Genetics 11:2409–2418.

Gotelli, N. J. 1991. Metapopulation Models: The rescue effect, the propagule rain, and the core-satellite hypothesis. The American Naturalist 138:768–776.

Grimm, V., E. Revilla, U. Berger, F. Jeltsch, W. M. Mooij, S. F. Railsback, H.-H. Thulke, J. Weiner, T. Wiegand, and D. L. DeAngelis. 2005. Pattern-oriented modeling of agent-based complex systems: lessons from ecology. Science 310:987–991.

Guillem, E. E., A. P. Barnes, M. D. A. Rounsevell, and A. Renwick. 2009. Farmer-induced land-use change and its impact on farmland bird populations. Aspects of Applied Biology:193–197.

Guzy, M., C. Smith, J. Bolte, D. Hulse, and S. Gregory. 2008. Policy research using agent-based modeling to assess future impacts of urban expansion into farmlands and forests. Ecology and Society 13.

Hale, R., E. A. Treml, and S. E. Swearer. 2015. Evaluating the metapopulation consequences of ecological traps. Proceedings of the Royal Society of London B: Biological Sciences 282:20142930.

Hall, L. 2015. Linked landscapes: metapopulation connectivity of secretive wetland birds. UC Berkeley.

Hall, L. A., N. D. Van Schmidt, and S. R. Beissinger. 2018. Validating dispersal distances inferred from autoregressive occupancy models with genetic parentage assignments. Journal of Animal Ecology 87:691–702.

Hames, R. S., K. V. Rosenberg, J. D. Lowe, and A. A. Dhondt. 2001. Site reoccupation in fragmented landscapes: testing predictions of metapopulation theory. Journal of Animal Ecology 70:182–190.

Hanski, I. 1994. A practical model of metapopulation dynamics. Journal of Animal Ecology 63:151–162.

Hanski, I. 1998. Metapopulation dynamics. Nature 396:41–49.

Hanski, I. A. 1999. Metapopulation Ecology. Oxford University Press.

Hanski, I., A. Moilanen, T. Pakkala, and M. Kuussaari. 1996. The quantitative incidence function model and persistence of an endangered butterfly metapopulation. Conservation Biology 10:578–590.

Hanski, I., T. Pakkala, M. Kuussaari, and G. Lei. 1995. Metapopulation persistence of an endangered butterfly in a fragmented landscape. Oikos 72:21–28.

Heard, G. W., M. A. McCarthy, M. P. Scroggie, J. B. Baumgartner, and K. M. Parris. 2013. A Bayesian model of metapopulation viability, with application to an endangered amphibian. Diversity and Distributions 19:555–566.

Henderson, M. T., G. Merriam, and J. Wegner. 1985. Patchy environments and species survival: Chipmunks in an agricultural mosaic. Biological Conservation 31:95–105.

Hines, J. E. 2013. PRESENCE - Software to estimate patch occupancy and related parameters. U.S.G.S. Patuxent Wildlife Research Center, Laurel, MD, USA.

Hodgson, D., J. L. McDonald, and D. J. Hosken. 2015. What do you mean, ‘resilient’? Trends in Ecology & Evolution 30:503–506.

Hof, C., M. B. Araújo, W. Jetz, and C. Rahbek. 2011. Additive threats from pathogens, climate and land-use change for global amphibian diversity. Nature 480:516–519.

Holling, C. S. 1973. Resilience and stability of ecological systems. Annual Review of Ecology and Systematics 4:1–23.

Holling, C. S. 1996. Engineering resilience versus ecological resilience. Pages 31–43 Engineering Within Ecological Constraints.

Hooper, D. U., F. S. Chapin, J. J. Ewel, A. Hector, P. Inchausti, S. Lavorel, J. H. Lawton, D. M. Lodge, M. Loreau, S. Naeem, B. Schmid, H. Setälä, A. J. Symstad, J. Vandermeer, and D. A. Wardle. 2005. Effects of Biodiversity on Ecosystem Functioning: A Consensus of Current Knowledge. Ecological Monographs 75:3–35.

Hruska, T., L. Huntsinger, M. Brunson, W. Li, N. Marshall, J. L. Oviedo, and H. Whitcomb. 2017. Rangelands as social–ecological systems. Pages 263–302 *in* D. D. Briske, editor. Rangeland Systems. Springer International Publishing.

Huntsinger, L., H. Tracy, J. L. Oviedo, M. W. K. Shapero, G. A. Nader, R. S. Ingram, and S. R. Beissinger. 2017. Save water or save wildlife? Water use and conservation in the Central Sierran foothill oak woodlands of California, USA. Ecology and Society 22:12.

Ims, R. A. 2005. The role of experiments in landscape ecology. Pages 70–78 *in* J. A. Wiens and M. R. Moss, editors. Issues and Perspectives in Landscape Ecology. Cambridge University Press.

Ingrisch, J., and M. Bahn. 2018. Towards a comparable quantification of resilience. Trends in Ecology & Evolution 33:251–259.

Iwamura, T., E. F. Lambin, K. M. Silvius, J. B. Luzar, and J. M. V. Fragoso. 2014. Agent-based modeling of hunting and subsistence agriculture on indigenous lands: understanding interactions between social and ecological systems. Environmental Modelling & Software 58:109–127.

Janssen, M., and E. Ostrom. 2006. Empirically based, agent-based models. Ecology and Society 11.

Kareiva, P., and M. Marvier. 2012. What is conservation science? BioScience 62:962–969.

Kauffman, E. B., S. A. Jones, A. P. Dupuis, K. A. Ngo, K. A. Bernard, and L. D. Kramer. 2003. Virus detection protocols for west nile virus in vertebrate and mosquito specimens. Journal of Clinical Microbiology 41:3661–3667.

Kilpatrick, A. M., and W. J. Pape. 2013. Predicting human West Nile virus infections with Mosquito surveillance data. American Journal of Epidemiology 178:829–835.

Kilpatrick, A. M., R. J. Peters, A. P. Dupuis, M. J. Jones, P. Daszak, P. P. Marra, and L. D. Kramer. 2013. Predicted and observed mortality from vector-borne disease in wildlife: West Nile virus and small songbirds. Biological Conservation 165:79–85.

Kovach, T. J., and A. M. Kilpatrick. 2018. Increased human incidence of West Nile virus disease near rice fields in California but not in southern United States. The American Journal of Tropical Medicine and Hygiene:10.4269/ajtmh.18-0120.

Kramer, D., J. Hartter, A. Boag, M. Jain, K. Stevens, K. Nicholas, W. McConnell, and J. Liu. 2017. Top 40 questions in coupled human and natural systems (CHANS) research. Ecology and Society 22.

Lee, D. E., and D. T. Bolger. 2017. Movements and source–sink dynamics of a Masai giraffe metapopulation. Population Ecology 59:157–168.

Lee, J.-S., T. Filatova, A. Ligmann-Zielinska, B. Hassani-Mahmooei, F. Stonedahl, I. Lorscheid, A. Voinov, J. G. Polhill, Z. Sun, and D. C. Parker. 2015. The complexities of agent-based modeling output analysis. Journal of Artificial Societies and Social Simulation 18:4.

Lemly, A. D., R. T. Kingsford, and J. R. Thompson. 2000. Irrigated agriculture and wildlife conservation: conflict on a global scale. Environmental Management 25:485–512.

Leslie, P., and J. T. McCabe. 2013. Response diversity and resilience in social-ecological systems. Current Anthropology 54:114–143.

Levins, R. 1969. Some demographic and genetic consequences of environmental heterogeneity for biological control. Bulletin of the Entomological Society of America 15:237–240.

Liu, J., T. Dietz, S. R. Carpenter, M. Alberti, C. Folke, E. Moran, A. N. Pell, P. Deadman, T. Kratz, J. Lubchenco, E. Ostrom, Z. Ouyang, W. Provencher, C. L. Redman, S. H. Schneider, and W. W. Taylor. 2007. Complexity of coupled human and natural systems. Science 317:1513–1516.

Liu, J., H. Mooney, V. Hull, S. J. Davis, J. Gaskell, T. Hertel, J. Lubchenco, K. C. Seto, P. Gleick, C. Kremen, and S. Li. 2015. Systems integration for global sustainability. Science 347:1258832.

Lunde, K. B., and V. H. Resh. 2012. Development and validation of a macroinvertebrate index of biotic integrity (IBI) for assessing urban impacts to Northern California freshwater wetlands. Environmental Monitoring and Assessment 184:3653–3674.

MacKenzie, D. I., J. D. Nichols, J. E. Hines, M. G. Knutson, and A. B. Franklin. 2003. Estimating site occupancy, colonization, and local extinction when a species is detected imperfectly. Ecology 84:2200–2207.

MacPherson, J. L., and P. W. Bright. 2011. Metapopulation dynamics and a landscape approach to conservation of lowland water voles (*Arvicola amphibius*). Landscape Ecology 26:1395–1404.

Matthysen, E. 1999. Nuthatches (*Sitta europaea*) in forest fragments: demography of a patchy population. Oecologia 119:501–509.

Moilanen, A., and M. Nieminen. 2002. Simple connectivity measures in spatial ecology. Ecology 83:1131–1145.

Moreno-Mateos, D., C. Pedrocchi, and F. A. Comín. 2009. Avian communities' preferences in recently created agricultural wetlands in irrigated landscapes of semi-arid areas. Biodiversity and Conservation 18:811–828.

O'Geen, A. T., J. J. Maynard, and R. A. Dahlgren. 2007. Efficacy of constructed wetlands to mitigate non-point source pollution from irrigation tailwaters in the San Joaquin Valley, California, USA. Water Science and Technology 55:55–61.

Olivier, P. I., R. J. V. Aarde, and S. M. Ferreira. 2009. Support for a metapopulation structure among mammals. Mammal Review 39:178–192.

Olsson, P., L. H. Gunderson, Carpenter, P. Ryan, L. Lebel, C. Folke, and C. S. Holling. 2006. Shooting the rapids: navigating transitions to adaptive governance of social-ecological systems. Ecology and Society 11.

O'Sullivan, D., T. Evans, S. Manson, S. Metcalf, A. Ligmann-Zielinska, and C. Bone. 2016. Strategic directions for agent-based modeling: avoiding the YAAWN syndrome. Journal of Land Use Science 11:177–187.

Ozgul, A., K. B. Armitage, D. T. Blumstein, D. H. Vanvuren, and M. K. Oli. 2006. Effects of patch quality and network structure on patch occupancy dynamics of a yellow-bellied marmot metapopulation. Journal of Animal Ecology 75:191–202.

Palta, M. M., N. B. Grimm, and P. M. Groffman. 2017. "Accidental" urban wetlands: ecosystem functions in unexpected places. Frontiers in Ecology and the Environment 15:248–256.

Parker, D. C., S. M. Manson, M. A. Janssen, M. J. Hoffmann, and P. Deadman. 2003. Multi-agent systems for the simulation of land-use and land-cover change: a review. Annals of the Association of American Geographers 93:314–337.

Parry, H. R., C. J. Topping, M. C. Kennedy, N. D. Boatman, and A. W. A. Murray. 2013. A Bayesian sensitivity analysis applied to an agent-based model of bird population response to landscape change. Environmental Modelling & Software 45:104–115.

Peterson, G., C. R. Allen, and C. S. Holling. 1998. Ecological resilience, biodiversity, and scale. Ecosystems 1:6–18.

Piessens, K., O. Honnay, and M. Hermy. 2005. The role of fragment area and isolation in the conservation of heathland species. Biological Conservation 122:61–69.

Poos, M. S., and D. A. Jackson. 2012. Impact of species-specific dispersal and regional stochasticity on estimates of population viability in stream metapopulations. Landscape Ecology 27:405–416.

Pulliam, H. R. 1988. Sources, sinks, and population regulation. The American Naturalist 132:652–661.

Quinlan, A. E., M. Berbés-Blázquez, L. J. Haider, and G. D. Peterson. 2015. Measuring and assessing resilience: broadening understanding through multiple disciplinary perspectives. Journal of Applied Ecology 53:677–687.

R Core team. 2013. R: A language and environment for statistical computing. R Foundation for Statistical Computing, Vienna, Austria.

Ranius, T., P. Bohman, O. Hedgren, L.-O. Wikars, and A. Caruso. 2014. Metapopulation dynamics of a beetle species confined to burned forest sites in a managed forest region. Ecography 37:797–804.

Richmond, O. M., J. Tecklin, and S. R. Beissinger. 2008. Distribution of California black rails in the Sierra Nevada foothills. Journal of Field Ornithology 79:381–390.

Richmond, O. M. W., S. K. Chen, B. B. Risk, J. Tecklin, and S. Beissinger. 2010a. California black rails depend on irrigation-fed wetlands in the Sierra Nevada foothills. California Agriculture 64:85–93.

Richmond, O. M. W., J. E. Hines, and S. R. Beissinger. 2010b. Two-species occupancy models: a new parameterization applied to co-occurrence of secretive rails. Ecological Applications 20:2036–2046.

Risk, B. B., P. de Valpine, and S. R. Beissinger. 2011. A robust-design formulation of the incidence function model of metapopulation dynamics applied to two species of rails. Ecology 92:462–474.

Runge, J. P., M. C. Runge, and J. D. Nichols. 2006. The role of local populations within a landscape context: defining and classifying sources and sinks. The American Naturalist 167:925–938.

Salas, J. D. 1993. Analysis and modelling of hydrological time series. Pages 1–72 *in* D. Maidment, editor. Handbook of Hydrology. McGraw-Hill Inc., New York, NY.

Sanford, T., P. C. Frumhoff, A. Luers, and J. Gulledge. 2014. The climate policy narrative for a dangerously warming world. Nature Climate Change 4:164–166.

Schlüter, M., R. R. J. Mcallister, R. Arlinghaus, N. Bunnefeld, K. Eisenack, F. Hölker, E. j. Milner-Gulland, B. Müller, E. Nicholson, M. Quaas, and M. Stöven. 2012. New horizons for managing the environment: a review of coupled social-ecological systems modeling. Natural Resource Modeling 25:219–272.

Schooley, R. L., and L. C. Branch. 2007. Spatial heterogeneity in habitat quality and cross-scale interactions in metapopulations. Ecosystems 10:846–853.

Schouten, M., P. Opdam, N. Polman, and E. Westerhof. 2013. Resilience-based governance in rural landscapes: Experiments with agri-environment schemes using a spatially explicit agent-based model. Land Use Policy 30:934–943.

Schreinemachers, P., and T. Berger. 2011. An agent-based simulation model of human–environment interactions in agricultural systems. Environmental Modelling & Software 26:845–859.

Sinsch, U. 1992. Structure and dynamic of a natterjack toad metapopulation (*Bufo calamita*). Oecologia 90:489–499.

Sjögren-Gulve, P., and I. Hanski. 2000. Metapopulation viability analysis using occupancy models. Ecological Bulletins 48:53–71.

Sorice, M. G., U. P. Kreuter, B. P. Wilcox, and W. E. Fox. 2014. Changing landowners, changing ecosystem? Land-ownership motivations as drivers of land management practices. Journal of Environmental Management 133:144–152.

Stacey, P. B., M. L. Taper, and V. A. Johnson. 1997. 12 - Migration within metapopulations: the impact upon local population dynamics. Pages 267–291 *in* I. Hanski and M. E. Gilpin, editors. Metapopulation Biology. Academic Press, San Diego.

Sueltenfuss, J. P., D. J. Cooper, R. L. Knight, and R. M. Waskom. 2013. The creation and maintenance of wetland ecosystems from irrigation canal and reservoir seepage in a semi-arid landscape. Wetlands 33:799–810.

Sutherland, C., D. A. Elston, and X. Lambin. 2012. Multi-scale processes in metapopulations: contributions of stage structure, rescue effect, and correlated extinctions. Ecology 93:2465–2473.

de Szalay, F. A., L. C. Carroll, J. A. Beam, and V. H. Resh. 2003. Temporal overlap of nesting duck and aquatic invertebrate abundances in the Grasslands Ecological Area, California, USA. Wetlands 23:739–749.

Thornton, P. K., P. G. Jones, G. Alagarswamy, and J. Andresen. 2009. Spatial variation of crop yield response to climate change in East Africa. Global Environmental Change 19:54–65.

Tilman, D., R. M. May, C. L. Lehman, and M. A. Nowak. 1994. Habitat destruction and the extinction debt. Nature 371:65–66.

Tobin, J. 1958. Estimation of relationships for limited dependent variables. Econometrica 26:24–36.

U.S. Bureau of Reclamation, and California Department of Water Resources. 2009, September 1. Private Water Districts. MPGIS Service Center.

US Environmental Protection Agency. 2013. Level III ecoregions of the conterminous United States. U.S. EPA Office of Research and Development (ORD) - National Health and Environmental Effects Research Laboratory (NHEERL), Corvallis, OR.

Vergara, P. M., A. Saravia-Zepeda, N. Castro-Reyes, and J. A. Simonetti. 2016. Is metapopulation patch occupancy in nature well predicted by the Levins model? Population Ecology 58:335–343.

Wilensky, U. 2018. NetLogo. Center for connected learning and computer-based modeling, Northwestern University, Evanston, IL.

Wolfe, N., P. Daszak, A. M. Kilpatrick, and D. Burke. 2005. Bushmeat hunting, deforestation, and prediction of zoonotic emergence. Emerging Infectious Diseases 11:1822–1827.

Appendices

Appendix S1.1: Supplementary information for Chapter 1

This appendix contains model selection tables, regression and factor analysis results, and West Nile virus analysis figures for Chapter 1.

Appendix S1.1: Table S1. AIC table for Tobit (censored 0–1) models of wetness of Sierra Nevada foothills wetlands, 2013–2016, with a random effect for site. Period is a factor representing 12 sampling time periods, source is a factor representing three water sources (natural-only, irrigation-only, both-source) and area was natural log of wetland size in hectares.

Model	**ΔAIC**	**AIC**	***w***	***K***
Period + source + source×period + area	0.00	294.95	0.766	45
Period + source + source×period + area + area×period	2.44	297.39	0.226	58
Period + source + source×period + area + area×period + source×area	10.26	305.21	0.005	60
Period + source + source×period + area + source×area	10.47	305.42	0.004	47
Period + source + source×period + area + area×period + source×area + source×area×period	25.63	320.58	0.000	86
Period + source + source×period	52.98	347.93	0.000	44
Period + source + area + area×period + source×area	61.65	356.60	0.000	32
Period + source + area + source×area	66.92	361.88	0.000	34
Period + area + area×period	74.11	369.06	0.000	30
Period + source + area + area×period	90.50	385.45	0.000	19
Period + source + area	93.50	388.45	0.000	21
Period + area	101.49	396.44	0.000	17
Period + source	139.21	434.16	0.000	18
Period	164.36	459.31	0.000	16

Appendix S1.1: Table S2. Landowner typologies in California's Sierra Nevada foothills as determined via weightings in a factorial analysis from a survey question on 20 reasons for land ownership (n = 354). These six typologies accounted for 64% of the variance in reasons for land ownership. Loadings are grouped and shown in bold by their landowner type.

Landowner typology (% of sample)	Reason for land ownership	Factor 1	2	3	4	5	6
Lifestyle-motivated (16.9%)	I want to escape or stay away from the city	**0.839**	0.140	0.049	0.180	0.028	0.021
	I like to live in a smaller community	**0.839**	0.158	0.045	0.189	0.020	0.030
	This is a healthy place to live	**0.631**	0.421	0.147	0.128	0.120	0.054
	I like to live near natural beauty	**0.599**	0.516	-0.060	0.126	-0.030	0.172
	To grow some of my own food	**0.539**	0.272	0.410	0.078	0.045	-0.016
Environment-motivated (15.3%)	My land allows me to protect the environment	0.267	**0.773**	0.058	0.129	-0.024	0.190
	To preserve open space	0.163	**0.759**	0.125	0.111	0.065	-0.120
	I want to restore and manage this land	0.126	**0.672**	0.388	0.191	0.073	0.022
	I enjoy improving this land	0.253	**0.620**	0.416	0.055	0.050	0.016
	I enjoy seeing wildlife and/or birds	0.518	**0.565**	-0.119	0.053	0.186	-0.044
Profit-motivated (15.8%)	To raise cattle or sheep	0.077	0.024	**0.775**	0.174	-0.059	-0.139
	My land is a source of income	-0.070	0.170	**0.771**	0.195	-0.066	0.270
	Living on this land is a family business	0.040	0.086	**0.742**	0.408	-0.006	0.125
	To contribute to the local economy	0.075	0.337	**0.681**	0.131	0.124	0.172
	To raise horses, ponies, donkeys, or mules	0.375	0.039	**0.429**	-0.257	0.202	-0.021
Tradition-motivated (16.7%)	I was born here or near here	0.030	-0.013	0.319	**0.704**	0.043	-0.202
	A good place to raise my children	0.220	0.066	0.175	**0.678**	0.089	0.012
	I want to pass this land to my heirs	0.055	0.320	0.072	**0.608**	0.069	0.121
	I am closer to friends and family here	0.363	0.191	0.139	**0.581**	0.102	0.094
Recreation-motivated (20.1%)	For vacations	0.025	0.082	-0.008	0.062	**0.760**	0.078
	For recreation	0.258	0.347	-0.051	0.113	**0.677**	-0.066
	To develop the land for future residential use	-0.220	-0.183	-0.025	0.034	**0.554**	0.406
	I enjoy hunting or fishing	0.193	-0.071	0.398	0.122	**0.507**	-0.263
Investment-motivated (15.3%)	My land is a financial investment	0.166	0.076	0.184	0.010	0.057	**0.827**

Appendix S1.1: Table S3. Logistic regression coefficients (SE in parentheses) for Sierra Nevada foothills landowners' management actions in response to a hypothetical water availability cutback (either 20, 50, or 100%; included as a continuous covariate) from all sources (*n = 274)*. Asterisks (*, **, ***) denote significance at the 10, 5, and 1% levels.

Parameter	**Wetland-impacting action[a]**	**Landowner-impacting action [b]**
Intercept (investment-motivated)	-1.1503*** (0.3732)	-0.7160** (0.3385)
Profit-motivated	2.2133*** (0.5032)	2.0702*** (0.4937)
Tradition-motivated	1.1467** (0.4924)	0.7343 (0.4615)
Lifestyle-motivated	1.1178** (0.4763)	0.7979* (0.4474)
Environment-motivated	0.2088 (0.5165)	0.7538 (0.4597)
Recreation-motivated	0.1437 (0.4857)	-0.1673 (0.4572)
Water cutback (%)	-0.1934 (0.2690)	0.2178 (0.2590)
Household income ($ 2013)	0.7315*** (0.2781)	0.1301 (0.2662)
Property size (acres)	0.6822* (0.3935)	0.6105* (0.3666)

[a] Includes responses "Repair leaks in ditches, pipes, dams and/or ponds", "Recycle and/or reuse tailwater, irrigation or pond runoff", "Stop or use less water to irrigate pasture(s)" and "Reduce area of irrigated pasture".

[b] Includes responses "Stop or reduce growing crops or gardening", "Sell livestock or reduce stocking rate", "Find other grazing land", "Sell some or all the land", "Purchase water from outside (non-district) sources" and "Change to a different land use."

Appendix S1.1: Table S4. Backwards stepwise AIC model selection table for a multi-season occupancy model for the Sierra Nevada foothills metapopulation of the black rail (*Laterallus jamaicensis*), 2012–2016. Starting with the full model (step 0), nuisance parameters (area, isolation, and year) were removed one at a time, and the lowest AIC was selected. The process was repeated until we found the lowest AIC (bold). Water source (natural, irrigated, or both; irrigated left out) was in all models.

Step	Model	ΔAIC	AIC	*w*	*K*
3	Ψ(area, nat[B], both), γ(year, area, nat, both), ε(area, nat, both), p(.)	1.32	1450.17	0.2199	16
3	Ψ(area, nat, both), γ(year, nat, both), ε(year, area, nat, both), p(.)	3.78	1452.63	0.0643	18
3	Ψ(area, nat, both), γ(area, nat, both), ε(year, area, nat, both), p(.)[A]	7.43	1456.28	0.0104	16
2	**Ψ(area, nat, both), γ(year, area, nat, both), ε(year, area, nat, both), p(.)**	**0.00**	**1448.85**	**0.4255**	**19**
2	Ψ(area, iso[C], nat, both), γ(year, area, iso, nat, both), ε(area, nat, both), p(.)	3.79	1452.64	0.064	18
2	Ψ(area, iso, nat, both), γ(year, iso, nat, both), ε(year, area, nat, both), p(.)	4.71	1453.56	0.0404	20
2	Ψ(area, iso, nat, both), γ(area, iso, nat, both), ε(year, area, nat, both), p(.)[A]	9.73	1458.58	0.0033	18
2	Ψ(area, nat, both), γ(year, area, nat, both), ε(year, nat, both), p(.)	29.91	1478.76	0.0000	18
1	Ψ(area, iso, nat, both), γ(year, area, iso, nat, both), ε(year, area, nat, both), p(.)	2.58	1451.43	0.1171	21
1	Ψ(area, nat, both), γ(year, area, nat, both), ε(year, area, nat, both), p(year)	4.97	1453.82	0.0355	23
1	Ψ(area, iso, nat, both), γ(year, area, iso, nat, both), ε(area, nat, both), p(year)	8.03	1456.88	0.0077	22
1	Ψ(area, iso, nat, both), γ(year, iso, nat, both), ε(year, area, nat, both), p(year)	10.18	1459.03	0.0026	24
1	Ψ(area, iso, nat, both), γ(area, iso, nat, both), ε(year, area, nat, both), p(year)[A]	15.33	1464.18	0.0002	22
1	Ψ(area, iso, nat, both), γ(year, area, iso, nat, both), ε(year, nat, both), p(.)	32.02	1480.87	0.0000	20
1	Ψ(area, iso, nat, both), γ(year, area, iso, nat, both), ε(year, nat, both), p(year)	34.44	1483.29	0.0000	24
0	Ψ(area, iso, nat, both), γ(year, area, iso, nat, both), ε(year, area, nat, both), p(year)	7.68	1456.53	0.0091	25
Null	Ψ(.), γ(.), ε(.), p(.)	111.10	1559.95	0.0000	4

[A] Models that did not include a year effect on γ had convergence problems (the "natural" beta estimate became infinitely negative)
[B] Natural
[C] Isolation

Appendix S1.1: Table S5. AIC table for multi-season occupancy models for the Sierra Nevada foothills metapopulation of the black rail (*Laterallus jamaicensis*), 2012–2016, to assess the impact of water source on occupancy. All models except for the "true null model" have area as a covariate for Ψ, γ, and ε, and year dummy variables as covariates for γ and ε.

Model	**ΔAIC**	**AIC**	***w***	***K***
Ψ(natural, both), γ(natural, both), ε(natural), p(.)	0.00	1447.35	0.3017	18
Ψ(natural, both), γ(natural, both), ε(.), p(.)	0.60	1447.95	0.2235	17
Ψ(natural, both), γ(natural, both), ε(natural, both), p(.)	1.50	1448.85	0.1425	19
Ψ(natural, both), γ(natural, both), ε(both), p(.)	2.43	1449.78	0.0895	18
Ψ(natural), γ(natural), ε(natural), p(.)	3.02	1450.37	0.0667	16
Ψ(natural, both), γ(both), ε(natural), p(.)	3.61	1450.96	0.0496	17
Ψ(natural), γ(natural), ε(.), p(.)	3.68	1451.03	0.0479	15
Ψ(natural, both), γ(both), ε(natural, both), p(.)	5.02	1452.37	0.0245	18
Ψ(natural, both), γ(natural), ε(natural, both), p(.)	5.10	1452.45	0.0236	18
Ψ(natural, both), γ(natural), ε(both), p(.)	5.93	1453.28	0.0156	17
Ψ(both), γ(both), ε(.), p(.)	6.86	1454.21	0.0098	15
Ψ(both), γ(both), ε(both), p(.)	8.72	1456.07	0.0039	16
Ψ(natural), γ(.), ε(natural), p(.)	11.81	1459.16	0.0008	15
Ψ(natural, both), γ(.), ε(natural, both), p(.)	13.84	1461.19	0.0003	17
Ψ(both), γ(.), ε(both), p(.)	17.78	1465.13	0.0000	15
Ψ(.), γ(.), ε(.), p(.)	17.84	1465.19	0.0000	13
True null model	112.60	1559.95	0.0000	4

Appendix S1.1: Table S6. AIC table for bias-reduced general linear models (binomial distribution and offsets accounting for differences in number of mosquitoes per pool) used to estimate West Nile virus prevalence at wetlands (n = 63) in the Sierra Nevada foothills.

Model	**ΔAIC**	**AIC**	***w***	***K***
site + date + date^2 + year	0.0	1561.30	0.501	67
site + date + date^2	0.5	1561.78	0.394	65
site	3.8	1565.09	0.075	63
site + date	5.7	1566.95	0.030	64
site×date + date2 + year	76.9	1638.23	0.000	129
site×date + site×date^2 + year	183.1	1744.44	0.000	191
site×date + site×date^2 + site*year	207.4	1768.69	0.000	215

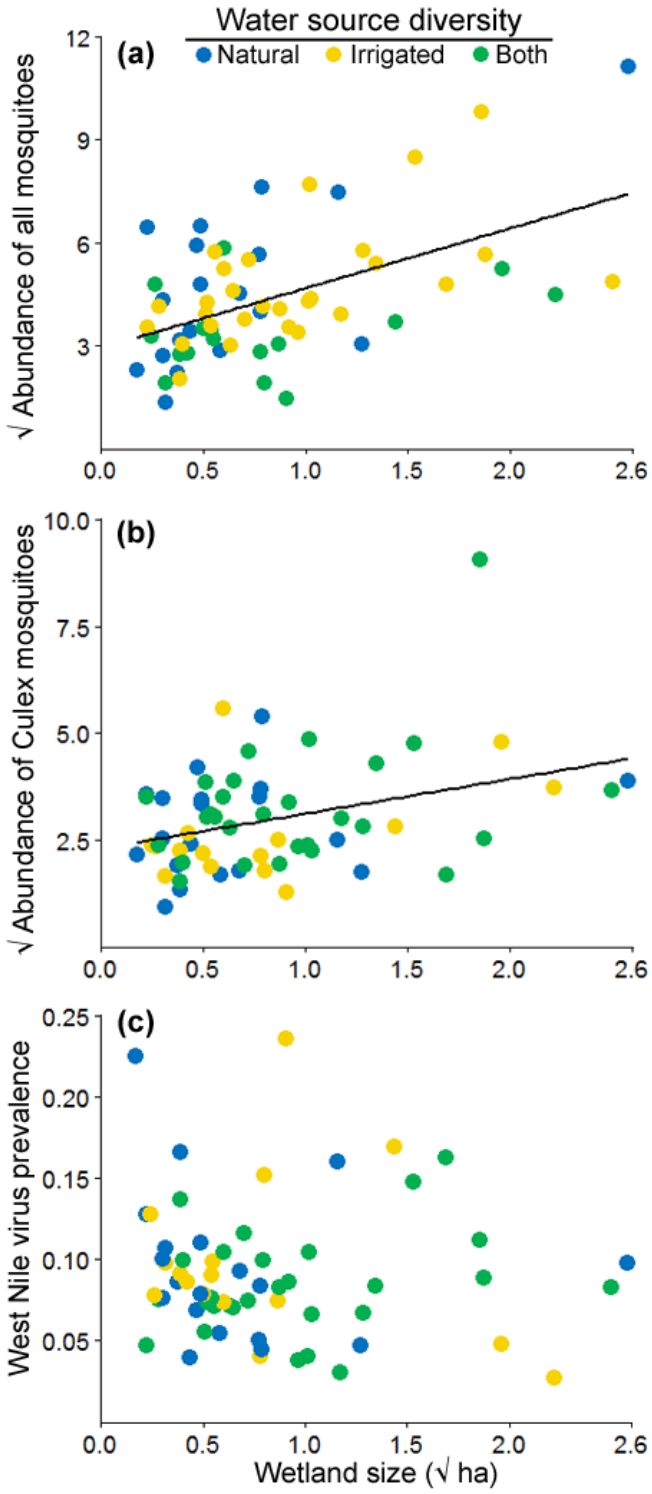

Appendix S1.1: Figure S1. Relationships between wetland size and three elements of West Nile virus transmission risk in the Sierra Nevada foothills. (a) Mean number of all mosquitoes caught per trap/night increased with wetland size ($abundance^{0.5} = 2.94 + 1.74 * size^{0.5}$, $r^2 = 0.27$, $p < 0.001$). (b) Mean number of *Culex* mosquitoes caught per trap/night increased with wetland size ($abundance^{0.5} = 2.31 + 0.81 \times size^{0.5}$, $r^2 = 0.12$, $p = 0.005$). (c) There was no relationship between mean West Nile virus prevalence in *Culex* and wetland size ($p = 0.671$).

Appendix S2.1: Preliminary rescue effect modeling and additional results

We surveyed 205 wetlands annually for black and Virginia rail occupancy from 2002–2006 during the breeding season (late May to early August). Wetlands were surveyed with call broadcast methods as described in (Richmond et al. 2008, 2010b), with up to 3 visits each summer (5 in 2002) to use in occupancy models that correct for detection probability (MacKenzie et al. 2003). We began recording Virginia rail responses in 2004, but did not use Virginia rail calls during all three visits until 2006 (Richmond et al. 2010b).

We analyzed these data using multi-season occupancy models in Program PRESENCE v12.19 (Hines 2013); see main text for details and isolation measures used. Our original preliminary analysis used only single-covariate models and the only isolation measure was the geometric mean distance to the nearest three naïvely occupied sites in the previous year ("DTN"). To facilitate direct comparison with results for the 2013–2016 nonequilibrium period, we here present a revised preliminary analysis with all three measures, using the same base models that used for the nonequilibrium analysis. Year-specific detection probabilities were included for both species to account for differences in surveyors; because Virginia rail playback was not conducted at all visits in 2004–2005, "no playback" was also included as a dummy variable in Virginia rail models for visits when only black rail calls were played. We then ran a model set for each species that included the DTN, IFM, and BRM on γ only, ε only, or both. AIC model selection results are in Appendix S2.1: Table S1. The black rail and Virginia rail "DTN γ, ε" model (because this was the measure used in our original preliminary analysis) are in Appendix S2.1: Table S2 and Appendix S2.1: Table S3, respectively, along with the same model from the 2013–2016 nonequilibrium period for comparison (see main text). Isolation-extinction relationships from these models are shown in the main text Fig. 2.1. Model parameters had high standard errors, indicating uncertainty due to low Virginia rail detectability in the first years of the study (Appendix S2.1: Table S3). For comparison with the main text Fig. 2.2, We graphed the estimated rescue effect for an average site within our full sample in 2006 (median area = 0.47 ha, median elevation = 123 m, slope geomorphology, both water sources) for 2006, the final year of our equilibrium surveys (Appendix S2.1: Fig. S1).

Appendix S2.1: Table S1. AIC model selection table for isolation effects on colonization and extinction rates of two rail species occupying wetlands in the foothills of California's Sierra Nevada during a period of dynamic equilibrium (2002–2006). Base model included area, slope, water source, and elevation (Virginia rail only) as covariates. DTN = distance to nearest 3 sites with detections; BRM = autoregressive buffer radius measure; IFM = autoregressive incidence function measure.

Black rail (*n* = 205)					**Virginia rail (*n* = 204)**				
Model	**ΔAIC**	**AIC**	***w***	***K***	**Model**	**ΔAIC**	**AIC**	***w***	***K***
DTN γ, ε	0.00	1020.89	0.675	22	BRM γ, ε*	0.00	636.75	0.208	17
DTN γ	1.53	1022.42	0.314	21	IFM ε*	0.47	637.22	0.164	16
BRM γ, ε	9.96	1030.85	0.004	22	BRM ε*	1.00	637.75	0.126	16
BRM γ	10.48	1031.37	0.004	21	Base	1.02	637.77	0.125	15
DTN ε	14.02	1034.91	0.001	21	DTN γ	1.76	638.51	0.086	16
IFM γ	14.08	1034.97	0.001	21	IFM γ*, ε*	2.11	638.86	0.072	17
BRM ε	15.24	1036.13	0.000	21	IFM γ*	2.16	638.91	0.071	16
IFM ε	15.49	1036.38	0.000	21	DTN γ, ε*	2.76	639.51	0.052	17
IFM γ, ε	15.61	1036.50	0.000	22	DTN ε	2.90	639.65	0.049	16
Base	18.72	1039.61	0.000	20	BRM γ*	2.96	639.71	0.047	16
Null	108.83	1129.72	0.000	4	Null	67.41	704.16	0.000	4

* Anti-rescue or anti-colonization effect (opposite direction predicted by theory)

Appendix S2.1: Table S2. Occupancy models of black rail metapopulation dynamics with DTN isolation effects on both γ and ε, comparing a preliminary analysis during a period of equilibrium from 2004–2006 (n = 205) to the main analysis during a nonequilibrium period from 2013–2016 (n = 125) in the foothills of the California Sierra Nevada. All continuous variables were standardized.

Metapopulation parameter	**Beta parameter**	**Equilibrium**		**Nonequilibrium**	
		Coefficient	**SE**	**Coefficient**	**SE**
Initial Occupancy	Intercept	-0.166641	0.468735	-1.809821	0.712555
	Area	0.798365	0.294622	1.956714	0.418720
	Slope	1.483825	0.506288	2.424694	0.756191
	Both-source	0.526529	0.574059	-0.217229	0.531284
	Natural-only	-0.934062	0.635976	-2.573195	1.298110
Colonization	Intercept	-1.825006	0.286126	-3.252210	0.585790
	DTN	-0.704070	0.196825	-0.770591	0.327804
	Area	0.680988	0.223210	0.501904	0.382515
	Precipitation	0.209098	0.186610	0.449925	0.305281
	Slope	0.717003	0.361086	0.833128	0.711268
	Both-source	0.922160	0.357742	0.925068	0.523820
Extinction	Intercept	-0.503457	0.363743	-2.578650	1.667735
	DTN	0.366804	0.195251	0.742201	0.551277
	Area	-1.244863	0.274979	-6.299527	2.358499
	Precipitation	-0.168581	0.197743	-2.192498	0.905586
	Slope	-1.415289	0.381023	-0.623872	1.194655
	Both-source	0.145162	0.338158	1.384684	1.054823
Detection	Year 1	1.201021	0.268529	0.566506	0.216458
	Year 2	0.687618	0.445742	0.658941	0.254266
	Year 3	1.386824	0.540752	0.534112	0.255978
	Year 4	0.756782	0.416041	0.723539	0.213903
	Year 5	0.416160	0.368087	N/A	N/A

Appendix S2.1: Table S3. Occupancy models of Virginia rail metapopulation dynamics with DTN isolation effects on both γ and ε, comparing a preliminary analysis during a period of equilibrium from 2004–2006 (n = 204) to the main analysis during a nonequilibrium period from 2013–2016 (n = 125) in the foothills of the California Sierra Nevada. All continuous variables were standardized.

Metapopulation parameter	Beta parameter	Equilibrium		Nonequilibrium	
		Coefficient	SE	Coefficient	SE
Initial Occupancy	Intercept	-1.734467	0.431999	-0.248108	0.366249
	Area	0.179714	0.284565	3.371013	0.786409
Colonization	Intercept	-0.777823	0.270694	-0.109219	0.360094
	DTN	-0.252815	0.221477	0.176127	0.219648
	Area	1.177128	0.352145	2.462479	0.558792
	Precipitation	-0.735557	0.481237	0.168061	0.264936
Extinction	Intercept	0.630716	2.338087	0.038389	0.517006
	DTN	-1.055661	1.143147	0.434717	0.336559
	Area	-8.740836	4.531453	-2.150335	0.716163
	Precipitation	-13.649935	8.212092	-0.153485	0.374585
	Both-source	2.590981	2.117164	-1.026861	0.648411
	Natural-only	4.972297	3.526329	-1.278843	1.222667
	Elevation	-1.852821	0.981271	-0.247767	0.358514
Detection	Year 1	0.270892	0.732147	0.137586	0.226184
	Year 2	0.783363	0.420755	0.225297	0.217023
	Year 3	0.883685	0.220964	0.719381	0.236710
	Year 4	N/A	N/A	0.256375	0.211114
	No playback	-1.046973	0.423452	N/A	N/A

Appendix S2.1: Table S4. Detection probabilities per visit (p) and site-level detection probabilities over all three visits (p^*) for black rail and Virginia rails in the foothills of the California Sierra Nevada. Probabilities were estimated from occupancy models fit to 2013–2016 winter and summer data (n = 125), utilizing the base model (see main text) with season-specific intercepts substituted in lieu of annual rainy reason precipitation.

	Black rail			**Virginia rail**		
Season	***p***	**SE**	***p****	***p***	**SE**	***p****
Summer 2013	0.631	0.052	0.950	0.535	0.057	0.900
Winter 2014	0.839	0.078	0.996	0.645	0.074	0.955
Summer 2014	0.712	0.057	0.976	0.540	0.062	0.903
Winter 2015	0.839	0.061	0.996	0.902	0.027	0.999
Summer 2015	0.692	0.058	0.971	0.682	0.051	0.968
Winter 2016	0.981	0.018	1.000	0.883	0.032	0.998
Summer 2016	0.726	0.050	0.979	0.560	0.053	0.915

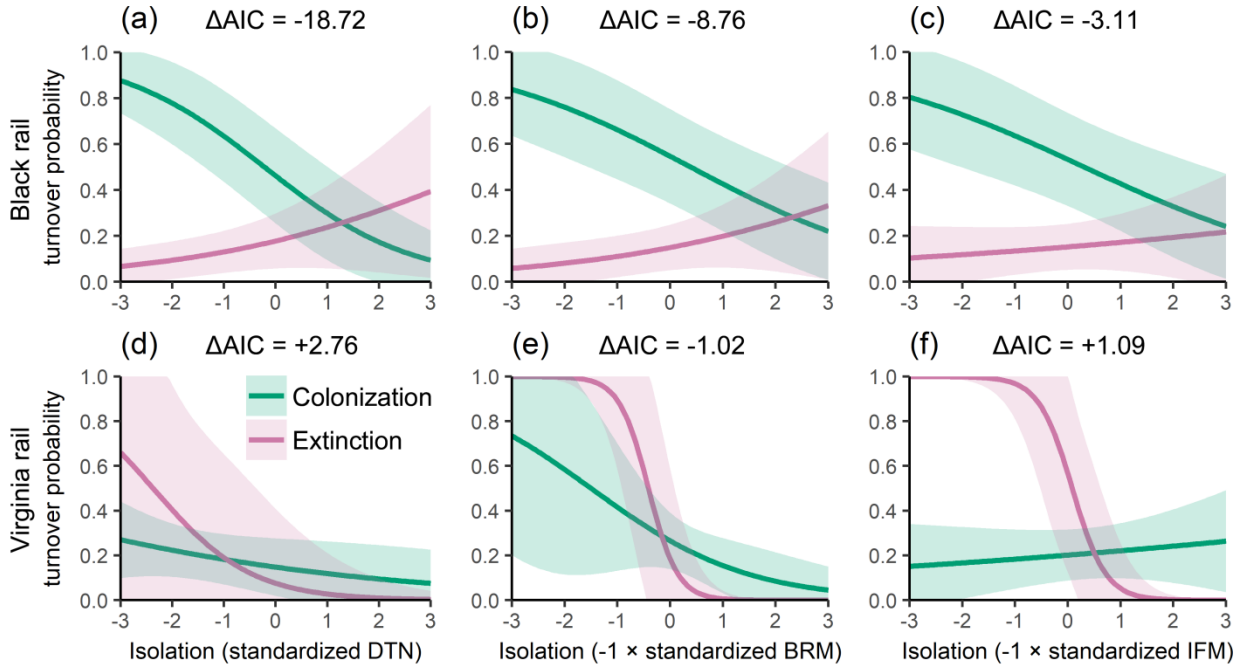

Appendix S2.1: Figure S1. An average wetland's predicted rescue effects metapopulations of (a–b) black rails and (d–f) Virginia rails in the foothills of California's Sierra Nevada during a period of equilibrium from 2002–2006 (*n* = 205 & 204; 2006 values shown). DTN = distance to nearest 3 sites with detections; BRM = autoregressive buffer radius measure; IFM = autoregressive incidence function measure. ΔAIC values show the amount of support for including both graphed relationships compared to a model without isolation effects (negative values indicate improvement).

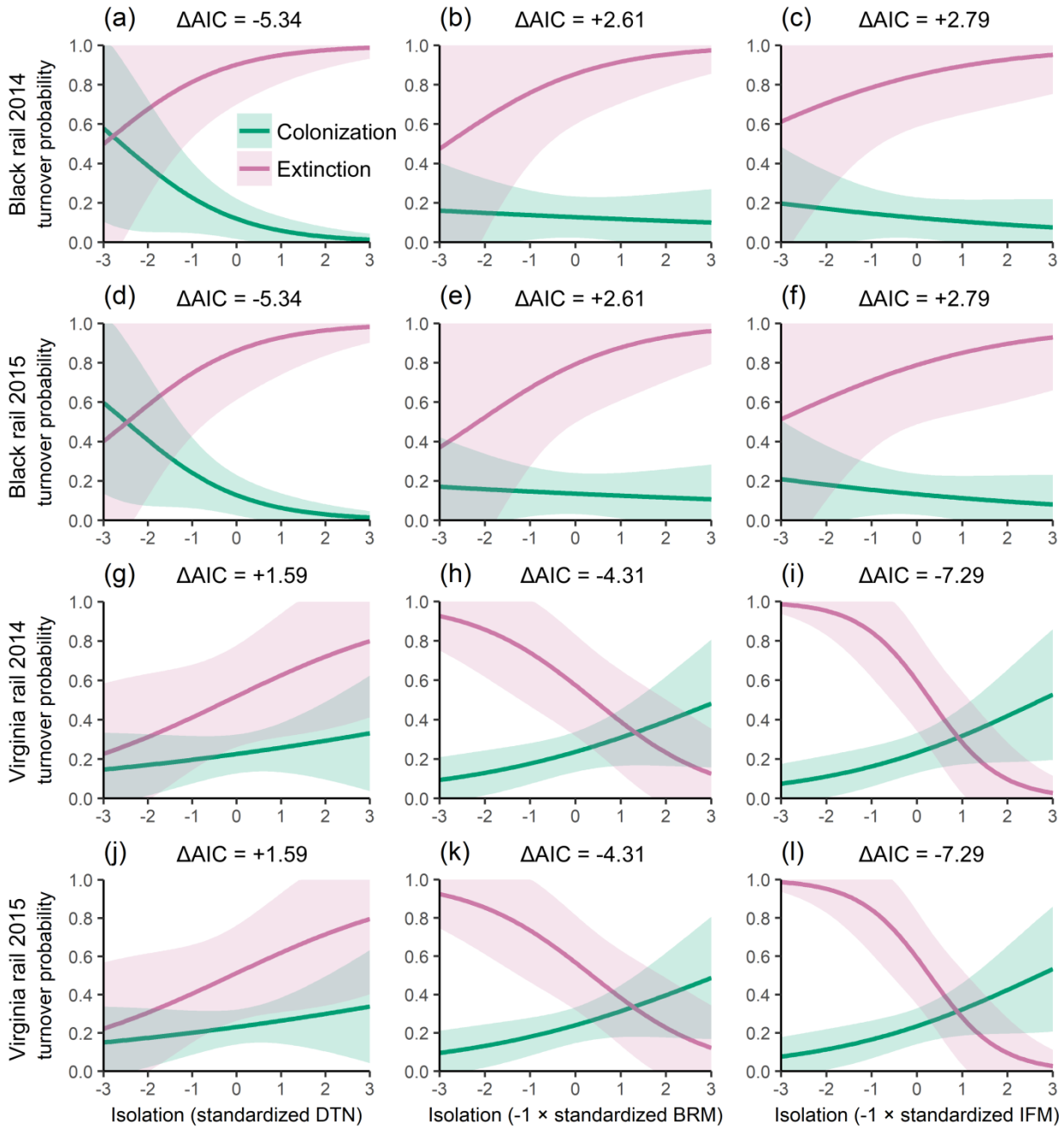

Appendix S2.1: Figure S2. An average wetland's predicted isolation effects on metapopulation dynamics of black rails in (a–c) 2014 and (d–f) 2015, and Virginia rails in 2014 (g–i) and 2015 (j–l) in the foothills of California's Sierra Nevada during a period of nonequilibrium metapopulation dynamics from 2013–2016 (n = 125; 2016 graph in main text). DTN = distance to nearest 3 sites with detections; BRM = autoregressive buffer radius measure; IFM = autoregressive incidence function measure. ΔAIC values show the amount of support for including both graphed relationships compared to a model without isolation effects (negative values indicate improvement).

Appendix S2.2: Fitting autoregressive connectivity measures for Virginia rails

We followed the analysis of Hall et al. (2018) to create incidence function (IFM) and buffer radius (BRM) autoregressive connectivity measures for Virginia rails that were equivalent to those for black rails, which we obtained from that paper. We first conducted a model selection exercise to obtain the best model for non-connectivity covariates to use in the autoregression, which was necessary due to long computation times for the autoregression procedure. We fit standard multi-season occupancy models (MacKenzie et al. 2003) using the 2002–2015 occupancy dataset on $n = 259$ surveyed and $n = 1853$ total wetlands, including those outside the core study area in a 1-km buffer to reduce edge effects (see Hall et al. 2018 for details on measurements). As in Hall et al. (2018), all years 2002–2015 were used because we were interested in obtaining the most accurate possible estimates of $\psi^c_{i,t}$. Fourteen sites surveyed only in 2015 were excluded from model fitting because they caused convergence problems, but their survey histories were included in R scripts when calculating $\psi^c_{i,t}$. Variables assessed were wetland patch area ($\log_{10}$ (ha +1)), elevation (m / 100, mean value per wetland from the 10 m National Elevation Dataset; U.S. Geological Survey 2009), fringe, fluvial, and impoundment (a set of dummy variables indicating geomorphology type, with slope the reference category), and year (a set of dummy variables). For detection we used Year-NP, a set of dummy variables for year with separate intercepts for visits in 2004 and 2005 when no playback of Virginia rail calls was conducted (black rail calls only; see Richmond et al. 2010). We started with the full model:

$$\Psi_i \sim \text{Area} + \text{Elevation} \quad \text{(S1)}$$

$$\gamma_{i,t}, \varepsilon_{i,t} \sim \text{Area} + \text{Elevation} + \text{Fringe} + \text{Fluvial} + \text{Impoundment} + \text{Year} \quad \text{(S2)}$$

$$\Psi_v \sim \text{Year-NP} \quad \text{(S3)}$$

for site i, year t, and visit v. Geomorphology covariates were excluded from ψ because they caused convergence issues due to the low number of detections in the first year. We then carried out a backwards stepwise model selection procedure using AIC, removing all variables one at a time, selecting the model with the lowest AIC, and iterating until the removing variables no longer reduced AIC. Results of the stepwise regression and the selected model are in Table S1.

We used the parameters estimated from the selected model to calculate autocovariate BRMs and IFMs in R (ver. 3.0.2; R Core Team 2013) for values of 1–10, 15, 20, 25, and 30 km for r and $1/\alpha$ (see main text). We then fit 28 models in PRESENCE with each measure included as an autocovariate on ψ (without the one-year lag in Eq. 2 and 3), γ, and ε (see Hall et al. 2018 for details and code). Each model was then iteratively refit until convergence of autocovariate values was achieved after 5 iterations (Augustin et al. 1996). We compared the AIC table of the resulting fifth iteration model sets for BRM and IFM separately, and selected the BRM and IFM model with the lowest AIC score (Supplementary Table S2). However for the IFM AIC scores were flat and not markedly better than the model with no connectivity measure, indicating none of the measures fit well.

Appendix S2.2: Table S1. Backwards stepwise AIC model selection table for multi-season (2004–2015) occupancy models of Virginia rails (*Rallus limicola*) for $n = 258$ wetlands in the foothills of the California Sierra Nevada. Step indicates the iteration of the stepwise procedure. Elev. = elevation, Imp. = Impoundment. Final model is bolded.

Step	Model	ΔAIC	AIC	*w*	*K*
7	ψ(Area), γ(Area, Fringe), ε(Year, Area, Fluvial, Elev.), p(Year-NP)	0.50	3771.84	0.079	33
7	ψ(.), γ(Year, Area, Fringe), ε(Year, Area, Fluvial, Elev.), p(Year-NP)	1.02	3772.36	0.061	42
7	ψ(Area), γ(Year, Area), ε(Year, Area, Fluvial, Elev.), p(Year-NP)	1.07	3772.41	0.059	42
7	ψ(Area), γ(Year, Area, Fringe), ε(Year, Area, Elev.), p(Year-NP)	1.91	3773.25	0.039	42
7	ψ(Area), γ(Year, Area, Fringe), ε(Year, Area, Fluvial, Elev.), p(.)	6.81	3778.15	0.003	30
7	ψ(Area), γ(Year, Area, Fringe), ε(Area, Fluvial, Elev.), p(Year-NP)	12.20	3783.54	0.000	33
7	ψ(Area), γ(Year, Area, Fringe), ε(Year, Area, Fluvial), p(Year-NP)	18.43	3789.77	0.000	42
7	ψ(Area), γ(Year, Fringe), ε(Year, Area, Fluvial, Elev.), p(Year-NP)	92.96	3864.30	0.000	42
7	ψ(Area), γ(Year, Area, Fringe), ε(Year, Fluvial, Elev.), p(Year-NP)	101.38	3872.72	0.000	42
6	**ψ(Area), γ(Year, Area, Fringe), ε(Year, Area, Fluvial, Elev.), p(Year-NP)**	**0.00**	**3771.34**	**0.101**	**43**
6	ψ(Area), γ(Year, Area, Fringe, Imp.), ε(Year, Area, Fluvial, Elev.), p(Year-NP)	0.92	3772.26	0.064	44
6	ψ(Area), γ(Area, Fringe, Imp.), ε(Year, Area, Fluvial, Elev.), p(Year-NP)	1.56	3772.90	0.046	34
6	ψ(.), γ(Year, Area, Fringe, Imp.), ε(Year, Area, Fluvial, Elev.), p(Year-NP)	1.85	3773.19	0.040	43
6	ψ(Area), γ(Year, Area, Imp.), ε(Year, Area, Fluvial, Elev.), p(Year-NP)	2.36	3773.70	0.031	43
6	ψ(Area), γ(Year, Area, Fringe, Imp.), ε(Year, Area, Elev.), p(Year-NP)	3.00	3774.34	0.023	43
6	ψ(Area), γ(Year, Area, Fringe, Imp.), ε(Year, Area, Fluvial, Elev.), p(.)	8.02	3779.36	0.002	31
6	ψ(Area), γ(Year, Area, Fringe, Imp.), ε(Area, Fluvial, Elev.), p(Year-NP)	13.13	3784.47	0.000	34
6	ψ(Area), γ(Year, Area, Fringe, Imp.), ε(Year, Area, Fluvial), p(Year-NP)	19.70	3791.04	0.000	43
6	ψ(Area), γ(Year, Fringe, Imp.), ε(Year, Area, Fluvial, Elev.), p(Year-NP)	78.62	3849.96	0.000	43
6	ψ(Area), γ(Year, Area, Fringe, Imp.), ε(Year, Fluvial, Elev.), p(Year-NP)	101.97	3873.31	0.000	43
5	ψ(Area), γ(Year, Area, Fringe, Imp.), ε(Year, Area, Fluvial, Elev.), p(Year-NP)	0.92	3772.26	0.064	44
5	ψ(Area), γ(Year, Area, Fringe), ε(Year, Area, Fluvial, Imp., Elev.), p(Year-NP)	1.66	3773.00	0.044	44

Step	Model	ΔAIC	AIC	*w*	*K*
5	ψ(Area), γ(Area, Fringe, Imp.), ε(Year, Area, Fluvial, Imp., Elev.), p(Year-NP)	2.16	3773.50	0.034	35
5	ψ(Area), γ(Year, Area, Imp.), ε(Year, Area, Fluvial, Imp., Elev.), p(Year-NP)	3.72	3775.06	0.016	44
5	ψ(Area), γ(Year, Area, Fringe, Imp.), ε(Year, Area, Imp., Elev.), p(Year-NP)	3.80	3775.14	0.015	44
5	ψ(.), γ(Year, Area, Fringe, Imp.), ε(Year, Area, Fluvial, Imp., Elev.), p(Year-NP)	4.49	3775.83	0.011	44
5	ψ(Area), γ(Year, Area, Fringe, Imp.), ε(Year, Area, Fluvial, Imp., Elev.), p(.)	9.71	3781.05	0.001	32
5	ψ(Area), γ(Year, Area, Fringe, Imp.), ε(Area, Fluvial, Imp., Elev.), p(Year-NP)	14.57	3785.91	0.000	35
5	ψ(Area), γ(Year, Area, Fringe, Imp.), ε(Year, Area, Fluvial, Imp.), p(Year-NP)	18.73	3790.07	0.000	44
5	ψ(Area), γ(Year, Fringe, Imp.), ε(Year, Area, Fluvial, Imp., Elev.), p(Year-NP)	80.45	3851.79	0.000	44
5	ψ(Area), γ(Year, Area, Fringe, Imp.), ε(Year, Fluvial, Imp., Elev.), p(Year-NP)	103.80	3875.14	0.000	44
4	ψ(Area), γ(Year, Area, Fringe, Imp.), ε(Year, Area, Fluvial, Imp., Elev.), p(Year-NP)	2.30	3773.64	0.032	45
4	ψ(Area), γ(Area, Fringe, Imp.), ε(Year, Area, Fringe, Fluvial, Imp., Elev.), p(Year-NP)	2.63	3773.97	0.027	36
4	ψ(Area), γ(Year, Area, Fringe, Imp.), ε(Year, Area, Fringe, Fluvial, Elev.), p(Year-NP)	2.63	3773.97	0.027	45
4	ψ(Area), γ(Year, Area, Fringe), ε(Year, Area, Fringe, Fluvial, Imp., Elev.), p(Year-NP)	3.16	3774.50	0.021	45
4	ψ(Area), γ(Year, Area, Fringe, Imp.), ε(Year, Area, Fringe, Imp., Elev.), p(Year-NP)	4.44	3775.78	0.011	45
4	ψ(.), γ(Year, Area, Fringe, Imp.), ε(Year, Area, Fringe, Fluvial, Imp., Elev.), p(Year-NP)	4.69	3776.03	0.010	45
4	ψ(Area), γ(Year, Area, Imp.), ε(Year, Area, Fringe, Fluvial, Imp., Elev.), p(Year-NP)	5.52	3776.86	0.006	45
4	ψ(Area), γ(Year, Area, Fringe, Imp.), ε(Year, Area, Fringe, Fluvial, Imp., Elev.), p(.)	11.38	3782.72	0.000	33
4	ψ(Area), γ(Year, Area, Fringe, Imp.), ε(Area, Fringe, Fluvial, Imp., Elev.), p(Year-NP)	16.01	3787.35	0.000	36
4	ψ(Area), γ(Year, Area, Fringe, Imp.), ε(Year, Area, Fringe, Fluvial, Imp.), p(Year-NP)	17.99	3789.33	0.000	45
4	ψ(Area), γ(Year, Fringe, Imp.), ε(Year, Area, Fringe, Fluvial, Imp., Elev.), p(Year-NP)	80.64	3851.98	0.000	45
4	ψ(Area), γ(Year, Area, Fringe, Imp.), ε(Year, Fringe, Fluvial, Imp., Elev.), p(Year-NP)	103.79	3875.13	0.000	45
3	ψ(Area), γ(Year, Area, Fringe, Imp.), ε(Year, Area, Fringe, Fluvial, Imp., Elev.), p(Year-NP)	3.76	3775.10	0.015	46
3	ψ(Area), γ(Year, Area, Fringe, Imp., Elev.), ε(Year, Area, Fluvial, Imp., Elev.), p(Year-NP)	3.83	3775.17	0.015	46
3	ψ(Area), γ(Year, Area, Fringe, Imp., Elev.), ε(Year, Area, Fringe, Fluvial, Elev.), p(Year-NP)	4.17	3775.51	0.013	46

Step	Model	ΔAIC	AIC	*w*	*K*
3	ψ(Area), γ(Area, Fringe, Imp., Elev.), ε(Year, Area, Fringe, Fluvial, Imp., Elev.), p(Year-NP)	4.55	3775.89	0.010	37
3	ψ(Area), γ(Year, Area, Fringe, Elev.), ε(Year, Area, Fringe, Fluvial, Imp., Elev.), p(Year-NP)	4.88	3776.22	0.009	46
3	ψ(Area), γ(Year, Area, Fringe, Imp., Elev.), ε(Year, Area, Fringe, Imp., Elev.), p(Year-NP)	5.91	3777.25	0.005	46
3	ψ(.), γ(Year, Area, Fringe, Imp., Elev.), ε(Year, Area, Fringe, Fluvial, Imp., Elev.), p(Year-NP)	6.43	3777.77	0.004	46
3	ψ(Area), γ(Year, Area, Imp., Elev.), ε(Year, Area, Fringe, Fluvial, Imp., Elev.), p(Year-NP)	7.13	3778.47	0.003	46
3	ψ(Area), γ(Year, Area, Fringe, Imp., Elev.), ε(Year, Area, Fringe, Fluvial, Imp., Elev.), p(.)	12.58	3783.92	0.000	34
3	ψ(Area), γ(Year, Area, Fringe, Imp., Elev.), ε(Area, Fringe, Fluvial, Imp., Elev.), p(Year-NP)	16.08	3787.42	0.000	37
3	ψ(Area), γ(Year, Area, Fringe, Imp., Elev.), ε(Year, Area, Fringe, Fluvial, Imp.), p(Year-NP)	18.03	3789.37	0.000	46
3	ψ(Area), γ(Year, Fringe, Imp., Elev.), ε(Year, Area, Fringe, Fluvial, Imp., Elev.), p(Year-NP)	80.28	3851.62	0.000	46
3	ψ(Area), γ(Year, Area, Fringe, Imp., Elev.), ε(Year, Fringe, Fluvial, Imp., Elev.), p(Year-NP)	104.34	3875.68	0.000	46
2	ψ(Area), γ(Year, Area, Fringe, Imp., Elev.), ε(Year, Area, Fringe, Fluvial, Imp., Elev.), p(Year-NP)	5.26	3776.60	0.007	47
2	ψ(Area), γ(Year, Area, Fringe, Fluvial, Imp.), ε(Year, Area, Fringe, Fluvial, Imp., Elev.), p(Year-NP)	5.39	3776.73	0.007	47
2	ψ(Area), γ(Year, Area, Fringe, Fluvial, Imp., Elev.), ε(Year, Area, Fluvial, Imp., Elev.), p(Year-NP)	5.57	3776.91	0.006	47
2	ψ(Area), γ(Year, Area, Fringe, Fluvial, Imp., Elev.), ε(Year, Area, Fringe, Fluvial, Elev.), p(Year-NP)	5.89	3777.23	0.005	47
2	ψ(Area), γ(Area, Fringe, Fluvial, Imp., Elev.), ε(Year, Area, Fringe, Fluvial, Imp., Elev.), p(Year-NP)	6.09	3777.43	0.005	38
2	ψ(Area), γ(Year, Area, Fringe, Fluvial, Elev.), ε(Year, Area, Fringe, Fluvial, Imp., Elev.), p(Year-NP)	6.50	3777.84	0.004	47
2	ψ(Area), γ(Year, Area, Fringe, Fluvial, Imp., Elev.), ε(Year, Area, Fringe, Imp., Elev.), p(Year-NP)	7.82	3779.16	0.002	47
2	ψ(.), γ(Year, Area, Fringe, Fluvial, Imp., Elev.), ε(Year, Area, Fringe, Fluvial, Imp., Elev.), p(Year-NP)	7.94	3779.28	0.002	47
2	ψ(Area), γ(Year, Area, Fluvial, Imp., Elev.), ε(Year, Area, Fringe, Fluvial, Imp., Elev.), p(Year-NP)	8.44	3779.78	0.002	47
2	ψ(Area), γ(Year, Area, Fringe, Fluvial, Imp., Elev.), ε(Year, Area, Fringe, Fluvial, Imp., Elev.), p(.)	14.58	3785.92	0.000	35
2	ψ(Area), γ(Year, Area, Fringe, Fluvial, Imp., Elev.), ε(Area, Fringe, Fluvial, Imp., Elev.), p(Year-NP)	16.77	3788.11	0.000	38
2	ψ(Area), γ(Year, Area, Fringe, Fluvial, Imp., Elev.), ε(Year, Area, Fringe, Fluvial, Imp.), p(Year-NP)	19.96	3791.30	0.000	47
2	ψ(Area), γ(Year, Fringe, Fluvial, Imp., Elev.), ε(Year, Area, Fringe, Fluvial, Imp., Elev.), p(Year-NP)	82.21	3853.55	0.000	47
2	ψ(Area), γ(Year, Area, Fringe, Fluvial, Imp., Elev.), ε(Year, Fringe, Fluvial, Imp., Elev.), p(Year-NP)	104.93	3876.27	0.000	47

Step	Model	ΔAIC	AIC	*w*	*K*
1	ψ(Area), γ(Year, Area, Fringe, Fluvial, Imp., Elev.), ε(Year, Area, Fringe, Fluvial, Imp., Elev.), p(Year-NP)	7.04	3778.38	0.003	48
1	ψ(Area, Elev.), γ(Year, Area, Fringe, Imp., Elev.), ε(Year, Area, Fringe, Fluvial, Imp., Elev.), p(Year-NP)	7.20	3778.54	0.003	48
1	ψ(Area, Elev.), γ(Year, Area, Fringe, Fluvial, Imp.), ε(Year, Area, Fringe, Fluvial, Imp., Elev.), p(Year-NP)	7.36	3778.70	0.003	48
1	ψ(Area, Elev.), γ(Year, Area, Fringe, Fluvial, Imp., Elev.), ε(Year, Area, Fluvial, Imp., Elev.), p(Year-NP)	7.51	3778.85	0.002	48
1	ψ(Area, Elev.), γ(Year, Area, Fringe, Fluvial, Imp., Elev.), ε(Year, Area, Fringe, Fluvial, Elev.), p(Year-NP)	7.83	3779.17	0.002	48
1	ψ(Area, Elev.), γ(Year, Area, Fringe, Fluvial, Elev.), ε(Year, Area, Fringe, Fluvial, Imp., Elev.), p(Year-NP)	8.45	3779.79	0.002	48
1	ψ(Area, Elev.), γ(Area, Fringe, Fluvial, Imp., Elev.), ε(Year, Area, Fringe, Fluvial, Imp., Elev.), p(Year-NP)	9.19	3780.53	0.001	39
1	ψ(Area, Elev.), γ(Year, Area, Fringe, Fluvial, Imp., Elev.), ε(Year, Area, Fringe, Imp., Elev.), p(Year-NP)	9.75	3781.09	0.001	48
1	ψ(Elev.), γ(Year, Area, Fringe, Fluvial, Imp., Elev.), ε(Year, Area, Fringe, Fluvial, Imp., Elev.), p(Year-NP)	9.88	3781.22	0.001	48
1	ψ(Area, Elev.), γ(Year, Area, Fluvial, Imp., Elev.), ε(Year, Area, Fringe, Fluvial, Imp., Elev.), p(Year-NP)	10.36	3781.70	0.001	48
1	ψ(Area, Elev.), γ(Year, Area, Fringe, Fluvial, Imp., Elev.), ε(Year, Area, Fringe, Fluvial, Imp., Elev.), p(.)	16.19	3787.53	0.000	36
1	ψ(Area, Elev.), γ(Year, Area, Fringe, Fluvial, Imp., Elev.), ε(Area, Fringe, Fluvial, Imp., Elev.), p(Year-NP)	20.79	3792.13	0.000	39
1	ψ(Area, Elev.), γ(Year, Area, Fringe, Fluvial, Imp., Elev.), ε(Year, Area, Fringe, Fluvial, Imp.), p(Year-NP)	21.86	3793.2	0.000	48
1	ψ(Area, Elev.), γ(Year, Fringe, Fluvial, Imp., Elev.), ε(Year, Area, Fringe, Fluvial, Imp., Elev.), p(Year-NP)	89.74	3861.08	0.000	48
1	ψ(Area, Elev.), γ(Year, Area, Fringe, Fluvial, Imp., Elev.), ε(Year, Fringe, Fluvial, Imp., Elev.), p(Year-NP)	106.57	3877.91	0.000	48
0	ψ(Area, Elev.), γ(Year, Area, Fringe, Fluvial, Imp., Elev.), ε(Year, Area, Fringe, Fluvial, Imp., Elev.), p(Year-NP)	9.00	3780.34	0.001	49
0	ψ(.), γ(.), ε(.), p(.)	4133.68	362.34	0.000	4

Appendix S2.2: Table S2. Model selection table to determine best dispersal distance for buffer radius and incidence function connectivity measure models of Virginia rail occupancy in $n = 258$ wetlands (plus 1853 autoregressive unsurveyed wetlands) in the foothills of the California Sierra Nevada. Connectivity measures were included on ψ, γ, and ε. All models except Null included the base model: ψ(Area), γ(Year, Area, Fringe), ε(Year, Area, Fluvial, Elevation), p(Year-NP).

Buffer radius measure (BRM)					**Incidence function measure (IFM)**				
r	**ΔAIC**	**AIC**	***w***	***K***	**1/α**	**ΔAIC**	**AIC**	***w***	***K***
20 km	0.00	3766.91	0.451	45	10 km	0.00	3770.62	0.107	45
8 km	3.22	3770.13	0.090	45	9 km	0.03	3770.65	0.106	45
25 km	3.22	3770.13	0.090	45	8 km	0.13	3770.75	0.100	45
9 km	3.44	3770.35	0.081	45	15 km	0.15	3770.77	0.099	45
15 km	4.05	3770.96	0.060	45	7 km	0.31	3770.93	0.092	45
10 km	4.35	3771.26	0.051	45	20 km	0.39	3771.01	0.088	45
Base	4.43	3771.34	0.049	43	6 km	0.64	3771.26	0.078	45
7 km	5.49	3772.4	0.029	45	Base	0.72	3771.34	0.075	43
30 km	6.11	3773.02	0.021	45	30 km	0.74	3771.36	0.074	45
5 km	6.16	3773.07	0.021	45	5 km	1.14	3771.76	0.061	45
1 km	6.22	3773.13	0.020	45	4 km	1.81	3772.43	0.043	45
6 km	6.88	3773.79	0.015	45	3 km	2.51	3773.13	0.031	45
3 km	7.4	3774.31	0.011	45	2 km	2.99	3773.61	0.024	45
4 km	7.45	3774.36	0.011	45	1 km	3.14	3773.76	0.022	45
Null	363.06	4133.68	0.000	4	Null	353.06	4133.68	0.000	4

Appendix S3.1: Wetlands-Irrigation CHANS Model (WICM) ODD Protocol

This appendix provides a comprehensive description of the design, construction, and function of the Wetlands-Irrigation CHANS Model (WICM) following the Overview, Design concepts, and Details (ODD) protocol standard for agent-based models (ABMs; Grimm et al. 2010).

S3.1.1 Purpose

The WICM is designed to simulate the wetlands of the Sierra Nevada foothills as a coupled human and natural system (CHANS). It models the linkages, feedbacks, and emergent behaviors of wetlands, climate and weather, irrigation districts, wildlife policy, landowners and land managers, West Nile virus (WNV), and the metapopulations of two rail species: the black rail (*Laterallus jamaicensis*) and the Virginia rail (*Rallus limicola*). The study area was the the EPA zone III Sierra Nevada Foothills eco-region (US Environmental Protection Agency 2013) for Nevada, Yuba, and southern Butte county. This region has a Mediterranean climate with hot, dry summers and cool, wet winters. Natural vegetation transitioned from open oak (*Quercus* spp.) savannah below 500 m elevation to oak woodland and mixed deciduous-conifer forest at higher elevations. It was historically dominated by rangeland-based cattle ranchers that utilized irrigation to create green pasture the dry season. High rates of development over the past two decades has led to subdivision of grazing lands and conversion into smaller "ranchettes" where people may keep small livestock, construct ponds, and enjoy a rural lifestyle (Wacker and Kelly 2004). The lowest elevations at the eastern edge of the study area were dominated by rice farms and large managed waterfowl hunting impoundments to the north of the Yuba River, and open grasslands with large pond fringe wetlands in Beale Air Force Base to the south.

Most wetlands (93%) in this region are on private lands, and landowners can accidentally or deliberately eliminate, create, and change the size of wetlands through irrigation practices. Regional irrigation districts deliver water to landowners through a combination of pipes, ditches, and natural waterways. Most wetland creation appears unintentional with roughly three-quarters of irrigated wetlands that we determined the water sources of fed by some kind of "waste" water: oversaturated pasture, ditch or pond leaks, or unmowed areas along rice fringes. Intentional irrigation of wetlands on private lands was largely limited to decorative ponds scattered throughout the foothills and in the rice-growing areas on the edge of the Central Valley. Two State Wildlife Areas, Spenceville and Daugherty Hill, intentionally create irrigated wetlands for rail habitat, but these composed only a small percentage of all wetlands.

The WICM combines a land-use change agent-based model (ABM) with a metapopulation stochastic patch occupancy model (SPOM). It runs stochastic submodels based on regression models parameterized from field data, in order to assess the coupled effects of annual rainy season precipitation, irrigation district water management, and landowner irrigation decisions on wetland patch change, metapopulation occupancy dynamics, and WNV. The model is used to determine the dominant drivers of overall system behavior and metapopulation extinction risk under climate change. Scenarios representing different WNV, irrigation district drought response, and wetland incentive policies are input to see how the system responds.

S3.1.2 Entities, variables, and scales

WICM was constructed in NetLogo v6.0.3 (Wilensky 2018). It represents the CHANS as three types of spatially explicit agents—wetlands, landowners, and irrigation districts—overlaid on a 100 m resolution (388 × 424 cells) raster map of the study area (Fig. 2b). Raster cells (called "patches" by NetLogo, though we use this term to refer to wetland agents in line with the metapopulation literature) contain spatial covariates (elevation and distance to rice fields) and represent spatial domains of agents with variables indicating landowner parcels and irrigation district service areas. All agents other than raster cells are represented in continuous space. Wetlands are represented as points with associated variables (e.g., area). Rails and WNV are represented as variables stored by the wetland agents (i.e., wetlands have *black-rail-occupancy* = 0 or 1). Landowners are agents with their own variables, and make decisions that affect wetlands that originate on their property. Irrigation districts are agents that provide irrigation to landowners within their service areas, have variables representing reservoirs that store precipitation, and make irrigation cutbacks to landowners when reservoirs levels fall too low.

S3.1.3 Process overview and scheduling

The model runs on an annual time step for 100 years, with submodels executed in an order approximating the seasonal cycle or sampling period used when gathering data (Fig. 2a). All agent-based processes were executed by agents in a randomized order. First, during the winter rainy season, precipitation is generated based on the RCP 8.5 climate scenario (Flint and Flint 2012). Districts then update their reservoir water storage by subtracting water used over the previous summer and adding recharge based on winter rainfall, and implement 20–50% water allocation cutbacks if minimum storage thresholds are not met. Landowners may transfer their property to a new landowner due to sale or deaths, and then make a series of irrigation decisions. Wetland patches first change in size, number, and distribution based on changes in their irrigation state (on or off). Next, landowners can respond to irrigation cutbacks (if implemented) by permanently fixing leaks, temporarily cutting off water from pasture or rice fields until cutbacks are lifted, or deciding to sell their land in the next year (or some combination of these). When irrigation is turned off, wetlands shrink in size if fed by both irrigated and natural water sources, or are eliminated altogether if fed by irrigation only. Landowners may then participate in a wetland protection incentive program that permanently prevents them from turning irrigation off for their largest wetland (impoundments, rice fringes, fluvial creeks, and wetlands fed by runoff from other properties excluded). Lastly, landowners may participate in a wetland creation incentive program, receiving ~2.5 miner's inches (~0.12 acre-feet/day) of free water to create a new wetland on their property. Landowners may enroll in each program only once, and total water allocation for creation incentive programs was capped at 2% of each district's storage. Because created wetlands use additional (i.e., surplus) irrigation water, they were all turned off and new enrollments suspended during water cutbacks. These policies represent different strategies for promoting wetland habitats—one aims to maintain wetlands during drought and one to increase wetlands outside of drought. Next, rail colonization and extinction occurs during late spring (matching the onset of our field surveys) by running a SPOM over the new landscape. Rails occupying wetlands eliminated by irrigation turning off go deterministically extinct. Finally, WNV vector strength is determined by wetland distribution as mosquito densities peak in late summer, affecting the probability of colonization and extinction for rails in the following year. In the fall, measurements are taken and then time steps forward.

S3.1.4 Design concepts

Basic principles—Our model is not designed to test any one theory, but can test predictions that have been made about the behavior of metapopulations in dynamic landscape CHANS (Sjögren-Gulve and Hanski 2000, Amarasekare and Possingham 2001, Gimona and Polhill 2011). Moreover it is designed to determine key drivers of system dynamics and identify management policies that can increase the likelihood of the persistence of the rail metapopulations and landowners' desired land uses. We created the WICM as an iterative, participatory process by interviewing landowners and water district employees before data collection (except rails) at the start of the study. We used their qualitative feedback to design our data collection. We conducted a second round of interviews after initial model design was complete, presenting a first draft of the model to get their feedback, which was incorporated into the final design. WICM was based on disciplinary theories that drove the design of underlying submodels (covered in more detail in **Submodels**), which we linked with regression equations empirically fit from field data. We used AIC model selection and selected the model with <2 ΔAIC that had the fewest numbers of parameters (to increase parsimony). Model selection results are in Appendix S3.2.

After construction of each submodel, it was tested using a range of realistic and extreme values to ensure proper function. The entire model it was proofed three times for errors after it was completed. Following the concept of pattern-oriented evaluation (Grimm et al. 2005), we tested whether the model was able to reproduce qualitatively similar patterns to three emergent phenomena: (1) frequency of irrigation cutbacks, (2) occupancy dynamics of black and Virginia rails pre-WNV, and (3) occupancy dynamics of black and Virginia rails post-WNV. We used precipitation data fit to historic 1947–2016 PRISM data ($\mu = 1.09$, $\sigma = 0.17$), assessed occurrences of both mean values and reproduction of variability (troughs and peaks). We were able to reproduce all three patterns (Fig. 2b, Appendix S3.3: Fig. S5). Droughts severe enough to trigger irrigation cutbacks occurred approximately every 20–40 years, in line with actual occurrences in our system. Rails pre-WNV showed higher occupancy for black rails with colonization and extinction at roughly equal rates. After WNV, black rail occupancy declined to a lower equilibrium with periodic extinction spikes in drought years. Virginia rails had higher and more stable occupancy overall, with less impact from WNV, as in our observed data. Quantitative validation analysis showed the model was able to reasonably accurately predict observed occupancy and land-use change dynamics in 2017–2018 (see main text).

Emergence—The model explores how the emergent behavior of the coupled system changes in response to land-use change rates, landowner characteristics, climate change, the presence of WNV, and different irrigation district and wildlife agency policies. The key emergent states of the model we examine are potential future values of: (1) wetland abundance, (2) rail metapopulation size (the number of occupied wetlands), and (3) rail metapopulation quasi-extinction risk (the minimum number of occupied wetlands; Beissinger and Westphal 1998). Certain model results are built in; for instance all models with WNV included have WNV as a permanent feature (i.e., WNV cannot be eliminated) and all models of rail dynamics include almost no risk of total metapopulation extinction (because our model does not include Allee effects that could cause extinction vortices).

Adaptation—Agents do not adapt explicitly to meet certain goals, but rather react in stochastic but pre-determined ways to circumstances. Irrigation districts react to drought by reducing their water usage by 20% or 50%, depending on the severity. Landowners may adapt to these reductions in water deliveries by reducing their pasture or rice irrigation, fixing leaks, or selling

their land. Black rails and Virginia rails could be seen as adapting to changing wetland conditions by going extinct from wetlands that change to less suitable conditions and colonizing newly suitable ones.

Objectives / Learning / Prediction—No entities explicitly do any of these. Landowners make decisions based on reported rates in survey data, not in an attempt to achieve any specific goal, and do not alter their decision-making processes over time (unless replaced by a new landowner).

Sensing—Landowners have perfect knowledge of the extent of their property, the irrigation and wildlife policies affecting them, and the state of wetlands on their property. Irrigation districts have perfect knowledge of their service areas and amount of water stored. Wetlands have perfect "knowledge" of sum area of wetlands within 2.5 km (used to calculate WNV risk) and other black rail occupied wetlands within 7 km (used to calculate connectivity).

Interaction—Irrigation districts and the wildlife agency interact with landowners by issuing policies that landowners may respond to, using raster cells as intermediaries communicating district membership information. Landowners interact with their wetlands by turning irrigation on or off to them, or protecting them. Landowners interact with the raster cells comprising their property by creating wetlands on them via incentive policies. Wetlands interact with each other by affecting their WNV risk and black rail colonization probabilities. Raster cells interact with wetlands by providing distance to rice field and elevation covariates, which affect WNV risk and Virginia rail extinction probability respectively.

Stochasticity—Most of the modeled processes are stochastic: initialization of many wetland and landowner characteristics, rainy season precipitation, water storage usage and recharge, landowner turnover, patch change rates, and rail colonization and extinction (see main text Table 3.1). Stochasticity in these instances represents underlying variability in these processes for which it is not possible to model deterministically—for instance, an individual black rail's probability of successfully dispersing into a wetland on the landscape is poorly understood, but the probability of a wetland's colonization based on patch area and isolation for black rails can be estimated with over a decade of data on colonization events. Using generalized linear regression models for these processes allows us to represent the overall system dynamics accurately without worrying about specifically accurate states of each individual agent.

Collectives—Collectives in our model are pre-defined by the input data rather than emergent. Raster cells and wetlands form collectives owned by landowners; landowners form collectives based on their membership within different irrigation districts; and all form one collective under the jurisdiction of the wildlife agency.

Observation—The scenarios being run are recorded at the start of the model run. Data is then collected after each summer, immediately before the simulation advances one time step ("tick"). We recorded mean wetland abundance (i.e., the number of wetlands with at least one active water source), the mean metapopulation size over years 10–50, ending metapopulation size at years 50 and 100, minimum metapopulation size for years 0–50 and 0–100, and the total cost and number of wetlands created and protected by incentive programs at year 50 and 100.

S3.1.5 Initialization

S3.1.5.1 Study area

Study area boundaries were defined using a polygon of the EPA zone III Sierra Nevada Foothills eco-region (US Environmental Protection Agency 2013) for Nevada, Yuba, and Butte county south of Bangor, CA. Large lakes and the Yuba River were hand-mapped by manually interpreting summer 2013 GeoEye-1 0.4 m imagery in Google Earth 7.1.5 (Google Inc.). These polygon layers were converted to raster maps based on the National Elevation Dataset 10 m (U.S. Geological Survey 2009) rescaled to 100 m, and projected to NAD 1983 UTM (all GIS processing was done in ArcMap v10; (Esri 2011). We explored different resolutions during model development and chose this resolution to balance computational demands with spatial accuracy. Finer resolutions sometimes resulted in memory errors, and scaling to a 100 m resolution resulted in little lost information because only 2 out of 7215 landowner properties were unable to be represented (see *S3.1.5.3 Landowners*) and the only other patch variables (elevation and distance to rice fields) changed fairly slowly over the landscape. These layers were subsequently loaded as variables into NetLogo's "patches" (i.e., raster cells) via the *gis* extension. Cells outside of the study area polygon, within large water bodies, or in parcels <1.2 ha (see *S3.1.5.3 Landowners*) were subsequently excluded from the land-use change submodels, though wetlands within water bodies were included in metapopulation and WNV submodels.

S3.1.5.2 Irrigation districts

There were 10 irrigation districts that serviced some parcels within our study area, but 8 of these were near the borders of our study area in the Central Valley and serviced very few parcels. To simplify the model we analyzed only the two largest irrigation districts in this region, Browns Valley Irrigation District (BVID) and Nevada Irrigation District (NID). Landowners serviced by one of the other 8 districts were assigned to BVID, which was spatially closer than NID. We used polygon maps of water district service areas (U.S. Bureau of Reclamation and California Department of Water Resources 2009) and manually edited them to include parcels on the edges of service areas that had visible private canals receiving water from the district. We converted polygons to 100 m rasters and applied them to the raster cells in WICM, representing the spatial domain of properties and wetlands that each district affected. Districts had their characteristics initialized and their water storage started full (see *S3.1.7.2 Water storage usage & recharge*).

S3.1.5.3 Landowners

Landowners were implemented into the model as spatial agents based on 2010 parcel layers, acquired from county assessors. Parcels with matching owners or addresses were dissolved into single polygons representing each landowner. We further used approximate string matching (R package *stringdist* (v0.9.4.6) to identify parcels that shared the same owner name within 3 characters, using the optimal string alignment method. Approximate matches, as well as known large properties that were under multiple names (e.g., some parcels listed under a company name), were then manually examined and merged if a true match. Polygon parcel layers were converted to 100 m raster maps matching the rest of the input data based on a "maximum area" rule. This resulted in 98 small parcels that were lost during conversion. In order to remedy this, we manually edited this raster map to reassign cells that touched these landowners. We were able to represent all but 2 properties on the landscape, resulting in 7213 modeled landowners. This

property raster layer was loaded into the landscape and stored as variables in NetLogo's raster cells that represented the landowner they belonged to. The polygon layer was converted to points, and subsequently loaded in as agents that contained all landowner variables. They were then randomly assigned to one of their cells, preferentially one serviced by an irrigation district; therefore if landowners' properties were on multiple irrigation district service areas, landowners were assigned to a single district probabilistically based on the relative number of cells that were in each district.

We designed and mailed a survey on land and water management to 862 landowners from the study area (Nevada, Yuba and Butte counties) with properties ≥1.2 ha (see Huntsinger et al. 2017 for details and a copy of the survey). Parcels <1.2 ha were excluded from the study because this was the Nevada county cutoff for Residential Agricultural zoning; Yuba county used a slightly larger threshold (2.0 ha) but we used the smaller cutoff to err on the side of including additional landowners. We obtained $n = 466$ valid questionnaires (54% success rate). We used survey respondents' reported acreage and names to identify their properties from this map. Respondents whose reported acreage could not be accurately matched were discarded from analysis, leaving $n = 464$ respondent-matched properties. To preserve respondent confidentiality, no private landowners were initialized to their actual survey values. Public landowners were assigned deterministically based on public land maps, were static, and did not respond to cutbacks or incentive programs. For private landowners, we initialized their characteristics via the submodels in *S3.1.7.5 Property transfer*.

S3.1.5.4 Wetlands

The core of our model was a map of all $n = 1759$ regional wetlands (minimum mapping unit 5×5 m), which we created via manual interpretation of the 2013 GeoEye imagery. We considered wetland any areas covered by emergent hydrophytes (*Typha* spp., *Scirpus* spp., *Juncus effusus*, *Leersia oryzoides*, and wetland sedges, including vegetation that appeared seasonally dry) as well as any green vegetation in a 5 m buffer from hydrophytes indicating a wetland-upland transition zone. We separately mapped patches of open water and rice fields for use in WNV models, but these were not included as "wetlands." Wetlands were considered separate patches (i.e., agents) if they were >100 m from each other or had different water sources (slope and fluvial geomorphologies), or were distinct management units (fringe and impoundment geomorphologies; e.g., around different rice fields). Some wetland patches were split or merged for landowner and metapopulation regression analyses: wetlands that crossed multiple properties were treated as separate wetlands for each landowner, and some wetlands considered multiple patches had been surveyed for occupancy as a single wetland.

We classified wetlands' geomorphology as slope (no open water body), fluvial (including vegetated irrigation ditches), pond or rice fringe, or waterfowl impoundment. We combined historical imagery, field surveys, and landowner interviews (described below) to determine the water sources of 934 wetlands (53%), including all public land, impoundment, rice fringe, and irrigation ditch wetlands. Wetlands were classified as three water source types: natural-only, irrigation-only, or both-source (even if irrigation was off in some years). Natural water type was further classified as creek or spring. Irrigation type was classified as pasture (which created wetlands when pooling in valleys, including bermed ponds built to recapture this water), leak (from a ditch or pipe), rice, runoff (from multiple uphill properties' irrigation), or water feature

(intentionally creating a wetland or pond). If wetlands received water from more than one type of irrigation they were assigned to what appeared to be their largest source.

Because changes in irrigation created, eliminated, or changed the area of wetlands in this landscape, we used historic aerial imagery to track individual wetlands through time, from 1947–2016. We acquired all imagery of our study area that was available from three online databases (USGS Earth Explorer, USDA Geospatial Data Gateway, and Google Earth) and three regional map libraries (U.C. Santa Barbara Map & Imagery Laboratory, U.C. Berkeley Earth Sciences & Map Library, and U.C. Davis Library Map Collection), resulting in two snapshots per decade and nearly annual measures after 2001 (Appendix S3.2: Table S1). Aerial frames from 1947–1998 were scanned and orthorectified in ERDAS Imagine Leica Photogrammetry Suite (v11; Hexagon Geospatial) using ≥50 tie points per image and a 10 m elevation map (U.S. Geological Survey 2009). Imagery from before 2004 often did not cover the entire study area; thus, not all tracked wetlands could be observed in all years. We measured the area and recorded changes in the irrigation state (presence/absence) of wetlands from our field surveys (n = 292; see *S3.1.7.9 Colonization & extinction*). We also tracked the parcels of the 464 landowner survey respondents whose properties could be identified, including parcels outside the main study area. We mapped all wetlands (n = 711, 598 of which were new) found on these properties in any of the 6 years preceding our survey (2009–2014), measuring their area and irrigation state in each year. In total we mapped 2035 wetlands. When imagery was ambiguous we conservatively assumed no change from the previous time step. To ensure consistency, all observations were reviewed twice by our two most experienced interpreters.

Wetlands were converted to point centroids for the WICM. Wetlands' area was a variable set to their measured 2013 area, unless they were irrigation-fed and their irrigation was off or their area was 0 (e.g., due to mowing) in this year, in which case their area was set to their area in the nearest year with irrigation on and/or a positive area. Unless otherwise noted, this measure of area was used in all analyses. Wetlands were assigned to landowners not according to their centroid location, but based on the property that their highest elevation was in (i.e., their hydrologic origin). We manually checked all wetlands whose point of highest elevation was within 50 meters of a property boundary and corrected them if necessary.

Wetlands with known water source were assigned these sources from GIS data. Following Berger and Schreinemachers (2006), to predict the water sources of the remaining 808 private-land pond fringe, slope, and fluvial wetlands we conducted three mixed-effect regressions with landowner as a random effect using the n = 606 assessed wetlands within the main study area. First, source type (natural-only, irrigation-only, both-source) was predicted using multinomial regression. Then, natural-fed wetlands' type was predicted with logistic regression (creek = 1, spring = 0) and irrigation-fed wetlands' type (pasture, leak, runoff, or water feature) was predicted with multinomial regression. Covariates tested were elevation ($\log_{10}$ m / 100), wetland area ($\log_{10}$ ha), property area ($\log_{10}$ ha), number of wetlands on the property ($\log_{10}$), geomorphology (fringe, slope, or fluvial; all other types had 100% assessed), whether the wetland was in an irrigation district service area (only for source type and irrigation type), and water source (only for irrigation type and natural type). Mixed-effect regressions were conducted in SPSS (v24.0) for multinomial and R (v3.4.3) package *lme4* (v1.1.14) for logistic. Multinomial regressions were weighted by the inverse of the proportion of each category in the dataset, to prevent models from converging to high accuracy by simply assigning all wetlands to the most

common categories. Model selection tables are shown in Appendix S3.2: Tables S2–S4 and final models in Appendix S3.1: Tables S1–S3.

We used logistic regression (R base package *stats*) to determine the probability of an irrigation-fed wetland's irrigation being active in the first year. We excluded from the regression natural-only wetlands, which were all initialized to irrigation-off, and rice irrigation type and irrigation-fed fluvial wetlands, which were all initialized to irrigation-on, as in our data. To reduce potential sampling bias caused by missing wetlands that had irrigation off during our 2013 mapping effort, we used only wetlands (n = 662) from our property-based 2009–2014 tracking of landowner respondents. Our effective sample size was low because most wetlands' irrigation was active, so we only tested three covariates: wetland area ($\log_{10}$ ha), leak irrigation type (because these had higher rates of irrigation deactivation; see *S3.1.7.6 Patch changes (baseline rates)*), and impoundment (because landowners cyclically dry impoundments to fallow them). Model selection table is in Appendix S3.2: Table S5 and best model is in Appendix S3.1: Table S4.

In the WICM area was divided between two variables, irrigated area and natural area (i.e., the area supported by each source in isolation). For irrigation- and natural-only wetlands the total mapped area was assigned to these respective sources. For both-source wetlands, we identified n = 36 both-source wetlands that had area measurements in our 1947–2016 dataset from before and after irrigation was added, without any major geomorphology changes. We then divided each site's average (across years) pre-irrigation area by the average post-irrigation area to estimate the percent of the both-source area that was supported by natural water alone. When square root transformed this data was approximately normally distributed between 0 and 1, so we used normal Tobit regression (R package *censReg* v0.5) censored at 0 and 1 to estimate the mean and SD (log-link) of the square root percent natural area. We included wetland area (ln ha post-irrigation) and irrigation type as possible covariates. We found an intercept-only model was best (μ = 0.6417 ± 0.0423 SE, σ = 0.2594 ± 0.1240); model selection table is in Appendix S3.2: Table S6. In the WICM both-source wetlands' predicted percent natural area was multiplied by their total area to assign their natural area, and the inverse of this was assigned to the irrigated area.

Finally, initial rail occupancy states (see *S3.1.7.9 Colonization & extinction*) and WNV risk (see *S3.1.7.10 West Nile virus risk*) were generated at each wetland.

S3.1.6 Input data

The model does not use input data to represent time-varying processes.

S3.1.7 Submodels

The following provides an integrated description of each submodel and the data collection and analysis used to parameterize it, in the schedule they are called.

S3.1.7.1 Rainy season precipitation

We focused on precipitation as a straightforward driver of reservoir recharge and wetland hydrology. We took historic monthly precipitation data from raster products, extracted for CIMIS weather station #84 near the center of the study area. We used historic 1947–2016 PRISM data (Daly Christopher et al. 2008) for covariates in data analysis and model verification,

and a downscaled 2017–2099 CCSM RCP 8.5 "high greenhouse gas emission" climate scenario (Flint and Flint 2012) for simulations. We chose this scenario because it is closest to present greenhouse gas emission trends (Sanford et al. 2014). We used the mean monthly precipitation over the rainy season (Nov–May), as this metric (1) accounted for the majority of rainfall in this region, with some precipitation in early summer and almost none in late summer and early fall, (2) aligned with the minimum and maximum respective storage levels in reservoirs in almost all years, and (3) coincided with the timing of districts' decision-making on whether to implement drought cutbacks and the start of our rail surveys at the end of May (see *S3.1.7.9 Colonization & extinction)*.

We stochastically generated annual time series of sum Nov–May precipitation based on the $n = 83$ years of CCSM data. We tried fitting both a lag-1 autoregressive model (Salas 1993) and a non-autoregressive model using R package *stats* (v3.4.3), square root transforming precipitation to increase normality. The model without an autoregressive term had lowest AIC (1.98 ΔAIC) so we selected it as the best model:

$$\text{Precipitation} \sim Normal(\mu = 1.023, \sigma = 0.189)^2 \quad \text{(S3.1)}$$

S3.1.7.2 Water storage usage & recharge

We combined information from interviews, documents, and online databases of reservoir levels (Browns Valley Irrigation District 2018b, California Department of Water Resources 2018) to create models of each irrigation district's water reservoir storage capacities, summer water use, winter water recharge, and drought water cutback thresholds. After gathering monthly reservoir level data, we calculated storage recharge for each year by subtracting the minimum start of rainy season reservoir storage levels (usually November) from the maximum end of rainy season storage (usually April–May). To calculate storage used during each summer irrigation season, we subtracted the end of summer (i.e., start next rainy season) minimum storage from the starting previous end of rainy season maximum storage. We then modeled the mean and SD (to account for annual differences caused by evaporation or snowpack) of these values for each district.

BVID's only water storage was the 49,500 acre-feet (AF) Collins Lake reservoir, fed entirely from local low-elevation rainfall. Only $n = 5$ years' (2013–2017) of data on reservoir levels was available to characterize storage usage and recharge. For usage we calculated the mean and SD of acre-feet (AF) used, assuming that this should be relatively constant with some variability due to differences in temperature and early summer precipitation. For recharge we used only the $n = 3$ years when maximum storage capacity was not reached. We divided annual recharge by precipitation to estimate the slope of AF recharge/m precipitation, calculating its mean and SD and assuming an intercept of 0 recharge (i.e., no precipitation equals no recharge).

NID used a complex series of 11 reservoirs totaling 280,380 AF, which were fed by both precipitation and snowmelt and were interconnected via a network of transfer pipelines to other out-of-district reservoirs. We modeled the overall behavior of NID based on the 5 reservoirs that had monthly storage data available, which accounted for 94.9% (266,190 AF) of NID's total storage. Because NID transfers water between them, we summed their individual storage data into one "reservoir" for analysis. We used $n = 51$ years of reservoir data (following completion of final reservoir in 1966), excluding only the severe drought year of 1977 as an outlier. We used normal Tobit regression to estimate mean and SD recharge (R package *crch* v1.0) because usage and recharge were censored by the minimum and maximum storage capacities. We used variable

censoring values, with each value censored at the maximum amount of usage or storage that would result completely draining or filling the reservoir respectively (i.e., the difference between the starting storage and the minimum and maximum storage, 266,190 AF). Since we were not modeling all storage in the system (5.1% of reservoir storage was missing and water can temporarily be moved into out-of-district reservoirs), if the modeled reservoirs were at >90% of the maximum storage we counted them as having reached capacity (based on 2011, a very rainy year following an average year that only reached 90% capacity in these 5 reservoirs). We fit models using only precipitation as a predictor. We tested precipitation as a predictor for usage as well, hypothesizing that because NID is partially fed by summer snowmelt, winter precipitation would result in lower rates of water use over the summer due to increased snowpack. However, precipitation's effect on storage used was non-significant ($p = 0.35$) so we dropped it and used an intercept-only model.

Resulting parameters controlling districts are summarized in Appendix S3.1: Table S5. These parameters were implemented into the WICM in AF/100, with annual storage used and recharge generated from a normal distribution with mean (calculated via regression equation for recharge) and SD (to account for additional annual variability driven by evaporation and snowpack). Annual storage was updated by subtracting the used and adding the recharge. If either 20% or 50% cutbacks were active, storage used was reduced by this percent. If cutbacks were not in place and creation incentives were active (see *Patch changes* subsections), storage used was increased by the corresponding percent:

$$\text{Additional \% of storage used} = \frac{\text{\# of extra MI used} \times 0.0905 \frac{AF}{MI}}{\text{AF Max storage capacity}} \quad \text{(S3.2)}$$

S3.1.7.3 Provide or cutback water

If the new storage fell below a 20% or 50% threshold (Appendix S3.1: Table S5), cutbacks were implemented for that year. BVID employees reported in interviews the storage thresholds at which 20% and 50% cuts would be implemented. NID has a drought contingency plan listing storage thresholds for 15–25% and 35–50% cutbacks (Nevada Irrigation District 2012), which we multiplied by 94.9% and then implemented as 20% and 50% thresholds respectively. Relative to their total storage, usage was lower and cutback thresholds were higher in NID due to contractual obligations to maintain water for minimum streamflow and hydropower.

S3.1.7.4 Provide wetland incentives

The wildlife agency acts deterministically according to our scenario design. If protection policies are in the scenario being run, it provides them. If creation policies are in the scenario, it pays for free water incentives for landowners in districts that do not have drought cutbacks active. Because creation wetlands were using additional irrigation water on top of current pre-existing allocations districts are obligated to provide, we modeled that they would all be turned off and new enrollments suspended during drought cutbacks. See *S3.1.7.8 Patch changes (incentive actions)* for details on policies' cost and effects.

S3.1.7.5 Property transfer

Underlying the patch change models were private landowners' characteristics. Landowner characteristics were fit from survey data. They were first assigned three variables that affected these landowner turnover rates. Landowner's age was generated from a normal distribution fit from the survey respondents' reported ages (μ = 63.175 and σ = 12.313; n = 429). We next probabilistically predicted whether the landowner planned to eventually sell their land based on the percent of respondents that said they would eventually sell (18.26%; n = 449); for those that planned to sell, we used a Poisson distribution to generate "years to sell," the number of years they expected to sell their land in (μ = 7.8; n = 81).

The survey included a question that asked respondents to rate (from one to four) 24 possible motivations for owning their property. All the 24 motivations were fully answered by n = 352 respondents. We then applied factor analysis to these responses and identified six different landowner typologies (factors): profit-oriented agricultural production ("profit"); family, tradition, and a sense of belonging to the land ("tradition"); the lifestyle associated with rural life ("lifestyle"); environmental and wildlife protection ("environment"); vacation and recreational use ("recreation"); and financial investment ("investment"; Appendix S3.2: Table S7). We assigned each respondent to one of these typologies based on the highest factor score obtained from applying the factor loadings to the standardized scores provided by each respondent in the landownership motivation questions. We then used these typology categories as explanatory variables in patch change submodels. We then used multinomial regression to predict landowner typologies, with observations weighted as the inverse of their typology's proportion in the dataset. Possible predictors were age, property area (ln ha), elevation (ln m/100), and number of wetlands on their property. The model selection table is in Appendix S3.2: Table S8 and the final model is in Appendix S3.1: Table S6. Lastly, we predicted landowner's response to drought cutbacks and willingness to participate in wetland protection and creation programs; see *S3.1.7.8 Patch changes (incentive actions)* for details.

These landowner characteristics were set during initialization and changed after landowners died or sold their land. Each landowner risked death annually in this submodel based on an exponential function fit from a US life table (U.S. Social Security Administration 2014) for ages 23 and up (the range of our respondents):

$$\text{Death probability} = 0.0001 \times e^{0.0779 \times \text{age}} \quad \text{(S3.3)}$$

If a landowner did not die, they next sold their land if they planned to sell, either because their "years to sell" reached zero or because they had decided due to drought cutbacks the previous year (see *S3.1.7.8 Patch changes (incentive actions)*). In case of death or sale, the land was transferred to a new landowner by generating new characteristics (the agent was recycled); new landowners were able to re-enroll in incentive programs even if the previous landowner already had. If land was not transferred, landowner's age increased and their "years to sell" decreased by one.

S3.1.7.6 Patch changes (baseline rates)

The process of patch changes was simulated as Markov process where wetlands transitioned between two states, irrigation on (1) or off (0). This was modeled via four subprocesses: baseline (i.e., without any policies) changes in existing wetlands, and landowners responding to irrigation cutbacks, protection incentives, and creation incentives.

We had a fifth planned submodel that estimated the baseline annual probability of a landowner creating a wholly new wetland, based on our 2009–2014 landowner property tracking data (n = 464 properties representing a surveyed area equal to 40% of the private land in study area, with 2335 total wetland observations). However, we found only 4 wetland creation events, 3 of which were minor leaks from ditches and rice fields that were too small to support black rails. The one wetland large enough to support a black rail was a pond leak that was fixed within two years. Thus, rates of new wetland creation on the landscape appeared negligible (<0.001 annual probability per landowner). Our 1947–2016 field-matched data supported this conclusion, with a period of steady growth in the number of irrigation-only wetlands beginning in the 1960s and leveling off by 2000 (data not shown). This result was not altogether unexpected because all regional irrigation allocations have been apportioned and there is a waiting list for new water (Huntsinger et al. 2017). Because rates were so low, to simplify the model we excluded baseline wetland creation from the WICM and only modeled changes in pre-existing wetlands.

Baseline changes were modeled using mixed logistic regression (R package *lme4* v1.1.14) with a random effect for site (i.e., panel data) on the occurrence of two irrigation transitions: irrigation being turned off at a wetland with irrigation on (deactivation probability), or irrigation being turned on at a preexisting but currently unirrigated wetland (activation probability). We included a random effect for site to account for repeat sampling of the same wetlands, as is common for time series data (Bell and Jones 2015). We used our patch change data from 2001–2016, and excluded data from earlier than this, under the assumption that modern rates would better represent future system dynamics that historic rates. We initially tried using our landowner-matched annual 2009–2014 patch change data, but rates of irrigation change were too low to fit both landowner typology and water source as covariates because they lead to some combinations of factor levels with no observations. Therefore, we focused on water source as the more likely important predictor, and expanded our dataset to include data from field-matched wetlands, 2001–2016. Because we were interested in the probability of a wetland that already existed in our model transitioning, when estimating activation probability we excluded the first "creation" irrigation activation of irrigation-only wetlands, and any observations before it. To account for differences in rates of first irrigation versus re-irrigation for both-source wetlands, we included in all activation probability models a separate "natural-only" dummy variable for natural-fed wetlands that had not previously been irrigated. Three groups of wetlands were excluded from the analysis, and assigned static irrigation states in the WICM, because they had no observed transitions: rice wetlands, fluvial wetlands, and natural-only wetlands that were outside of irrigation district service areas. Overall this left n = 4863 observations of 639 wetlands for activation probability, and n = 1062 observations of 183 wetlands for deactivation probability. Because of limited number of turnover events we conducted model selection only on wetland area, impoundment geomorphology, irrigation type as covariates. We attempted to include a random effect for landowner but the estimated variance of this effect was 0, but models with both random effects did not converge so we excluded it. Model selection tables for probability of deactivation and activation are in Appendix S3.2: Tables S9–S10; final models are in Appendix S3.1: Tables S7–S8.

When natural wetlands were irrigated for the first time in the WICM their source type was changed from "natural-only" to "both-source." We used the same data from our both-source natural vs. irrigated area initialization (n = 36) to estimate a Gamma distribution for the new irrigated size increase (α = 0.878 ± 0.180 SE, β = 2.228 ± 0.605).

S3.1.7.7 Patch changes (cutback actions)

Landowners next responded to drought cutbacks (if active), which we parameterized from a survey question asking landowners how they would respond to hypothetical water cutbacks of 20, 50, or 100%. We used logistic regression (NLOGIT v5.0) to model the probabilities of landowners reporting they would respond to cutbacks by taking the following actions: selling some or all land (n = 318 respondents), repairing leaks in ditches, pipes, dams, and/or ponds (only for n = 166 respondents with irrigation); stopping using or using less water to irrigate pasture(s) or reducing area of irrigated pasture (only for n = 93 respondents with pastures); and stopping or reducing growing crops (only for n = 12 respondents with rice fields). We selected these response options in the survey based on preliminary interviews; a write-in option was available but rarely used, indicating these choices captured the likely responses. We included typology in all models because we were interested in how landowner diversity might affect the system. We carried out model selection on property size and elevation (mean of their largest contiguous parcel), including linear, log and quadratic specifications. Because there were few landowners with rice fields, we did not include any covariates in the rice model. AIC tables are in Appendix S3.2: Table S11–S13 and final models in Appendix S3.1: Table S9.

In the WICM, landowners that responded they would take these actions were assigned to four corresponding groups: land-sellers, leak-fixers, pasture-reducers, and rice-reducers. If cutbacks were activated for a landowner's district in a year, land-seller landowners sold their land (i.e., transferred to a random new landowner) in the following year, and took any other actions as normal. All landowners deterministically turned off any irrigation to creation incentive wetlands. Pasture-reducer and rice-reducer landowners temporarily turned off all irrigation to pasture and rice irrigation type wetlands on their properties. While in reality landowners may not stop irrigating all of their pastures or rice fields, we believe this to be a reasonable simplification, as it is likely those fields that are over-irrigated (i.e., resulting in accidental wetlands) would be reduced first. Once cutbacks were lifted, irrigation was automatically turned back on at these sites (unless it was turned off via baseline changes). Leak-fixer landowners permanently turned irrigation off for all leaks on their properties.

We did not model changes for runoff and water feature irrigation type wetlands. Runoff wetlands were fed by runoff from multiple properties and thus difficult to model without a full hydrologic model; however, their multiple water sources also likely made them resistant to drying. Thus, we believe this to be a reasonable approach. Water feature wetlands were either (1) ponds, which landowner interviewees reported were important for storage during drought and would still remain wet albeit possibly with a lower water level, or (2) impoundments that interviewees and districts reported were mainly fed by separate, more resilient irrigation supplies from the Yuba River.

S3.1.7.8 Patch changes (incentive actions)

Lastly, landowners chose whether to participate in wetland-promoting incentive programs. We parameterized this via logistic regression (NLOGIT v5.0) on responses to a survey question asking landowners whether they would be interested in protecting a wetland for a one-time payment (only for n = 141 landowners with wetlands), or creating a wetland if given free water (n = 328). We used the same covariates as drought cutbacks, plus whether the property was in

Nevada county (because NID had higher water prices). AIC tables are in Appendix S3.2: Tables S14–S25 and final models in Appendix S3.1: Table S10.

All landowners instantaneously signing up for creation or incentive programs would be unrealistic behavior. Therefore, we set an annual enrollment rate of potential-creation-landowners and potential-protection-landowners in these programs of 5.263% (i.e., the probability that a landowner in one of these groups actually enrolled that year). We based this rate on the U.S. Wetlands Reserve Program, which had a linear rate of participation following inception that took 19 years to reach its original acreage goal (Ferris and Siikamäki 2009).

Protection-landowners were given a one-time payment of $10,000 by the wildlife agency to set their largest wetlands to "protected" status, preventing it from being turned off even during drought cutbacks. This was the maximum amount requested by landowners that said they would be willing to participate (minimum $1,000; median $5,000). Protection incentives excluded impoundments, rice fringes, and fluvial creeks since these were poorer black rail habitat and not in need of protection; if a landowner did not have a suitable wetland, they could not participate. Protected wetlands were automatically re-irrigated if irrigation had been turned off.

Creation-landowners received free water from their irrigation district to create a single slope geomorphology wetland, which was the best black rail habitat. Wetlands could only be created on cells of their property serviced by irrigation districts that did not already have a wetland on them; if a landowner did not have a suitable cell, they could not participate. We parameterized this model with data from $n = 18$ slope wetlands that were intentionally created for black rail habitat within the regional Spenceville and Daugherty Hill State Wildlife Areas. We divided the area of each wetland created by the amount of irrigation applied (acquired from refuge staff) to estimate a mean ± SD wetland creation of 0.213 ± 0.126 ha / MI. The average amount of water used was 2.67 MI, so we set the creation water amount supplied to landowners at 2.67 for BVID and 2.5 MI for NID based on the increments sold by each district. The costs for supplying this water for one summer was $893.10 for BVID and $550.00 for NID (Browns Valley Irrigation District 2018a, Nevada Irrigation District 2018), which would be paid by the state wildlife agency, similar to an existing program in the Central Valley (Duffy and Kahara 2011). Landowners could enroll in each program only once, and total water allocation for creation incentive programs was capped at 2% of each district's storage.

Finally, the areas of wetlands were updated based on the preceding changes to irrigation state. The wetland's overall area was set to the natural area, plus the irrigated area multiplied by 1 if irrigation was on and 0 if irrigation was off.

S3.1.7.9 Colonization & extinction

We conducted annual broadcast surveys for black rails and Virginia rails of $n = 273$ wetlands (43% of the 2013 acreage) during the breeding season, late May–early August from 2002–2016 (methodology described in Richmond et al. 2008, 2010b). Surveys for Virginia rails began in 2004, with revisits only using black rail calls in that year. We conducted up to 3 resurveys each summer to allow for occupancy modeling correcting for detection probability. These models jointly estimate wetland-specific probabilities of initial occupancy (Ψ), colonization (γ), and extinction (ε), with covariates fit to each probability via logit-link regression equations (MacKenzie et al. 2003). Previous studies have found no competition between black and Virginia rails so we analyzed and simulated their dynamics separately (Risk et al. 2011).

Area and connectivity were included in all models because they are the foundation of metapopulation theory (Hanski 1999). For area we used our annual measures of area to account for irrigation being turned on and off at sites, isolating the effects of precipitation on wetlands (i.e., substrate drying) from changes in irrigation behavior driven by changes precipitation. Isolation was included as an autoregressive connectivity metric, $\log_{10}$ sum ha of occupied wetlands within a 7 km radius, which had been previously found to be the best connectivity metric for black rails (Hall et al. 2018). This connectivity metric incorporates occupancy probability at sites that were unsurveyed or had non-detections when fitting the occupancy model, to best match the complete knowledge of the simulated occupancy status of all 1759 wetlands used when calculating the metric within the ABM. Following the same methodology used in (Hall et al. 2018) we carried out an equivalent analysis for Virginia rails (for brevity, data not shown). However, model selection only weakly supported dispersal limitation to their connectivity (best autoregressive metric ΔAIC 1.12 improvement compared to model without) with effect sizes in the opposite direction predicted by theory (i.e., lower colonization in well-connected areas), suggesting a spurious result. Earlier studies in this system found Virginia rails were not dispersal limited (Risk et al. 2011), supporting this conclusion. We thus excluded connectivity metrics from all the Virginia rail models.

We used R package *unmarked* (v0.12) to carry out multi-season occupancy models (MacKenzie et al. 2003). The remaining covariates for γ and ε were assessed via model selection: precipitation (ln m), WNV risk (see *S3.1.7.10 West Nile virus risk*), elevation (m/100), water source type (natural, irrigated, or both), and geomorphology type (slope, fringe, fluvial, or impoundment). Black rail Ψ included covariates if they were included as covariates for either γ or ε, with four exceptions: WNV because it had not arrived in the region in the first year of the study (2002), precipitation because it was a year-based effect, connectivity because it could not be initialized in the simulation, and impoundment because none were surveyed in the first year. Area was the only covariate for Virginia rail Ψ due to the small sample size in their first year of surveys. The results of model selection exercise are in Appendix S3.2: Table S16–S17. For the final black rail model, we re-ran the top model without connectivity's effect on ε because this term was a non-significant effect in the opposite direction predicted by theory.

We implemented the final model for each species as a series of 6 regression equations (Appendix S3.1: Table S11). Occupancy is initialized during model start-up with each wetland stochastically assigned as occupied with probability Ψ. At each subsequent year unoccupied wetlands risks stochastic colonization with probability γ, and occupied wetlands risks stochastic extinction with probability ε. These probabilities were site- and year-specific. Connectivity for black rails was calculated based on the buffer radius calculated in the previous year, as in the analysis model. It was necessary to include in WICM wetlands that were too small to support these rail species, in order to accurately model landowner behavior and WNV. To prevent stochastic colonization of these wetlands, we deterministically set unoccupied any wetland smaller than the minimum observed 95% kernel density estimates of breeding home ranges from radio-tracked black and Virginia rails in this region (0.16 and 0.28 ha, respectively; S.R. Beissinger, unpublished data).

S3.1.7.10 West Nile virus risk

We trapped mosquitoes at $n = 80$ of our field wetlands (range in area 0.03–8.92 ha) from June through October 2012–2014. We sampled 60 wetlands for one year and 20 wetlands in all 3

years. We visited each wetland weekly (1,658 total visits) and set up 4 Center for Disease Control traps baited with dry ice. Mosquitoes were then identified to species using established morphological keys (Darsie and Ward 2005). For each wetland, we estimated the abundance of the main WNV mosquito vectors as the mean number of *Culex* mosquitoes (*C. tarsalis, C. thriambus, C. pipiens,* and *C. stigmatasoma*) caught per trap/night (6,385 trap/nights).

To estimate WNV prevalence at each wetland, we first extracted RNA using RNeasy kits (Qiagen) followed by RT-PCR (Qiagen) on n = 3,706 pools (i.e., groups) of 1-50 *Culex* mosquitoes (mean of 19.4 mosquitoes/pool) (Kauffman et al. 2003). Alongside each set of 40 reactions, we included at least one positive and negative control and all WNV-positive mosquito pools were run twice to confirm presence of WNV. In the few cases where a pool tested positive and then negative, we used the results of a third test to determine WNV status. We then estimated average WNV *Culex* prevalence at each wetland using bias-reduced generalized linear models (R package *brglm*) with a binomial distribution and an offset for mosquito pool size. We accounted for differences in date and year by including the following predictors: site, date, date^2, and year, as well as interactions between these. We then used the model with the lowest AICc value (Appendix S3.2: Table S18) to estimate mean *Culex* WNV prevalence at each wetland site.

We used linear regression to model average *Culex* abundance and average *Culex* WNV prevalence across wetland sites. For *Culex* abundance we used the 6 potential predictor variables: elevation, distance to nearest rice field, percent of wetland cover in 2.5 km buffer, percent of open water cover in 2.5 km buffer, presence of flowing water, and presence of irrigation. For *Culex* WNV prevalence we used the same 6 potential predictors listed above and the average *Culex* abundance at each wetland site. We used backwards stepwise regression based on lowest AICc values (Appendix S3.2: Tables S19–S20) to find the best models for *Culex* abundance and *Culex* WNV prevalence (Appendix S3.1: Tables S12–S13).

We estimated WNV risk at each wetland as the infected vector abundance (the product of *Culex* mosquito abundance and *Culex* WNV prevalence). The validity of this measure of WNV disease risk has a strong theoretical basis, and it has been found to be a good predictor of spatial variation in human disease cases for WNV (Kilpatrick et al. 2006, Bolling et al. 2009, Kwan et al. 2012, Kilpatrick and Pape 2013) and many other vector borne pathogens (Beier et al. 1999, Pepin et al. 2012, Dobson and Auld 2016). For fitting rail occupancy models we used the actual values for mosquito trapping sites, and used the best models for abundance and prevalence to predict values for all other wetlands based on the 2013 landscape. In the WICM, at the end of each time step the best *Culex* abundance and *Culex* prevalence models were used at the end of each time step to predict each of these, and then their values were multiplied together estimate WNV risk. Effects on metapopulations were modeled with a one year delay because mosquito abundances peaked in late summer and early fall, after rail surveys had already concluded. Disease mortality therefore affected colonization and extinction rates over the winter, which determined occupancy in the following year.

Appendix S3.1: Table S1. Final model for mixed multinomial regression prediction of water source type (natural-only, irrigation-only, or both-source) of pond fringe, fluvial, and slope geomorphology wetlands in the California Sierra Nevada foothills (n = 606). The wetland's landowner was a random effect. Irrigation-only and slope geomorphology were reference categories.

Source type	Parameter	Coefficient	SE	p-value
Both-source	Intercept	-1.822	0.413	<0.001
	Fluvial geomorphology	2.234	0.365	<0.001
	Fringe geomorphology	-0.250	0.196	0.203
	Property area ($\log_{10}$ ha)	0.588	0.235	0.013
	No irrigation district	0.843	0.597	0.158
	Landowner σ	2.103	-	-
Natural-only	Intercept	-4.509	0.765	<0.001
	Fluvial geomorphology	-1.342	0.597	0.025
	Fringe geomorphology	-0.660	0.226	0.004
	Property area ($\log_{10}$ ha)	1.189	0.397	0.003
	No irrigation district	4.308	0.623	<0.001
	Landowner σ	2.933	-	-

Appendix S3.1: Table S2. Final model for mixed multinomial regression prediction of irrigation type (pasture, leak, runoff, or water feature) of irrigation-fed pond fringe, fluvial, and slope geomorphology wetlands in the California Sierra Nevadas foothills (n = 557). The wetland's landowner was a random effect. Pasture, irrigation-only water source and slope geomorphology were reference categories. All rice wetlands were assessed so this irrigation type is not included.

Irrigation type	Parameter	Coefficient	SE	p-value
Leak	Intercept	-0.802	0.707	0.257
	Both-source	-0.048	0.292	0.870
	Fluvial geomorphology	-1.113	0.627	0.076
	Fringe geomorphology	-2.143	0.418	<0.001
	Elevation (log_{10} m / 100)	0.289	0.334	0.387
	Property area (log_{10} ha)	-0.082	0.518	0.874
	Wetland area (log_{10} ha)	-1.548	0.224	<0.001
	# wetlands on property (log_{10})	-1.898	1.101	0.085
	Landowner σ	3.078	-	-
Runoff	Intercept	-1.932	0.592	0.001
	Both-source	1.015	0.280	<0.001
	Fluvial geomorphology	4.021	0.480	<0.001
	Fringe geomorphology	1.301	0.271	<0.001
	Elevation (log_{10} m / 100)	0.183	0.280	0.515
	Property area (log_{10} ha)	0.473	0.421	0.262
	Wetland area (log_{10} ha)	-0.823	0.198	<0.001
	# wetlands on property (log_{10})	-2.660	0.906	0.003
	Landowner σ	2.652	0.975	-
ater feature	Intercept	-2.116	0.648	0.001
	Both-source	-1.208	0.305	<0.001
	Fluvial geomorphology	3.042	0.587	<0.001
	Fringe geomorphology	3.363	0.291	<0.001
	Elevation (log_{10} m / 100)	0.068	0.296	0.818
	Property area (log_{10} ha)	-0.442	0.485	0.362
	Wetland area (log_{10} ha)	-0.986	0.196	<0.001
	# wetlands on property (log_{10})	-0.462	1.014	0.649
	Landowner σ	2.675	-	-

Appendix S3.1: Table S3. Final model for mixed logistic regression prediction of natural type (creek = 1, spring = 0) of natural-fed pond fringe, fluvial, and slope geomorphology wetlands in the California Sierra Nevada foothills (n = 217). The wetland's landowner was a random effect. Fluvial geomorphology was a reference category.

Parameter	**Coefficient**	**SE**	**p-value**
Intercept	3.388	0.925	<0.001
Fringe geomorphology	-4.033	1.016	<0.001
Slope geomorphology	-6.604	1.363	<0.001
Landowner σ	2.052	-	-

Appendix S3.1: Table S4. Best model for logistic regression on probability of irrigation being active in 2013 for irrigation-fed wetlands in the California Sierra Nevada foothills (n = 663).

Parameter	**Coefficient**	**SE**	**p-value**
Intercept	3.245	0.240	<0.001
Impoundment	-1.938	0.336	<0.001

Appendix S3.1: Table S5. Summary of parameters controlling water storage behavior of Nevada Irrigation District (NID) and Browns Valley Irrigation District (BVID) fit from reservoir data, district documents, and interviews. Values for BVID are for Collin's Lake reservoir; values for NID are for the sum of the 5 reservoirs modeled (Bowman, Scotts Flat, Rollin, French Lake, and Jackson Meadows reservoirs). All values are in 100s of acre-feet.

Characteristic	Parameter	BVID value	NID value
Storage capacity	Maximum	495.00	2661.90
	20% cutback threshold	225.00	1879.79
	50% cutback threshold	98.00	1443.07
Storage recharge	Intercept	0.00	-863.60
	Precipitation (Nov–May sum m)	281.02	1955.00
	Standard deviation	50.53	156.49
Storage used	Mean	282.68	947.06
	Standard deviation	85.36	172.78

Appendix S3.1: Table S6. Final model for multinomial regression prediction of landowner typologies in the California Sierra Nevada foothills (n = 350).

Typology	Parameter	Coefficient	SE	p-value
Investment-motivated	Intercept	0.061	0.389	0.875
	Property area (ln ha)	0.006	0.125	0.962
Lifestyle-motivated	Intercept	1.038	0.370	0.005
	Property area (ln ha)	-0.387	0.140	0.006
Profit-motivated	Intercept	-0.744	0.412	0.071
	Property area (ln ha)	0.282	0.120	0.019
Recreation-motivated	Intercept	-0.067	0.375	0.858
	Property area (ln ha)	0.146	0.116	0.206
Tradition-motivated	Intercept	-0.579	0.401	0.149
	Property area (ln ha)	0.253	0.119	0.033

Appendix S3.1: Table S7. Final model for mixed logistic regression (site random effect) on probability of irrigation activation (i.e., being turned on at a pre-existing wetland with irrigation currently off) in the California Sierra Nevada foothills (n = 4863).

Parameter	**Coefficient**	**SE**	**p-value**
Intercept	-3.529	0.576	<0.001
Natural-only	-3.903	0.757	<0.001
Precipitation (Nov–May sum m)	1.307	0.422	0.002
Impoundment	2.082	0.292	<0.001
Site σ	0.495	-	-

Appendix S3.1: Table S8. Final model for mixed logistic regression (site random effect) on the probability of irrigation deactivation (i.e., irrigation being turned off currently irrigated wetland) in the California Sierra Nevada foothills (n = 1062).

Parameter	**Coefficient**	**SE**	**p-value**
Intercept	-5.466	0.677	<0.001
Precipitation (Nov–May sum m)	-0.779	0.404	0.054
Impoundment	5.178	0.577	<0.001
Leak	1.109	0.586	0.058
Pasture	-0.566	0.617	0.359
Runoff	-1.296	0.899	0.150
Site σ	2.201	-	-

Appendix S3.1: Table S9. Final models for logistic regression analysis of the probability of landowners in the California Sierra Nevadas taking different management actions in response to water cutbacks of ≥20%. Values in parentheses are standard errors.

Parameter	**Dependent variable (take action = 1; otherwise = 0)**			
	Sell land	**Cut pasture**	**Cut rice**	**Fix leaks**
Intercept (investment typology)	-3.8501*** (1.0106)	0.0592 (0.8322)	0.3364 (0.3333)	-3.7165*** (1.0141)
Lifestyle typology	-0.1201 (1.4283)	2.5194** (1.1112)	-	0.9032 (1.2686)
Environment typology	0.0215 (1.4293)	0.9096 (1.0320)	-	-[A]
Profit typology	1.9894* (1.0892)	1.7633* (0.9840)	-	2.0853 (1.0977)
Tradition typology	1.5678 (1.1143)	2.2670** (1.0540)	-	0.5325 (1.3018)
Recreation typology	0.8544 (1.1710)	0.4804 (1.175)	-	1.6165 (1.1662)
Property elevation (m)	-	-0.0026** (0.0011)	-	-
Property area (acres)	-	0.0028** (0.0014)	-	0.0010** (0.0004)
Property area^2 (acres)	-	-0.4267×10^{-06}** (0.2096×10^{-06})	-	-
n	318	93	318	166

*, **, and *** indicate significance at the 10, 5, and 1% levels respectively.

[A] Environment typology had perfect separation (no leak fixers) so this factor level was grouped with investment for this analysis.

Appendix S3.1: Table S10. Final models for logistic regression analysis of the probability of landowners in the California Sierra Nevada foothills being willing to participate in two wetland incentive programs. Values in parentheses are standard errors.

Parameter	**Dependent variable (willing = 1; otherwise = 0)**	
	Wetland protection	**Wetland creation**
Intercept ("investment" typology)	-1.9097*** (0.7362)	-0.3980 (0.3507)
"Lifestyle" typology	-1.3323 (1.2120)	0.3899 (0.4076)
"Environment" typology	-0.1962 (0.9020)	0.4719 (0.4195)
"Profit" typology	-0.7942 (0.8812)	-0.2788 (0.4270)
"Tradition" typology	-0.1644 (0.8444)	0.1088 (0.4178)
"Recreation" typology	-0.1830 (0.8407)	0.1123 (0.3993)
Property Elevation	0.0013 (0.0012)	-0.0020** (0.0008)
Nevada Irrigation District	-	0.7856** (0.3646)
n	141	328

*, **, and *** indicate significance at the 10, 5, and 1% levels respectively.

Appendix S3.1: Table S11. Final occupancy models for black and Virginia rails in the California Sierra Nevadas. Dashes indicate parameters not in the top model for that species.

Occupancy parameter	Beta parameter	Black rail Coefficient	SE	*p*	Virginia rail Coefficient	SE	*p*
Initial Occ.	Intercept	0.421	0.632	0.505	-0.364	0.630	0.564
	Area	1.672	0.537	0.002	0.491	0.641	0.444
	Slope	1.759	0.573	0.002	-	-	-
	Fluvial	0.238	0.826	0.773	-	-	-
	Irrigation-only	-0.398	0.617	0.519	-	-	-
	Natural-only	-1.142	0.741	0.123	-	-	-
Colonization	Intercept	-5.107	0.583	<0.001	-1.040	0.121	<0.001
	Area	0.984	0.196	<0.001	1.910	0.196	<0.001
	Connectivity	1.507	0.273	<0.001	-	-	-
	Slope	1.091	0.250	<0.001	-	-	-
	Fluvial	-0.053	0.335	0.875	-	-	-
	Impoundment	0.046	0.458	0.920	-	-	-
	Irrigation-only	-0.595	0.241	0.014	-	-	-
	Natural-only	-0.720	0.272	0.008	-	-	-
	WNV risk	-0.359	0.113	0.002	-	-	-
	Precipitation	1.569	0.402	<0.001	1.070	0.371	0.004
Extinction	Intercept	-0.745	0.358	0.037	-0.620	0.240	0.010
	Area	-2.813	0.269	<0.001	-2.657	0.293	<0.001
	Slope	-0.796	0.295	0.007	-	-	-
	Fluvial	0.861	0.384	0.025	-	-	-
	Impoundment	3.451	0.757	<0.001	-	-	-
	Irrigation-only	-0.210	0.221	0.342	0.413	0.239	0.085
	Natural-only	1.409	0.388	<0.001	0.912	0.307	0.003
	WNV risk	0.198	0.127	0.119	-	-	-
	Precipitation	-1.443	0.512	0.005	-1.288	0.507	0.011
	Elevation	-	-	-	-0.558	0.118	<0.001
	Intercept	1.219	0.269	<0.001	-1.140	0.615	0.063
Detection	Year 2003	0.590	0.463	0.203	-	-	-
	Year 2004	1.367	0.542	0.012	-	-	-
	Year 2005	0.738	0.416	0.076	2.020	0.515	<0.001
	Year 2006	0.353	0.369	0.338	1.990	0.649	0.002
	Year 2007	-1.537	0.353	<0.001	1.340	0.647	0.039
	Year 2008	-0.070	0.329	0.832	1.830	0.639	0.004
	Year 2009	0.428	0.400	0.285	1.320	0.646	0.040
	Year 2010	0.500	0.392	0.203	2.160	0.650	0.001
	Year 2011	-0.218	0.334	0.514	1.810	0.640	0.005
	Year 2012	-0.542	0.350	0.122	1.720	0.645	0.008
	Year 2013	-0.608	0.328	0.064	1.170	0.644	0.069
	Year 2014	-0.538	0.365	0.141	1.360	0.642	0.035
	Year 2015	-0.587	0.353	0.096	1.990	0.646	0.002
	Year 2016	-0.240	0.354	0.498	1.570	0.646	0.015
	No playback	-	-	-	-1.010	0.415	0.015

Appendix S3.1: Table S12. Final model for linear regression on $\log_{10}$ *Culex* spp. abundance at *n* = 80 wetlands in the California Sierra Nevada foothills.

Parameter	**Coefficient**	**SE**	**p-value**
Intercept	0.889	0.325	0.008
% Wetland cover within 2.5 km (√)	4.909	1.211	<0.001
Distance to rice field (√km)	-0.138	0.083	0.101

Appendix S3.1: Table S13. Final model for linear regression on $\log_{10}$ estimated *Culex* spp. West Nile virus prevalence at $n = 80$ wetlands in the California Sierra Nevada foothills.

Parameter	**Coefficient**	**SE**	**p-value**
Intercept	-1.505	0.243	<0.001
Distance to rice field (√)	-0.118	0.058	0.046
Culex spp. abundance (Log_{10})	-0.407	0.105	<0.001

Appendix S3.2: Analysis and model selection tables for parameterization of WICM

This appendix contains analysis tables, chiefly AIC model selection, used in parameterizing the Wetlands-Irrigation CHANS Model (WICM). Unless otherwise noted, we used AIC model selection and selected the model with a ΔAIC or AICc <2 that had the fewest numbers of parameters (to increase parsimony).

Appendix S3.2: Table S1. Imagery used for mapping changes in Sierra Nevada foothills wetlands. Source provides company or programmatic names of satellites/flights. Resolution is provided for digital orthoimagery; original scale for scanned aerial frames.

Year	Source	Imagery Type	Color	Resolution (m) / Scale	# sampled wetlands
2016	NAIP	Orthoimagery	Color	0.6*	292
2015	DigitalGlobe	Satellite	Color	0.6*	292
2014	NAIP	Orthoimagery	Color	1.0	890
2013	DigitalGlobe	Satellite	Color	0.6*	2034
2012	NAIP	Orthoimagery	Color	1.0	890
2011	DigitalGlobe	Satellite	Color	0.6*	890
2010	DigitalGlobe	Satellite	Color	0.6*	890
2009	NAIP	Orthoimagery	Color	1.0	890
2007	USGS Aerials Express	Orthoimagery	Color	0.5	292
2006	DigitalGlobe; NAIP	Satellite; orthoimagery	Color	0.6*; 2.0	292
2005	NAIP	Orthoimagery	Color	1.0	292
2004	NAIP	Orthoimagery	Color	2.0	292
2003	DigitalGlobe; NAIP	Satellite; orthoimagery	Color	0.6; 2.0	264
2001	IKONOS	Satellite	Color	0.8	283
1998	NAPP-3C	Aerial frames	Grayscale	1:40,000	292
1993	NAPP-2C	Aerial frames	Grayscale	1:40,000	292
1987	GS-VFLL-C	Aerial frames	Color	1:24,000	289
1984	WAC-84C	Aerial frames	Grayscale	1:31,680	292
1978	78-102-02645; 78-131-02679	Optical bar scanner	Color infrared	1:32,500	290
1971	AR573	Aerial frames	Grayscale	1:20,000	32
1970	AAX-1970	Aerial frames	Grayscale	1:40,000	112
1969	CAS-2579	Aerial frames	Grayscale	1:20,000	240
1962	CAS-YUB; CAS-NEV; CAS-BUT	Aerial frames	Grayscale	1:20,000	286
1958	ABA-1958; AAX-1958	Aerial frames	Grayscale	1:20,000	53
1952	ABA-1952; DRG-1952	Aerial frames	Grayscale	1:20,000	199
1947	AAX-1952	Aerial frames	Grayscale	1:28,400	176

* Exact resolution unknown because accessed via Google Earth; estimated as the average of QuickBird II, GeoEye-1, and WorldView-3 satellites (range 0.46–0.65 m pan-sharpened resolution).

Appendix S3.2: Table S2. Model selection results for mixed multinomial regression on water source type (natural-only, irrigation-only, or both-source) of pond fringe, fluvial, and slope geomorphology wetlands in the California Sierra Nevada foothills (n = 606). The wetland's landowner was a random effect. Elevation was in m/100 and areas were in ha and # wetlands was the total on the property; all were $\log_{10}$ transformed. Geomorphology was a factor. Only the top 10 models and the intercept-only model are shown (out of 63); selected model is bolded.

Model	**ΔAIC**	**AIC**	***w***	***K***
Geomorphology + Property area + No district	**0.00**	**-6193.76**	**0.74**	**14**
Geomorphology + Property area + # wetlands + No district	2.13	-6191.63	0.26	16
Geomorphology + # wetlands + No district	39.79	-6153.97	0.00	14
Geomorphology + Elevation + Property area + No district	44.67	-6149.09	0.00	16
Geomorphology + Elevation + Property area + # wetlands + No district	47.43	-6146.33	0.00	18
Geomorphology + Property area + Wetland area + No district	70.48	-6123.28	0.00	16
Geomorphology + Property area + Wetland area + # wetlands + No district	70.87	-6122.89	0.00	18
Geomorphology + No district	73.45	-6120.31	0.00	12
Geomorphology + Elevation + Property area + Wetland area + No district	82.26	-6111.50	0.00	18
Geomorphology + Elevation + Property area + Wetland area + # wetlands + No district	83.03	-6110.73	0.00	20
Intercept-only	431.28	-5762.48	0.00	6

Appendix S3.2: Table S3. Model selection results for mixed multinomial regression prediction of irrigation type (pasture, creek, runoff, or water feature) of $n = 557$ irrigation-fed pond fringe, fluvial, and slope geomorphology wetlands in the California Sierra Nevada foothills. The wetland's landowner was a random effect. All rice wetlands were assessed so this irrigation type is not included. Continuous variables were $\log_{10}$ transformed, elevation was in m/100, areas were in ha, # wetlands was the total number on each property, and geomorphology was a factor. Only the top 10 models and the intercept-only model are shown (out of 127); selected model is bolded.

Model	ΔAIC	AIC	*w*	*K*
Both-source + Geomorphology + Elevation + Property area + Wetland area + # wetlands	**0.00**	**-8292.52**	**1.00**	**20**
Both-source + Geomorphology + Elevation + Wetland area + # wetlands	14.59	-8277.93	0.00	18
Both-source + Geomorphology + Property area + Wetland area + # wetlands	26.07	-8266.45	0.00	18
Both-source + Geomorphology + Elevation + Property area + Wetland area	26.14	-8266.39	0.00	18
Both-source + Geomorphology + Elevation + Property area + Wetland area + # wetlands + No district	28.52	-8264.00	0.00	20
Both-source + Geomorphology + Property area + Wetland area + # wetlands + No district	32.34	-8260.18	0.00	18
Both-source + Geomorphology + Wetland area + # wetlands	39.44	-8253.08	0.00	16
Both-source + Geomorphology + Elevation + Wetland area + # wetlands + No district	43.01	-8249.51	0.00	18
Both-source + Geomorphology + Wetland area + # wetlands + No district	46.23	-8246.29	0.00	16
Both-source + Geomorphology + Elevation + Property area + Wetland area + No district	49.79	-8242.74	0.00	18
Intercept-only	801.66	-7490.86	0.00	6

Appendix S3.2: Table S4. Model selection results for mixed logistic regression on natural type (creek = 1, spring = 0) of natural-fed pond fringe, fluvial, and slope geomorphology wetlands in the California Sierra Nevada foothills ($n = 217$). The wetland's landowner was a random effect. Continuous variables were $\log_{10}$ transformed, elevation was in m/100, areas were in ha, # wetlands was the total number on each property, and geomorphology was a factor. Only models with ≥0.01 AICc wt. and the intercept-only model are shown (out of 64); selected model is bolded.

Model	**ΔAICc**	**AICc**	***w***	***K***
Geomorphology + Elevation	0.00	190.74	0.10	5
Geomorphology + Elevation + # wetlands	0.74	191.48	0.07	6
Geomorphology + Elevation + Property area	0.77	191.52	0.07	6
Natural-only + Geomorphology + Elevation	0.82	191.56	0.07	6
Geomorphology	**1.28**	**192.02**	**0.06**	**4**
Natural-only + Geomorphology + Elevation + Property area	1.41	192.15	0.05	7
Natural-only + Geomorphology	1.49	192.24	0.05	5
Natural-only + Geomorphology + Elevation + # wetlands	1.53	192.27	0.05	7
Geomorphology + Elevation + Wetland area	2.09	192.83	0.04	6
Natural-only + Geomorphology + Property area	2.18	192.92	0.04	6
Geomorphology + Property area	2.21	192.95	0.03	5
Geomorphology + # wetlands	2.42	193.16	0.03	5
Natural-only + Geomorphology + # wetlands	2.56	193.30	0.03	6
Natural-only + Geomorphology + Elevation + Wetland area	2.60	193.34	0.03	7
Geomorphology + Elevation + Property area + # wetlands	2.69	193.44	0.03	7
Geomorphology + Elevation + Wetland area + # wetlands	2.86	193.61	0.03	7
Geomorphology + Elevation + Property area + Wetland area	2.91	193.65	0.02	7
Natural-only + Geomorphology + Wetland area	3.02	193.76	0.02	6
Geomorphology + Wetland area	3.31	194.05	0.02	5
Natural-only + Geomorphology + Elevation + Wetland area + # wetlands	3.37	194.11	0.02	8
Natural-only + Geomorphology + Elevation + Property area + Wetland area	3.40	194.14	0.02	8
Natural-only + Geomorphology + Elevation + Property area + # wetlands	3.41	194.15	0.02	8
Natural-only + Geomorphology + Property area + Wetland area	3.96	194.70	0.01	7
Natural-only + Geomorphology + Wetland area + # wetlands	4.13	194.87	0.01	7
Geomorphology + Property area + # wetlands	4.26	195.00	0.01	6
Natural-only + Geomorphology + Property area + # wetlands	4.28	195.02	0.01	7
Geomorphology + Property area + Wetland area	4.32	195.06	0.01	6
Geomorphology + Wetland area + # wetlands	4.48	195.22	0.01	6
Geomorphology + Elevation + Property area + Wetland area + # wetlands	4.85	195.59	0.01	8
Natural-only + Geomorphology + Elevation + Property area + Wetland area + # wetlands	5.37	196.11	0.01	9
Natural-only + Geomorphology + Property area + Wetland area + # wetlands	6.03	196.77	0.01	8
Intercept-only	79.70	270.44	0.00	2

Appendix S3.2: Table S5. Model selection results for logistic regression on probability of irrigation being active in 2013 for irrigation-fed wetlands in the California Sierra Nevada foothills (n = 663). Wetland area was in $\log_{10}$ ha.

Model	**ΔAICc**	**AICc**	***w***	***K***
Impoundment geomorphology + Leak	0.00	267.48	0.48	3
Wetland area + Impoundment geomorphology + Leak	1.40	268.87	0.24	4
Impoundment geomorphology	**1.92**	**269.4**	**0.18**	**2**
Wetland area + Impoundment geomorphology	3.05	270.53	0.10	3
Wetland area	28.36	295.84	0.00	2
Wetland area + Leak	29.47	296.94	0.00	3
Intercept-only	31.98	299.46	0.00	1
Leak	33.77	301.25	0.00	2

Appendix S3.2: Table S6. Model selection results for Tobit regression (censored at 0 and 1 with a standard deviation parameter) on the areal percent of a both-source wetland that is supported by natural water sources in the California Sierra Nevada foothills (n = 36). The response variable was square root transformed and irrigation type was a factor (pasture, leak, runoff, water feature; no rice wetlands were both-source). Selected model is bolded.

Model	**ΔAIC**	**AIC**	***w***	***K***
Intercept-only	**0.00**	**15.87**	**0.58**	**2**
Wetland area (ln ha)	1.76	17.63	0.24	3
Irrigation type	2.95	18.83	0.13	5
Wetland area (ln ha), irrigation type	4.95	20.82	0.05	6

Appendix S3.2: Table S7. Landowner typologies in California's Sierra Nevada foothills as determined via weightings in a factorial analysis from a survey question on 24 reasons for land ownership (n = 352). These six typologies accounted for 64% of the variance in reasons for land ownership. Loadings are grouped and shown in bold by their landowner type.

Landowner typology	**Reason for land ownership**	**Factor**					
(% of sample)		**1**	**2**	**3**	**4**	**5**	**6**
Lifestyle-motivated	I want to escape or stay away from the city	**0.835**	0.186	0.049	0.183	0.009	0.014
(16.8%)	I like to live in a smaller community	**0.830**	0.141	0.049	0.205	0.022	0.035
	This is a healthy place to live	**0.652**	0.439	0.128	0.107	0.093	0.024
	I like to live near natural beauty	**0.593**	0.515	-0.038	0.150	-0.035	0.148
	To grow some of my own food	**0.571**	0.280	0.359	0.117	-0.031	0.021
	To raise horses, ponies, donkeys, or mules	**0.439**	0.021	0.356	-0.205	0.164	0.074
Environment-motivated (14.5%)	My land allows me to protect the environment	0.267	**0.768**	0.076	0.140	-0.009	0.209
	To preserve open space	0.201	**0.756**	0.126	0.104	0.048	-0.100
	I want to restore and manage this land	0.121	**0.712**	0.384	0.156	0.085	0.015
	I enjoy improving this land	0.268	**0.610**	0.443	0.008	0.018	-0.003
	I enjoy seeing wildlife and/or birds	0.540	**0.582**	-0.129	0.088	0.131	-0.048
Profit-motivated	My land is a source of income	-0.046	0.196	**0.778**	0.164	-0.025	0.233
(15.9%)	To raise cattle or sheep	0.127	0.036	**0.749**	0.183	-0.105	-0.170
	Living on this land is a family business	0.057	0.105	**0.723**	0.414	0.005	0.146
	To contribute to the local economy	0.111	0.330	**0.659**	0.142	0.143	0.205
Tradition-motivated	A good place to raise my children	0.246	0.015	0.173	**0.708**	0.069	0.022
(17.0%)	I was born here or near here	0.003	0.014	0.298	**0.697**	0.043	-0.247
	I want to pass this land to my heirs	0.022	0.346	0.076	**0.592**	0.059	0.133
	I am closer to friends and family here	0.328	0.193	0.145	**0.591**	0.126	0.061
Recreation-motivated	For vacations	0.055	0.111	-0.023	0.051	**0.779**	0.039
(20.2%)	To develop the land for future residential use	-0.205	-0.149	0.013	0.053	**0.641**	0.276
	For recreation	0.324	0.319	-0.029	0.153	**0.624**	-0.111
	I enjoy hunting or fishing	0.222	-0.090	0.429	0.075	**0.450**	-0.347
Investment-motivated (15.6%)	My land is a financial investment	0.164	0.051	0.222	-0.003	0.137	**0.806**

Appendix S3.2: Table S8. Model selection results for multinomial regression on landowner typologies (investment-, environment-, lifestyle-, profit-, recreation-, or tradition-motivated) in the California Sierra Nevada foothills (n = 350). Elevation was in m / 100; property area was in ha. All continuous covariates except age were natural log transformed. Selected model is bolded.

Model	**ΔAIC**	**AIC**	***w***	***K***
Property area	**0.00**	**1232.60**	**0.87**	**10**
Property area + Elevation	5.65	1238.25	0.05	15
# wetlands + Property area	5.79	1238.39	0.05	15
Property area + Age	7.63	1240.24	0.02	15
# wetlands + Property area + Elevation	11.51	1244.12	0.00	20
Property area + Elevation + Age	12.32	1244.92	0.00	20
# wetlands + Property area + Age	13.28	1245.88	0.00	20
# wetlands + Property area + Elevation + Age	18.24	1250.84	0.00	25
# wetlands	24.31	1256.92	0.00	10
Intercept-only	27.33	1259.93	0.00	5
# wetlands + Elevation	30.05	1262.65	0.00	15
# wetlands + Age	31.41	1264.02	0.00	15
Elevation	32.66	1265.26	0.00	10
Age	34.51	1267.11	0.00	10
# wetlands + Elevation + Age	36.27	1268.88	0.00	20
Elevation + Age	38.91	1271.52	0.00	15
Property area	0.00	1232.60	0.87	10

Appendix S3.2: Table S9. Model selection results for mixed logistic regression (site random effect) on probability of irrigation activation (i.e., being turned on at a pre-existing wetland with irrigation currently off) in the California Sierra Nevada foothills (n = 4863). Wetland area is $\log_{10}$ ha + 0.01; precipitation is sum m Nov–May. "Natural-only" indicates natural-fed wetland that has never before been irrigated. Selected model is bolded.

Model	**ΔAICc**	**AICc**	***w***	***K***
Natural-only + Precipitation + Wetland area + Impoundment	0.00	525.13	0.54	6
Natural-only + Precipitation + Impoundment	**0.80**	**525.93**	**0.36**	**5**
Natural-only + Precipitation + Wetland area + Impoundment + Leak + Pasture + Runoff	4.37	529.50	0.06	9
Natural-only + Precipitation + Impoundment + Leak + Pasture + Runoff	4.97	530.10	0.04	8
Natural-only + Precipitation + Wetland area + Leak + Pasture + Runoff	18.89	544.02	0.00	8
Natural-only + Precipitation + Wetland area	19.66	544.78	0.00	5
Natural-only + Precipitation + Leak + Pasture + Runoff	33.26	558.38	0.00	7
Natural-only	56.15	581.28	0.00	3

Appendix S3.2: Table S10. Model selection results for mixed logistic regression (site random effect) on the probability of irrigation deactivation (i.e., irrigation being turned off currently irrigated wetland) in the California Sierra Nevada foothills (n = 1062). Wetland area is $\log_{10}$ ha + 0.01; precipitation is sum m Nov–May. Selected model is bolded.

Model	ΔAICc	AICc	*w*	*K*
Precipitation + Impoundment + Leak + Pasture + Runoff	**920.41**	**0.00**	**0.63**	**7**
Precipitation + Wetland area + Impoundment + Leak + Pasture + Runoff	921.75	1.35	0.32	8
Precipitation + Impoundment	926.02	5.61	0.04	4
Precipitation + Wetland area + Impoundment	927.72	7.31	0.02	5
Precipitation + Wetland area + Leak + Pasture + Runoff	1010.44	90.03	0.00	7
Precipitation + Leak + Pasture + Runoff	1037.68	117.28	0.00	6
Precipitation + Wetland area	1042.61	122.20	0.00	4
Intercept-only	1060.44	140.04	0.00	2

Appendix S3.2: Table S11. Model selection results for logistic regression on probability of a landowners in the California Sierra Nevada foothills taking the action "selling some or all land" when facing a water cutback of ≥20% (n = 318). Elevation was in m; property area was in ha. Selected model is bolded.

Model	**ΔAIC**	**AIC**	***w***	***K***
Typology (baseline model)	**0.00**	**139.89**	**0.19**	**6**
Typology + Elevation + Elevation^2	1.04	140.92	0.12	8
Typology + ln(Elevation)	1.32	141.21	0.10	7
Typology + Property area	1.57	141.45	0.09	7
Typology + ln(Property area)	1.82	141.70	0.08	7
Typology + Elevation	1.80	141.69	0.08	7
Typology + Elevation + Elevation^2 + Property area	2.64	142.52	0.05	9
Typology + Elevation + Elevation^2 + ln(Property area)	2.90	142.79	0.05	9
Typology + ln(Elevation) + Property area	2.94	142.83	0.04	8
Typology + ln(Elevation) + ln(Property area)	3.17	143.05	0.04	8
Typology + Property area + Property area^2	3.33	143.22	0.04	8
Typology + Elevation + Property area	3.40	143.29	0.04	8
Typology + Elevation + ln(Property area)	3.64	143.53	0.03	8
Typology + Elevation + Elevation^2 + Property area + Property area^2	4.14	144.02	0.02	10
Typology + ln(Elevation) + Property area + Property area^2	4.69	144.57	0.02	9
Typology + Elevation + Property area + Property area^2	5.11	145.00	0.02	9

Appendix S3.2: Table S12. Model selection results for logistic regression on probability of a landowners with pastures in the California Sierra Nevada foothills taking the actions "stop using or using less water to irrigate pasture(s)" or "reduce area of irrigated pasture" when facing a water cutback of ≥20% (n = 93). Elevation was in m and property area was in acres. Selected model is bolded.

Model	ΔAIC	AIC	*w*	*K*
Typology + Elevation + Property area + Property area^2	**0.00**	**100.54**	**0.41**	**9**
Typology + Elevation + Elevation2 + Property area + Property area^2	0.78	101.32	0.27	10
Typology + ln(Elevation) + Property area + Property area^2	3.71	104.24	0.06	9
Typology + Elevation	4.10	104.63	0.05	7
Typology + Property area + Property area^2	4.58	105.12	0.04	8
Typology + Elevation + ln(Property area)	5.46	106.00	0.03	8
Typology + Elevation + Elevation^2	5.26	105.80	0.03	8
Typology + Elevation + Property area	5.84	106.38	0.02	8
Typology + ln(Elevation)	6.42	106.95	0.02	7
Typology (baseline model)	6.59	107.13	0.02	6
Typology + Elevation + Elevation^2 + ln(Property area)	6.79	107.33	0.01	9
Typology + Elevation + Elevation^2 + Property area	6.90	107.44	0.01	9
Typology + ln(Elevation) + ln(Property area)	7.91	108.44	0.01	8
Typology + ln(Elevation) + Property area	8.25	108.79	0.01	8
Typology + ln(Property area)	8.42	108.96	0.01	7
Typology + Property area	8.48	109.01	0.01	7

Appendix S3.2: Table S13. Model selection results for logistic regression on probability of a landowner with irrigation in the California Sierra Nevada foothills taking the action "repairing leaks in ditches, pipes, dams, and/or ponds" when facing a water cutback of ≥20% (n = 166). Elevation was in m and property area was in acres. Quadratic terms were not included because they caused convergence issues. Selected model is bolded.

Model	**ΔAIC**	**AIC**	***w***	***K***
Typology + Property area + ln(Elevation)	0.00	104.88	0.28	7
Typology + Property area	**0.76**	**105.65**	**0.19**	**6**
Typology + Property area + Elevation	1.07	105.95	0.16	7
Typology + ln(Elevation)	2.39	107.28	0.08	6
Typology + ln(Property area) + ln(Elevation)	2.63	107.51	0.07	7
Typology + ln(Property area)	2.97	107.85	0.06	6
Typology	3.02	107.91	0.06	5
Typology + Elevation	3.61	108.49	0.05	6

Appendix S3.2: Table S14. Model selection results for logistic regression on probability of landowners with wetlands in the Sierra Nevada foothills being willing to protect a wetland for a one-time $10,000 payment ($n$ = 141). Elevation was in m, property area in acres, and NID indicated they were in Nevada Irrigation District's county. Selected model is bolded.

Model	**ΔAIC**	**AIC**	***w***	***K***
Typology + Elevation + ln(Property area)	-0.19	117.66	0.11	8
Typology + ln(Elevation) + ln(Property area)	-0.04	117.81	0.10	8
Typology + Elevation	**0.00**	**117.85**	**0.10**	**7**
Typology + ln(Elevation)	0.07	117.91	0.09	7
Typology + Elevation + ln(Property area) + NID	1.09	118.93	0.06	9
Typology + ln(Elevation) + NID	1.13	118.98	0.05	8
Typology + Elevation + NID	1.17	119.02	0.05	8
Typology + Elevation + Elevation^2 + ln(Property area)	1.65	119.50	0.04	9
Typology + Elevation + Elevation^2	1.82	119.67	0.04	8
Typology + Elevation + Property area	1.98	119.83	0.04	8
Typology + ln(Elevation) + Property area	2.05	119.90	0.03	8
Typology (baseline model)	2.59	120.43	0.03	6
Typology + Elevation + Elevation^2 + ln(Property area) + NID	3.09	120.93	0.02	10
Typology + ln(Elevation) + Property area + NID	3.10	120.94	0.02	9
Typology + Elevation + Property area + NID	3.12	120.97	0.02	9
Typology + Elevation + Elevation^2 + NID	3.17	121.02	0.02	9
Typology + ln(Property area)	3.44	121.28	0.02	7
Typology + Elevation + Property area + Property area^2	3.71	121.56	0.02	9
Typology + Elevation + Elevation2 + Property area	3.79	121.64	0.01	9
Typology + ln(Elevation) + Property area + Property area^2	3.82	121.67	0.01	9
Typology + NID	4.38	122.22	0.01	7
Typology + Property area	4.55	122.40	0.01	7
Typology + Elevation + Property area + Property area^2 + NID	4.67	122.52	0.01	10
Typology + ln(Elevation) + Property area + Property area^2 + NID	4.77	122.62	0.01	10
Typology + Elevation + Elevation^2 + Property area + NID	5.12	122.97	0.01	10
Typology + ln(Property area) + NID	5.26	123.11	0.01	8
Typology + Elevation + Elevation^2 + Property area + Property area^2	5.45	123.30	0.01	10
Typology + Property area + NID	6.32	124.17	0.00	8
Typology + Property area + Property area^2	6.53	124.38	0.00	8
Typology + Elevation + Elevation^2 + Property area + Property area^2 + NID	6.67	124.52	0.00	11
Typology + Property area + Property area^2 + NID	8.32	126.17	0.00	9

Appendix S3.2: Table S15. Model selection results for logistic regression on probability of a landowner in the Sierra Nevada Foothills being willing to create a wetland if given free irrigation water (n = 328). Elevation was in m, property area in acres, and NID indicated they were in Nevada Irrigation District's county. Selected model is bolded.

Model	ΔAIC	AIC	w	K
Typology + Elevation + NID	**0.00**	**437.50**	**0.20**	**8**
Typology + ln(Elevation) + NID	0.59	438.08	0.15	8
Typology + Elevation + ln(Property area) + NID	1.84	439.34	0.08	9
Typology + Elevation + Property area + NID	1.87	439.37	0.08	9
Typology + Elevation + Elevation^2 + NID	1.96	439.46	0.07	9
Typology + ln(Elevation) + Property area + NID	2.49	439.99	0.06	9
Typology + Elevation + Property area + Property area^2 + NID	3.36	440.86	0.04	10
Typology + Elevation	3.67	441.17	0.03	7
Typology + Elevation + Elevation^2 + ln(Property area) + NID	3.80	441.29	0.03	10
Typology + Elevation + Elevation^2 + Property area + NID	3.83	441.33	0.03	10
Typology + ln(Elevation) + Property area + Property area^2 + NID	4.16	441.66	0.02	10
Typology + ln(Elevation)	4.40	441.90	0.02	7
Typology + Elevation + Elevation^2	4.90	442.39	0.02	8
Typology + Elevation + Elevation^2 + Property area + Property area^2 + NID	5.34	442.84	0.01	11
Typology + Elevation + Property area	5.47	442.97	0.01	8
Typology + Elevation + ln(Property area)	5.51	443.01	0.01	8
Typology + ln(Elevation) + Property area	6.20	443.70	0.01	8
Typology + ln(Elevation) + ln(Property area)	6.22	443.72	0.01	8
Typology	6.25	443.75	0.01	6
Typology + Elevation + Elevation^2 + Property area	6.69	444.19	0.01	9
Typology + Elevation + Elevation^2 + ln(Property area)	6.75	444.25	0.01	9
Typology + Elevation + Property area + Property area^2	7.28	444.78	0.01	9
Typology + NID	7.46	444.96	0.00	7
Typology + ln(Elevation) + Property area + Property area^2	8.07	445.57	0.00	9
Typology + Property area	8.13	445.63	0.00	7
Typology + ln(Property area)	8.16	445.66	0.00	7
Typology + Elevation + Elevation^2 + Property area + Property area^2	8.42	445.91	0.00	10
Typology + ln(Property area) + NID	9.40	446.90	0.00	8
Typology + Property area + NID	9.41	446.91	0.00	8
Typology + Property area + Property area^2	9.82	447.32	0.00	8
Typology + Property area + Property area^2 + NID	10.90	448.40	0.00	9

Appendix S3.2: Table S16. Model selection results for occupancy models of black rails in California Sierra Nevada foothills wetlands ($n = 273$). All models had "Year" effects as detection covariates. Area was $\log_{10}$ (ha + 0.0001), precipitation was ln(∑ m Nov–May), elevation was m/100, and source was water source (a three-level factor); see text for calculation of connectivity and West Nile virus (WNV). Only models with ≥0.01 AICc wt. and the intercept-only model are shown (out of 256); selected model is bolded.

Model	ΔAICc	AICc	*w*	*K*
ψ ~ Area + Slope + Fluvial + Source	**0.00**	**3687.94**	**0.40**	**41**
γ ~ Area + Connectivity + Slope + Fluvial + Impoundment + Source + WNV + Precipitation				
ε ~ Area + Connectivity + Slope + Fluvial + Impoundment + Source + WNV + Precipitation				
ψ ~ Area + Elevation + Slope + Fluvial + Source	1.08	3689.02	0.24	43
γ ~ Area + Connectivity + Slope + Fluvial + Impoundment + Source + WNV + Precipitation				
ε ~ Area + Connectivity + Elevation + Slope + Fluvial + Impoundment + Source + WNV + Precipitation				
ψ ~ Area + Elevation + Slope + Fluvial + Source	2.97	3690.91	0.09	44
γ ~ Area + Connectivity + Elevation + Slope + Fluvial + Impoundment + Source + WNV + Precipitation				
ε ~ Area + Connectivity + Elevation + Slope + Fluvial + Impoundment + Source + WNV + Precipitation				
ψ ~ Area + Slope + Fluvial + Source	3.30	3691.24	0.08	39
γ ~ Area + Connectivity + Slope + Fluvial + Impoundment + WNV + Precipitation				
ε ~ Area + Connectivity + Slope + Fluvial + Impoundment + Source + WNV + Precipitation				
ψ ~ Area + Elevation + Slope + Fluvial + Source	4.13	3692.07	0.05	43
γ ~ Area + Connectivity + Elevation + Slope + Fluvial + Impoundment + Source + WNV + Precipitation				
ε ~ Area + Connectivity + Slope + Fluvial + Impoundment + Source + WNV + Precipitation				
ψ ~ Area + Elevation + Slope + Fluvial + Source	4.48	3692.42	0.04	41
γ ~ Area + Connectivity + Slope + Fluvial + Impoundment + WNV + Precipitation				
ε ~ Area + Connectivity + Elevation + Slope + Fluvial + Impoundment + Source + WNV + Precipitation				
ψ ~ Area + Slope + Fluvial + Source	5.02	3692.96	0.03	39

γ ~ Area + Connectivity + Slope + Fluvial + Impoundment + Source + Precipitation				
ε ~ Area + Connectivity + Slope + Fluvial + Impoundment + Source + Precipitation				
ψ ~ Area + Elevation + Slope + Fluvial + Source	6.25	3694.19	0.02	42
γ ~ Area + Connectivity + Elevation + Slope + Fluvial + Impoundment + WNV + Precipitation				
ε ~ Area + Connectivity + Elevation + Slope + Fluvial + Impoundment + Source + WNV + Precipitation				
ψ ~ Area + Elevation + Slope + Fluvial + Source	7.39	3695.33	0.01	41
γ ~ Area + Connectivity + Slope + Fluvial + Impoundment + Source + Precipitation				
ε ~ Area + Connectivity + Elevation + Slope + Fluvial + Impoundment + Source + Precipitation				
ψ ~ Area + Elevation + Slope + Fluvial + Source	7.46	3695.40	0.01	41
γ ~ Area + Connectivity + Elevation + Slope + Fluvial + Impoundment + WNV + Precipitation				
ε ~ Area + Connectivity + Slope + Fluvial + Impoundment + Source + WNV + Precipitation				
ψ ~ Area + Slope + Fluvial + Source	7.63	3695.57	0.01	37
γ ~ Area + Connectivity + Slope + Fluvial + Impoundment + Precipitation				
ε ~ Area + Connectivity + Slope + Fluvial + Impoundment + Source + Precipitation				
ψ ~ Area + Elevation + Slope + Fluvial + Source	8.32	3696.26	0.01	41
~ Area + Connectivity + Elevation + Slope + Fluvial + Impoundment + Source + Precipitation				
ε ~ Area + Connectivity + Slope + Fluvial + Impoundment + Source + Precipitation				
ψ ~ Area + Elevation + Slope + Fluvial + Source	8.44	3696.38	0.01	42
γ ~ Area + Connectivity + Elevation + Slope + Fluvial + Impoundment + Source + Precipitation				
ε ~ Area + Connectivity + Elevation + Slope + Fluvial + Impoundment + Source + Precipitation				
Intercept-only	510.19	4198.13	0.00	4

Appendix S3.2: Table S17. Model selection results for occupancy models of Virginia rails in California Sierra Nevada foothills wetlands (n = 272). All models had a set of "year" and a "no playback" dummy variables as detection covariates. Area was $\log_{10}$ (ha + 0.0001), precipitation was ln(∑ m Nov–May)), elevation was m/100, and source was water source (a three-level factor). Only models with ≥0.01 AICc wt. and the intercept-only model are shown (out of 256); selected model is bolded.

Model	ΔAICc	AICc	*w*	*K*
γ ~ Area + Precipitation, ε ~ Area + Elevation + Source + Precipitation	**0.00**	**4167.64**	**0.25**	**25**
γ ~ Area + Elevation + Precipitation, ε ~ Area + Elevation + Source + Precipitation	1.11	4168.75	0.14	26
γ ~ Area + Source + Precipitation, ε ~ Area + Elevation + Source + Precipitation	2.14	4169.79	0.08	27
γ ~ Area + Slope + Fluvial + Impoundment + Precipitation, ε ~ Area + Elevation + Source + Precipitation	2.36	4170.00	0.08	28
γ ~ Area + Elevation + Source + Precipitation, ε ~ Area + Elevation + Source + Precipitation	3.13	4170.77	0.05	28
γ ~ Area + Slope + Fluvial + Impoundment + Source + Precipitation, ε ~ Area + Elevation + Source + Precipitation	3.23	4170.87	0.05	30
γ ~ Area + Elevation + Slope + Fluvial + Impoundment + Precipitation, ε ~ Area + Elevation + Source + Precipitation	3.43	4171.07	0.04	29
γ ~ Area + WNV + Precipitation, ε ~ Area + Elevation + Source + WNV + Precipitation	4.11	4171.75	0.03	27
γ ~ Area + Elevation + Slope + Fluvial + Impoundment + Source + Precipitation, ε ~ Area + Elevation + Source + Precipitation	4.12	4171.76	0.03	31
γ ~ Area + Precipitation, ε ~ Area + Elevation + Precipitation	4.47	4172.11	0.03	23
γ ~ Area + Source + Precipitation, ε ~ Area + Elevation + Precipitation	4.63	4172.27	0.02	25
γ ~ Area + Precipitation, ε ~ Area + Elevation + Slope + Fluvial + Impoundment + Source + Precipitation	5.39	4173.04	0.02	28
γ ~ Area + Elevation + Source + Precipitation, ε ~ Area + Elevation + Precipitation	5.40	4173.04	0.02	26
γ ~ Area + Elevation + Precipitation, ε ~ Area + Elevation + Precipitation	5.49	4173.13	0.02	24
γ ~ Area + Elevation + WNV + Precipitation, ε ~ Area + Elevation + Source + WNV + Precipitation	5.70	4173.34	0.01	28

$\gamma \sim$ Area + Source + WNV + Precipitation, $\varepsilon \sim$ Area + Elevation + Source + WNV + Precipitation	5.86	4173.50	0.01	29
$\gamma \sim$ Area + Slope + Fluvial + Impoundment + Source + Precipitation, $\varepsilon \sim$ Area + Elevation + Precipitation	5.87	4173.51	0.01	28
$\gamma \sim$ Area + Elevation + Slope + Fluvial + Impoundment + Source + Precipitation, $\varepsilon \sim$ Area + Elevation + Precipitation	6.46	4174.10	0.01	29
$\gamma \sim$ Area + Elevation + Precipitation, $\varepsilon \sim$ Area + Elevation + Slope + Fluvial + Impoundment + Source + Precipitation	6.82	4174.46	0.01	29
$\gamma \sim$ Area + Slope + Fluvial + Impoundment + WNV + Precipitation, $\varepsilon \sim$ Area + Elevation + Source + WNV + Precipitation	7.05	4174.69	0.01	30
$\gamma \sim$ Area + Slope + Fluvial + Impoundment + Source + WNV + Precipitation, $\varepsilon \sim$ Area + Elevation + Source + WNV + Precipitation	7.07	4174.71	0.01	32
$\gamma \sim$ Area + Elevation + Source + WNV + Precipitation, $\varepsilon \sim$ Area + Elevation + Source + WNV + Precipitation	7.38	4175.02	0.01	30
$\gamma \sim$ Area + Source + WNV + Precipitation, $\varepsilon \sim$ Area + Elevation + WNV + Precipitation	7.61	4175.25	0.01	27
$\gamma \sim$ Area + Slope + Fluvial + Impoundment + Precipitation, $\varepsilon \sim$ Area + Elevation + Precipitation	7.61	4175.25	0.01	26
$\gamma \sim$ Area + Slope + Fluvial + Impoundment + Precipitation, $\varepsilon \sim$ Area + Elevation + Slope + Fluvial + Impoundment + Source + Precipitation	7.63	4175.27	0.01	31
$\gamma \sim$ Area + Source + Precipitation, $\varepsilon \sim$ Area + Elevation + Slope + Fluvial + Impoundment + Source + Precipitation	7.68	4175.32	0.01	30
Intercept-only	406.40	4574.04	0.00	4

Appendix S3.2: Table S18. Model selection results for bias-reduced generalized linear models (with binomial distribution and offset for mosquito pool size) estimating mean *Culex* spp. West Nile virus prevalence at a site from $n = 3{,}706$ pools trapped at wetlands in the California Sierra Nevada foothills. This model was not included in the agent-based model; rather, we used the lowest AICc value model (bolded) to estimate average *Culex* prevalence at each wetland site.

Model	**ΔAICc**	**AICc**	***w***	***K***
Site + Day + Day^2 + Year	**0.00**	**2345.29**	**0.70**	**84**
Site + Day + Day^2	1.66	2346.95	0.30	82
Intercept-only	14.83	2360.12	0.00	1
Site	22.04	2367.33	0.00	80
Site + Day	23.22	2368.51	0.00	81
Site + Day + Day^2 + Year + Site:Day	94.55	2439.85	0.00	163
Site + Day + Day^2 + Year + Site:Day + Site:Day^2	235.03	2580.33	0.00	242
Site + Day + Day^2 + Year + Site:Day + Site:Day^2 + Site:Year	286.88	2632.17	0.00	280

Appendix S3.2: Table S19. Model selection results for linear regression on $\log_{10}$ *Culex* spp. mosquito abundance at $n = 80$ wetlands in the California Sierra Nevada foothills. "Wetland" and "water" were square root % wetland and open water land cover in 2.5km buffer, respectively; elevation was in m, and rice distance was the square root of the distance to the nearest rice field in km. "Flowing" and "irrigated" were dummy variables indicating the presence of flowing and irrigation water in the wetland. Selected model is bolded.

Model	**ΔAICc**	**AICc**	***w***	***K***
Wetland + Rice distance	**0.00**	**48.93**	**0.57**	**3**
Wetland + Rice distance + Flowing	1.60	50.53	0.25	5
Wetland + Rice distance + Flowing + Irrigated	3.22	52.15	0.11	7
Wetland + Rice distance + Flowing + Irrigated + Elevation	4.83	53.76	0.05	8
Wetland + Rice distance + Flowing + Irrigated + Elevation + Open water	7.26	56.19	0.02	9

Appendix S3.2: Table S20. Model selection results for linear regression on $\log_{10}$ estimated *Culex* spp. West Nile virus prevalence at $n = 80$ wetlands in the California Sierra Nevada foothills. *Culex* abundance was $\log_{10}$ average count per trap/night; "wetland" and "water" were square root % wetland and open water land cover in 2.5km buffer, respectively; elevation was in m, and rice distance was the square root of the distance to the nearest rice field in km. "Flowing" and "irrigated" were dummy variables indicating the presence of flowing and irrigation water in the wetland. Selected model is bolded.

Model	**ΔAICc**	**AICc**	***w***	***K***
***Culex* abundance + Rice distance**	**0**	**50.55**	**0.59**	**3**
Culex abundance + Rice distance + Elevation	1.63	52.18	0.26	4
Culex abundance + Rice distance + Elevation + Wetland	3.52	54.07	0.10	5
Culex abundance + Rice distance + Elevation + Wetland + Flowing	5.7	56.25	0.03	7
Culex abundance + Rice distance + Elevation + Wetland + Flowing + Irrigated	7.97	58.52	0.01	9
Culex abundance + Rice distance + Elevation + Wetland + Flowing + Irrigated + Open water	10.45	61.00	0.00	10

Appendix S3.3: Additional results and discussion of the WICM

Black rails appear to be dispersal-limited (i.e., were strongly sensitive to connectivity), in agreement with earlier findings (Risk et al. 2011, Hall et al. 2018). Conversely, Virginia rail metapopulation dynamics were not dispersal-limited (see Appendix S3.1), but were highly sensitive to elevation (Fig. 3.4b, Appendix S3.3: Fig. S1b). Their higher extinction rates at lower elevations may be due to rainy season deep-water flooding of large fringe geomorphology Central Valley wetlands, which we observed in the field. Black rails are likely not sensitive to elevation because they were less likely to occupy these fringe wetlands in the first place, preferring slope geomorphology wetlands (Fig. 3.4a). Virginia rails were more generalist, showing no sensitivity to heterogeneity in wetland geomorphology types (Appendix S3.2: Table S17).

Most model outcomes for rail metapopulation dynamics showed no distinguishable sensitivity to landowner or wetland heterogeneity (Appendix S3.3: Fig. S3). One exception was wetland abundance, which showed small to moderate decreases with increases of profit-motivated landowners, irrigation-only wetlands, and leak-fed wetlands (Appendix S3.3: Fig. S2). However, these results should be interpreted with caution. We conducted a traditional sensitivity analysis that varied the percent of only one wetland or landowner type at a time, but overall diversity of agents on the landscape may average out the impact of changes in any one group (the portfolio effect; Schindler et al. 2010). For example, the 25% perturbation in percent of profit-motivated landowners changed the percent of profit-motivated landowners by only 2.4%. Notably, the metapopulations were more sensitive to wetland heterogeneity via the regression parameters for colonization and extinction (Fig. 3.4; Appendix S3.3: Fig. S2). Understanding the importance of landowner and wetland diversity as a whole thus requires different scenarios modifying these processes together, and is a focus of future research.

The sensitivity analysis results (Fig. 3.4) suggest three additional possible ways to reduce metapopulation extinction risk: (1) reducing "storage used" (i.e., water conservation by landowners), (2) lowering the "storage threshold" for when drought cutbacks are implemented, and (3) increasing water district "max storage" capacity. Water conservation measures are unlikely to help in the real world, as this would likely reduce the "waste" irrigation runoff and leaks that create wetlands in this working landscape in the first place. Reducing the storage threshold (e.g., BVID implementing cutbacks if below 35% max storage rather than 45%) showed diminishing increases in occupancy for higher perturbations (Fig. 3.4). In addition, our reservoir and hydrologic models are coarser than those used by irrigation districts to set these thresholds, so this may not be advisable. Increasing storage capacity by building reservoirs is a promising option, which some districts in the region are considering. If combined with guaranteed water allocations for wetlands that were preserved during drought, this may be a politically feasible middle ground. Such a policy would provide landowners with additional and more secure water supplies while providing environmental benefits to trade-off against the impacts of reservoir construction.

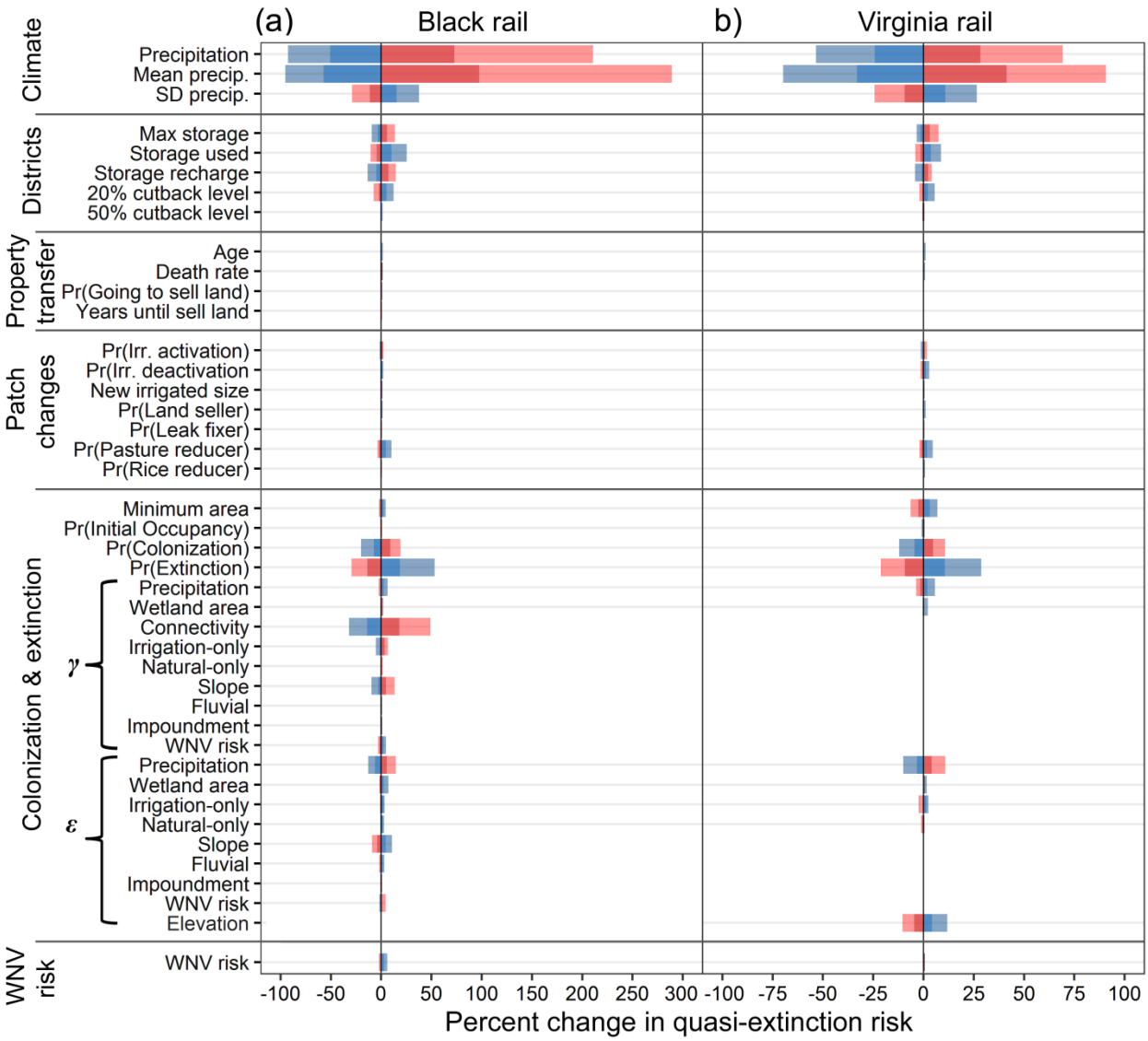

Appendix S3.3: Figure S1. Sensitivity analysis of (a) black and (b) Virginia rail quasi-extinction risk (minimum number of occupied wetlands) for WICM input parameters used in the simulation of the California Sierra Nevada foothills with drought cutbacks and no wetland incentives. γ and ε represent logistic regression parameters for colonization and extinction probabilities, respectively.

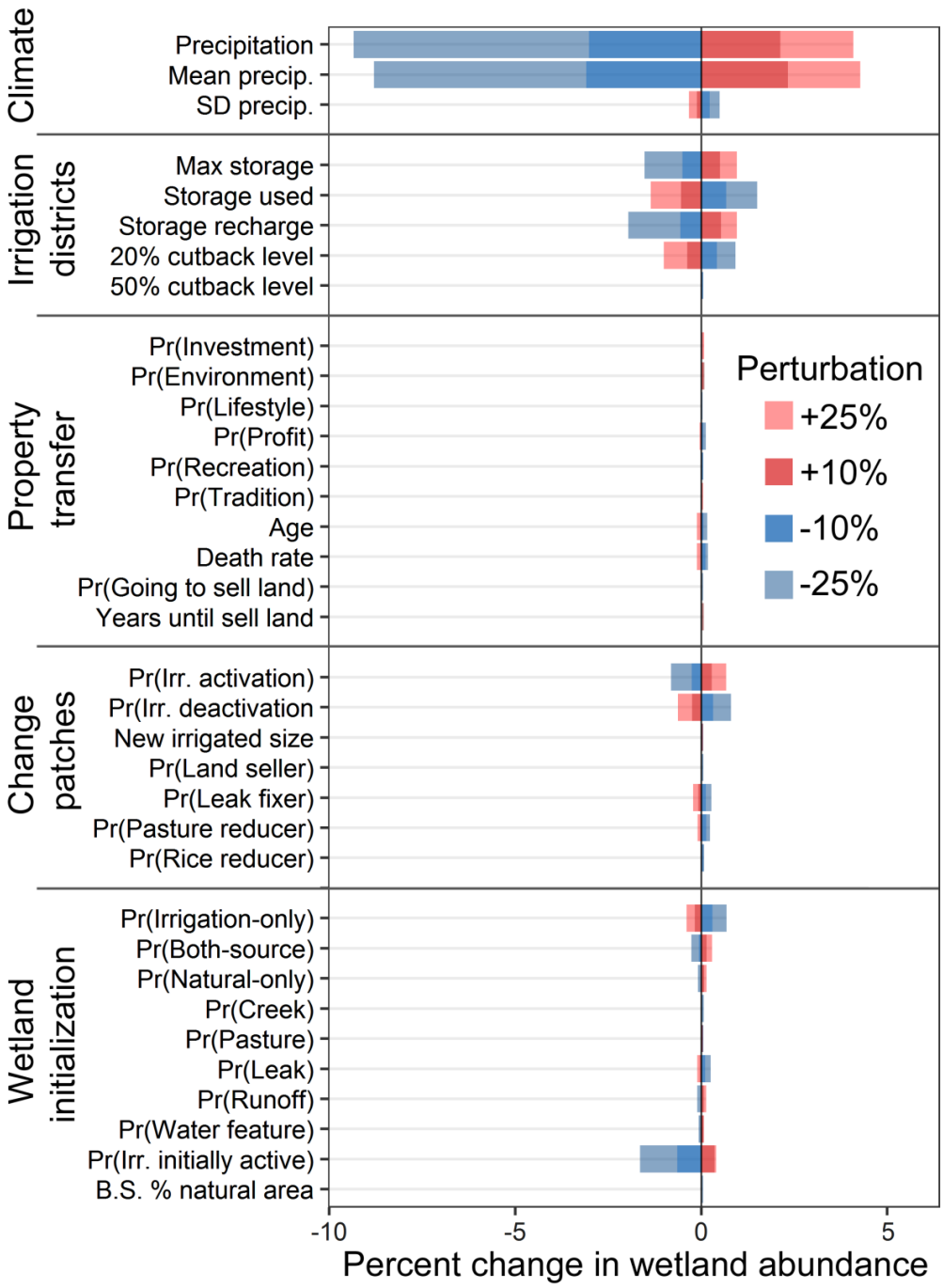

Appendix S3.3: Figure S2. Sensitivity analysis wetland abundance for WICM input parameters used in the simulation of the California Sierra Nevada foothills with drought cutbacks and no wetland incentives.. All geomorphology types and 53% of water sources are excluded because they were deterministically initialized to their real values.

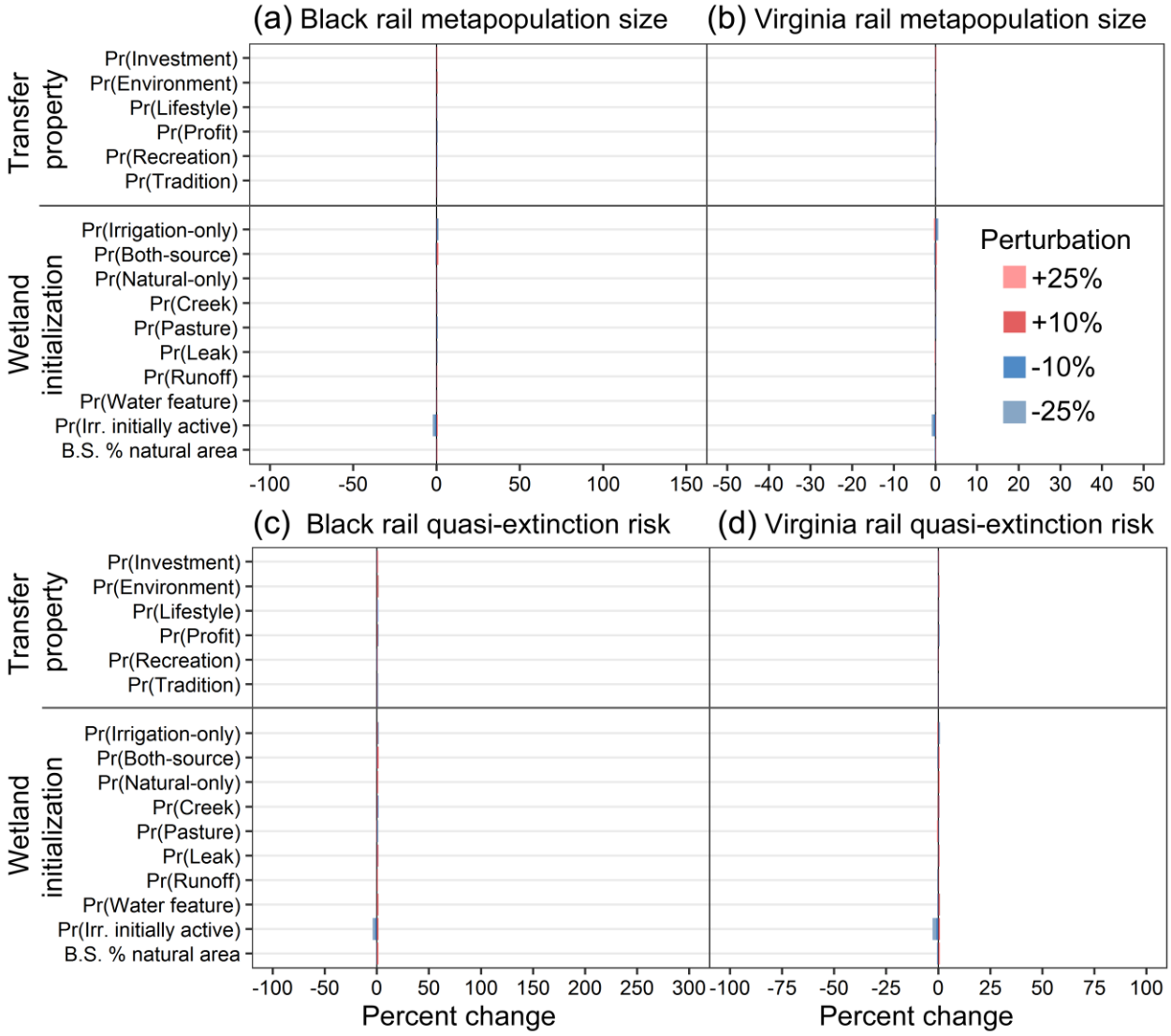

Appendix S3.3: Figure S3. Sensitivity analysis of landowner heterogeneity and wetland heterogeneity and initialization effects on black (a, c) and Virginia (b, d) rail metapopulation dynamics in the WICM. All geomorphology types and 53% of water sources were excluded because they were deterministically initialized to their real values.

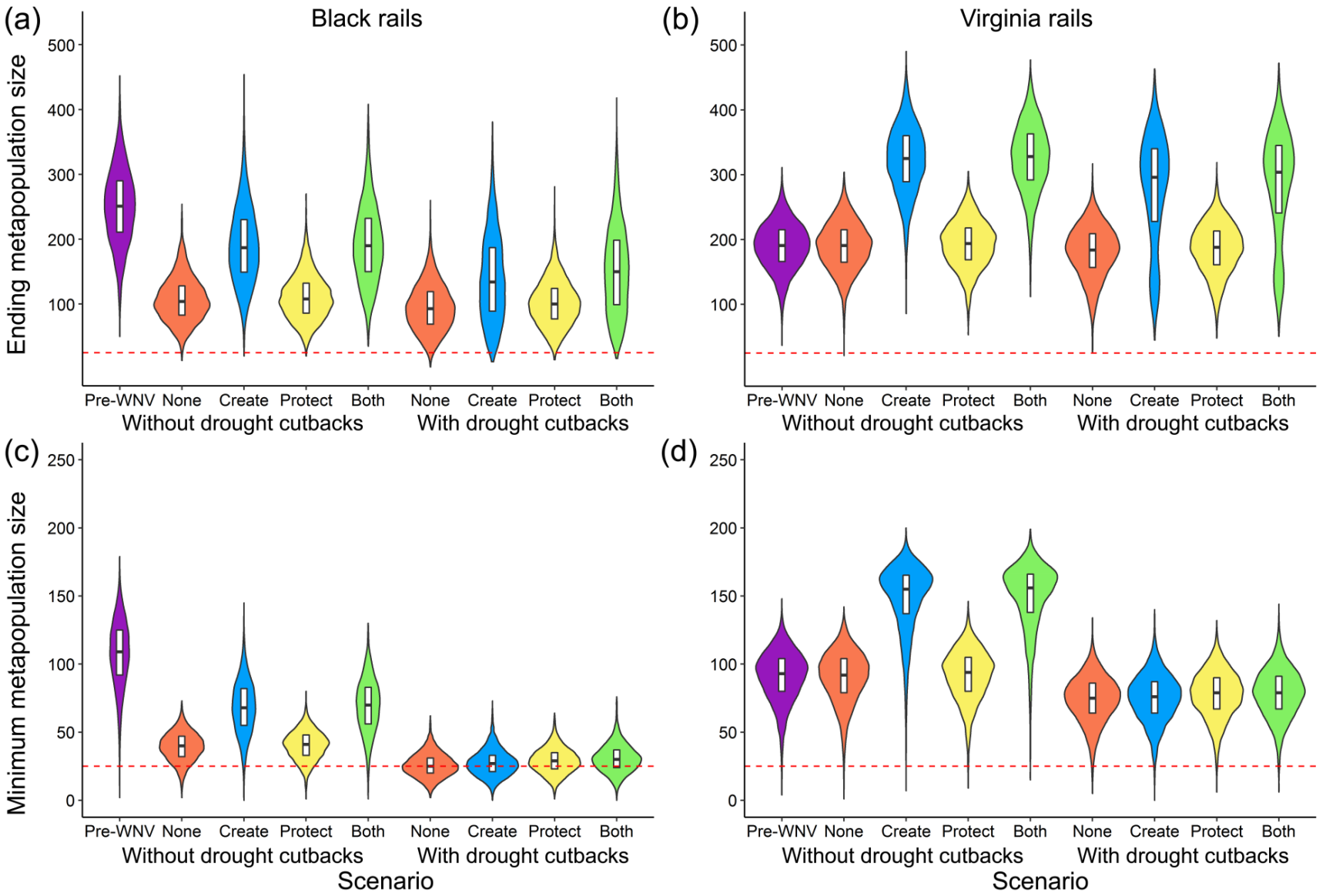

Appendix S3.3: Figure S4. Metapopulation size and quasi-extinction risk for black rails and Virginia rails after 100 years, for 8 different scenarios simulating the California Sierra Nevada foothill landscape.

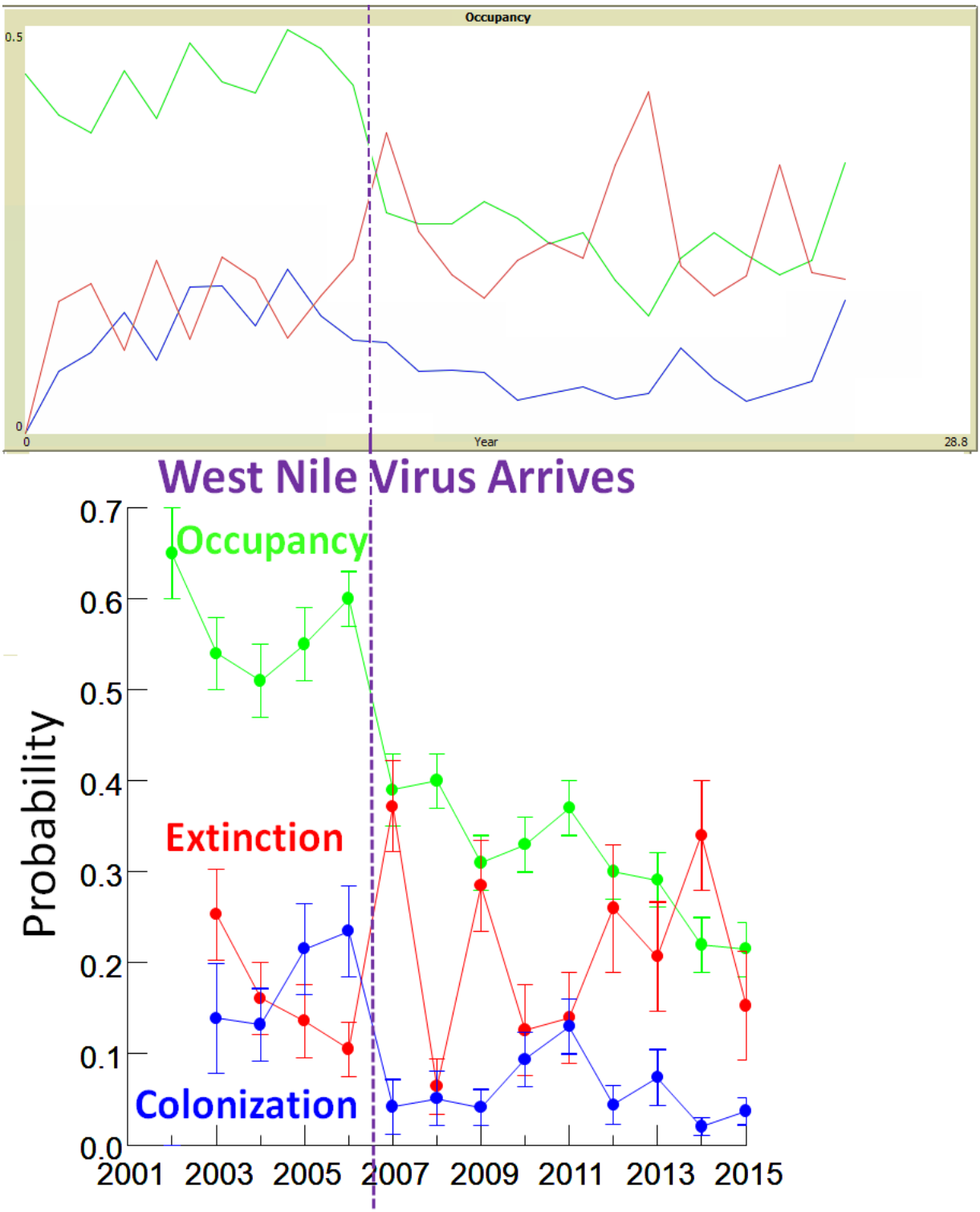

Appendix S3.3: Figure S5. The combination of West Nile virus and drought was able to reproduce the dynamics of the black rail decline. Bottom: estimates of black rail occupancy, colonization, and extinction rates fit from a year-only model (n = 274). Top: black rail occupancy, colonization, and extinction rates produced by the WICM over 10 pre-WNV and 15 post-WNV years, for the equivalent sites (some site definitions were different in the WICM).

Appendix References

Amarasekare, P., and H. Possingham. 2001. Patch dynamics and metapopulation theory: the case of successional species. Journal of Theoretical Biology 209:333–344.

Augustin, N. H., M. A. Mugglestone, and S. T. Buckland. 1996. An autologistic model for the spatial distribution of wildlife. Journal of Applied Ecology 33:339–347.

Beier, J. C., G. F. Killeen, and J. I. Githure. 1999. Short report: entomologic inoculation rates and Plasmodium falciparum malaria prevalence in Africa. The American Journal of Tropical Medicine and Hygiene 61:109–113.

Beissinger, S. R., and M. I. Westphal. 1998. On the use of demographic models of population viability in endangered species management. The Journal of Wildlife Management 62:821–841.

Bell, A., and K. Jones. 2015. Explaining fixed effects: random effects modeling of time-series cross-sectional and panel data. Political Science Research and Methods 3:133–153.

Bolling, B. G., C. M. Barker, C. G. Moore, W. J. Pape, and L. Eisen. 2009. Seasonal patterns for entomological measures of risk for exposure to *Culex* vectors and West Nile virus in relation to human disease cases in northeastern Colorado. Journal of Medical Entomology 46:1519–1531.

Browns Valley Irrigation District. 2018a. 2018 irrigation rates. https://www.bvid.org/files/2018_Rates_no_discount.pdf.

Browns Valley Irrigation District. 2018b, March 19. Collins Lake usable water. https://www.bvid.org/files/currentlakelevel.pdf.

California Department of Water Resources. 2018, March 19. Active monthly reservoirs. https://cdec.water.ca.gov/misc/monthly_res.html.

Daly Christopher, Halbleib Michael, Smith Joseph I., Gibson Wayne P., Doggett Matthew K., Taylor George H., Curtis Jan, and Pasteris Phillip P. 2008. Physiographically sensitive mapping of climatological temperature and precipitation across the conterminous United States. International Journal of Climatology 28:2031–2064.

Darsie, R., and R. Ward. 2005. Identification and geographical distribution of the mosquitoes of North America, north of Mexico. University of Flordia Press, Gainesville, Florida.

Dobson, A. D. M., and S. K. J. R. Auld. 2016. Epidemiological implications of host biodiversity and vector biology: key insights from simple models. The American Naturalist 187:405–422.

Duffy, W. G., and S. N. Kahara. 2011. Wetland ecosystem services in California's Central Valley and implications for the Wetland Reserve Program. Ecological Applications 21:S128–S134.

Esri. 2011. ArcGIS Desktop. Esri, Redlands, CA.

Ferris, J., and J. Siikamäki. 2009. Conservation reserve program and wetland reserve program: primary land retirement programs for promoting farmland conservation. Resources for the Future, Washington, DC.

Flint, L. E., and A. L. Flint. 2012. Downscaling future climate scenarios to fine scales for hydrologic and ecological modeling and analysis. Ecological Processes 1:2.

Gimona, A., and J. G. Polhill. 2011. Exploring robustness of biodiversity policy with a coupled metacommunity and agent-based model. Journal of Land Use Science 6:175–193.

Grimm, V., U. Berger, D. L. DeAngelis, J. G. Polhill, J. Giske, and S. F. Railsback. 2010. The ODD protocol: A review and first update. Ecological Modelling 221:2760–2768.

Grimm, V., E. Revilla, U. Berger, F. Jeltsch, W. M. Mooij, S. F. Railsback, H.-H. Thulke, J. Weiner, T. Wiegand, and D. L. DeAngelis. 2005. Pattern-oriented modeling of agent-based complex systems: lessons from ecology. Science 310:987–991.

Hall, L. A., N. D. Van Schmidt, and S. R. Beissinger. 2018. Validating dispersal distances inferred from autoregressive occupancy models with genetic parentage assignments. Journal of Animal Ecology 87:691–702.

Hanski, I. A. 1999. Metapopulation Ecology. Oxford University Press.

Hines, J. E. 2013. PRESENCE - Software to estimate patch occupancy and related parameters. U.S.G.S. Patuxent Wildlife Research Center, Laurel, MD, USA.

Huntsinger, L., H. Tracy, J. L. Oviedo, M. W. K. Shapero, G. A. Nader, R. S. Ingram, and S. R. Beissinger. 2017. Save water or save wildlife? Water use and conservation in the Central Sierran foothill oak woodlands of California, USA. Ecology and Society 22:12.

Kauffman, E. B., S. A. Jones, A. P. Dupuis, K. A. Ngo, K. A. Bernard, and L. D. Kramer. 2003. Virus detection protocols for west nile virus in vertebrate and mosquito specimens. Journal of Clinical Microbiology 41:3661–3667.

Kilpatrick, A. M., L. D. Kramer, M. J. Jones, P. P. Marra, and P. Daszak. 2006. West Nile virus epidemics in North America are driven by shifts in mosquito feeding behavior. PLOS Biology 4:e82.

Kilpatrick, A. M., and W. J. Pape. 2013. Predicting human West Nile virus infections with mosquito surveillance data. American Journal of Epidemiology 178:829–835.

Kwan, J. L., B. K. Park, T. E. Carpenter, V. Ngo, R. Civen, and W. K. Reisen. 2012. Comparison of enzootic risk measures for predicting West Nile disease, Los Angeles, California, USA, 2004–2010. Emerging Infectious Diseases 18:1298–1306.

MacKenzie, D. I., J. D. Nichols, J. E. Hines, M. G. Knutson, and A. B. Franklin. 2003. Estimating site occupancy, colonization, and local extinction when a species is detected imperfectly. Ecology 84:2200–2207.

Nevada Irrigation District. 2012. Drought contingency plan. Page 9. Nevada Irrigation District.

Nevada Irrigation District. 2018. Schedule of rates and charges.

Pepin, K. M., R. J. Eisen, P. S. Mead, J. Piesman, D. Fish, A. G. Hoen, A. G. Barbour, S. Hamer, and M. A. Diuk-Wasser. 2012. Geographic variation in the relationship between human Lyme disease incidence and density of infected host-seeking *Ixodes scapularis* nymphs in the eastern United States. The American Journal of Tropical Medicine and Hygiene 86:1062–1071.

R Core team. 2013. R: A language and environment for statistical computing. R Foundation for Statistical Computing, Vienna, Austria.

Richmond, O. M., J. Tecklin, and S. R. Beissinger. 2008. Distribution of California black rails in the Sierra Nevada foothills. Journal of Field Ornithology 79:381–390.

Richmond, O. M. W., S. K. Chen, B. B. Risk, J. Tecklin, and S. Beissinger. 2010a. California black rails depend on irrigation-fed wetlands in the Sierra Nevada foothills. California Agriculture 64:85–93.

Richmond, O. M. W., J. E. Hines, and S. R. Beissinger. 2010b. Two-species occupancy models: a new parameterization applied to co-occurrence of secretive rails. Ecological Applications 20:2036–2046.

Risk, B. B., P. de Valpine, and S. R. Beissinger. 2011. A robust-design formulation of the incidence function model of metapopulation dynamics applied to two species of rails. Ecology 92:462–474.

Salas, J. D. 1993. Analysis and modelling of hydrological time series. Pages 1–72 in D. Maidment, editor. Handbook of Hydrology. McGraw-Hill Inc., New York, NY.

Sanford, T., P. C. Frumhoff, A. Luers, and J. Gulledge. 2014. The climate policy narrative for a dangerously warming world. Nature Climate Change 4:164–166.

Schindler, D. E., R. Hilborn, B. Chasco, C. P. Boatright, T. P. Quinn, L. A. Rogers, and M. S. Webster. 2010. Population diversity and the portfolio effect in an exploited species. Nature 465:609–612.

Sjögren-Gulve, P., and I. Hanski. 2000. Metapopulation viability analysis using occupancy models. Ecological Bulletins 48:53–71.

U.S. Bureau of Reclamation, and California Department of Water Resources. 2009, September 1. Private Water Districts. MPGIS Service Center.

US Environmental Protection Agency. 2013. Level III Ecoregions of the Conterminous United States. U.S. EPA Office of Research and Development (ORD) - National Health and Environmental Effects Research Laboratory (NHEERL), Corvallis, OR.

U.S. Geological Survey. 2009. National Elevation Dataset. https://lta.cr.usgs.gov/NED.

U.S. Social Security Administration. 2014. Actuarial life table. https://www.ssa.gov/oact/STATS/table4c6_2010.html.

Wacker, M. J., and N. M. Kelly. 2004. Ranchers vs. ranchettes in California's oak rangelands. Rangelands 26:17–22.

Wilensky, U. 2018. NetLogo. Center for Connected Learning and Computer-Based Modeling, Northwestern University, Evanston, IL.